Expanding the potential of mutasynthetic approaches for pseudomonic acids

by

Yusra Alsammarraie

A thesis submitted to the University of Birmingham for the degree of DOCTOR OF PHILOSOPHY

Institute of Microbiology and infection
School of Biosciences
College of Life and Environmental Sciences
The University of Birmingham
August 2015

UNIVERSITY OF
BIRMINGHAM

University of Birmingham Research Archive

e-theses repository

This unpublished thesis/dissertation is copyright of the author and/or third parties. The intellectual property rights of the author or third parties in respect of this work are as defined by The Copyright Designs and Patents Act 1988 or as modified by any successor legislation.

Any use made of information contained in this thesis/dissertation must be in accordance with that legislation and must be properly acknowledged. Further distribution or reproduction in any format is prohibited without the permission of the copyright holder.

Abstract

Natural products, particularly polyketides are among the most important sources of antimicrobial compounds. 20% of the top selling drugs are polyketide based. In recent years genetic engineering has played a critical role in modifying biosynthetic pathways of different polyketide compounds as a way to create novel structures with improved clinical properties. Further investigation and understanding of these giant multi-enzyme complexes is necessary to achieve efficient synthetic engineering.

In many PKS systems including the mupirocin biosynthesis pathway, the thioesterase (TE) is normally considered as the end of the assembly line. However, expressing the CoA-ligase *tmlU* from the thiomarinol pathway in the mupirocin producer strain (*Pseudomonas fluorescens* NCIMB10586) revealed that TmlU could only release truncated pseudomonic acid when a TE domain was present. This finding led to the hypothesis that perhaps the TE domain could act as a tether for TmlU, in order for the latter to be able to capture the growing chain and perhaps load it onto the post TE pathway. This study also presents the first evidence of MmpB being involved in producing the 9-hydroxynonanoic acid in the mupirocin biosynthesis pathway.

Table of Contents

List of figures

Chapter 1

Chapter 2

Chapter 3

Chapter 4

Chapter 5

Chapter 6

List of tables

CHAPTER 1

1 Introduction

1.1 Antibiotics

The concept of using antibacterial compounds to treat wounds and various other infections goes back thousands of years, way before the period we consider as "the modern antibiotic era". In Nippur, in the Euphrates valley, circa 2000 BC, a prescription for using honey to treat skin infections and ulcers was found written on a clay tablet (Munn and Jones, 2001). Other ancient civilizations have also utilized honey and used it for various medical applications sometimes combined with other ingredients like red ochre or powdered alabaster. Metals have also contributed to the collection of early antibacterial agents. Silver for example was used by the settlers of North America to preserve beverages like milk, wine and water by dropping silver coins in transport containers (Swathy *et al*., 2014). This practice was later modified and used by Japanese soldiers to prevent the spread of dysentery (Joseph *et al*., 2013). In ancient Rome herbs were used widely as antimicrobial agents, Myrrh and barbarum were one of the earliest examples (around 400 BC) used to treat many septic processes. While the ancient world mostly depended on the process of trial and error to discover the therapeutic properties of certain compounds, in the 18th century drug discovery started to take a more advanced approach where scientific logic and technique were applied to identify possible antimicrobial compounds. One of the earliest examples was Edward Jenner's experiment which paved the way for the use of vaccination against some infectious diseases (Timmins, 2009), and then in 1864 Louis Pasteur discovered that virus attenuation can be a very useful way to gain protection against some viral diseases like Rabies (Enrique Ravina, 2011). However, what we refer to as the modern antibiotic era did not start until the early 1900s, when Paul Ehrlich, together with chemist Alfred Bertheim and bacteriologist Sahachiro Hata produced Neosalvarsan, a

compound that cured syphilis. Ehrlich, in addition to his drug discovery career, also pioneered the systematic screening approach on which pharmaceutical companies rely upon to this day. The major medical breakthrough though came in 1928 when Alexander Fleming noticed that the *Staphylococcus aureus* he grew on a petri dish contaminated with fungus, had lysed and turned translucent instead of their normal yellow opaque colour. The fungus was identified as *Penicillium notatum* and Fleming called the lytic compound produced by the mould penicillin (Clardy *et al*., 2009). Although discovering penicillin was a big achievement, the process of isolating and purifying the active substance was a tedious task and it was not until 1940 that penicillin was mass produced and distributed to pharmaceutical companies using a protocol developed by Howard Florey and Ernest Chain that allows penicillin purification in quantities suitable for clinical trials (Aminov, 2010). By 1944 Charles Pfizer and Co became the largest producers of penicillin turning out 100,000 million units a month (Sneader, 2006).

1.1.1 Antibiotic Targets

Antibiotics can be classified on the basis of their cellular or molecular target into four major divisions: inhibitors of DNA replication, RNA synthesis, cell wall synthesis and protein synthesis (Walsh, 2003). In order for a bacterial cell to be able to contain 1000 μm of double stranded DNA, it has to control the topology of the chromosomal DNA, by reducing the space it occupies. In *Escherichia coli* this is achieved by producing enzymes called DNA topoisomerases, of which fluoroquinolones target DNA gyrase and DNA topoisomerase IV (Hawkey, 2003). This class of antibiotics inhibits DNA synthesis by interacting with the enzyme-bound DNA complex, forming a drug-enzyme–DNA complex. This leads to chromosomal DNA fragmentation and prevents the re-ligation of

these fragments, resulting in impaired DNA replication and initiation of the apoptotic pathway (Guan *et al*., 2013) (Schroder *et al*., 2012).

RNA synthesis is another valid target for antibiotics like Rifamycins (Floss and Yu, 2005). It works by binding strongly to the DNA-dependent RNA polymerase during initiation, clashing sterically with the growing oligonucleotide. After RNA synthesis has progressed to the elongation stage the process is no longer sensitive to the effect of the Rifamycins (Artsimovitch and Vassylyev, 2006).

Given the vital role of the ribosome for the bacterial cellular functions, it is not surprising that many clinically relevant antibiotics target different aspects of the ribosomal processes as a way to inhibit protein synthesis. The importance of the 30S subunit lies in its decoding site (A-site), which monitors codon – anticodon pairing between mRNA and tRNA respectively, the function of which is to screen for the accurate match between the mRNA codon and the aminoacylated–tRNA anticodon. Among the antibiotics that target this site are aminoglycosides, which facilitate amino acid mis-incorporation and consequently interfere with translational fidelity (Hermann, 2005). Tetracyclines, in use since the 1940s, inhibit protein synthesis by blocking the tRNA binding site (Brodersen *et al*., 2000). By contrast, the antibiotic Pactamycin prevents the formation of the functional 70S ribosome by causing conformational changes in the 30S subunit and thus blocking the tRNA binding site (Brodersen *et al*., 2000). Other antibiotics also target the ribosomal 50S subunit, which contains the peptidyl-transferase centre (PTC), the active site of the ribosome, in addition to the peptide exit tunnel (Tenson and Mankin, 2006). Chloramphenicol interacts with the PTC and prevents binding to the A-site tRNA. Virginiamycin M on the other hand binds to both the A- and P-sites and causes structural changes in the PTC, while macrolides like erythromycin hinder protein biosynthesis by

stopping the growing peptide chain from passing through the ribosomal exit tunnel (Hermann, 2005).

The cell wall is the first line of defence for the bacterium and very critical for its survival. Inhibiting bacterial cell wall synthesis can have a variety of effects on the bacterial cell such as changes to cell shape and size, induction of a cellular stress response and cell lysis. Penicillin, which belongs to the β-lactam class of antibiotics, targets the transpeptidase known as penicillin-binding protein (PBP), which catalyses the peptide bond formation that crosslinks the peptidoglycan blocks. Cell wall synthesis can also be inhibited through blocking both transglycosidase and transpeptidase activity, a strategy that is utilized by vancomycin via binding to the D-Ala-D-Ala C- terminus of the pentapeptide. This blocks the addition of late precursors by transglycosylation to the nascent peptidoglycan chain, and consequently results in reduction of the cellular mechanical strength and an incomplete cell wall (Kohanski *et al*., 2010). Fosfomycin works by inhibiting MurA, the enzyme involved in catalysing the first step of the peptidoglycan synthesis, and Daptomycin induces calcium–dependent membrane depolarisation, which leads to disruption of the bacterial cellular membrane (Bush, 2012). Exploiting bacterial Folic acid biosynthesis as an antibiotic target has been recognised for years. Sulfonamides were the first folic acid pathway inhibitors introduced as early as the 1930s. They work as alternative substrates for dihydropteroate synthase, one of the pathway's enzymes, leading to depletion of the folate pool and therefore inhibition of bacterial growth by preventing DNA replication. Dihydrofolate reductase (DHFR) is the final enzyme in the pathway, and it is targeted by the diaminopyrimidine (Bermingham and Derrick, 2002), (Figure 1.1).

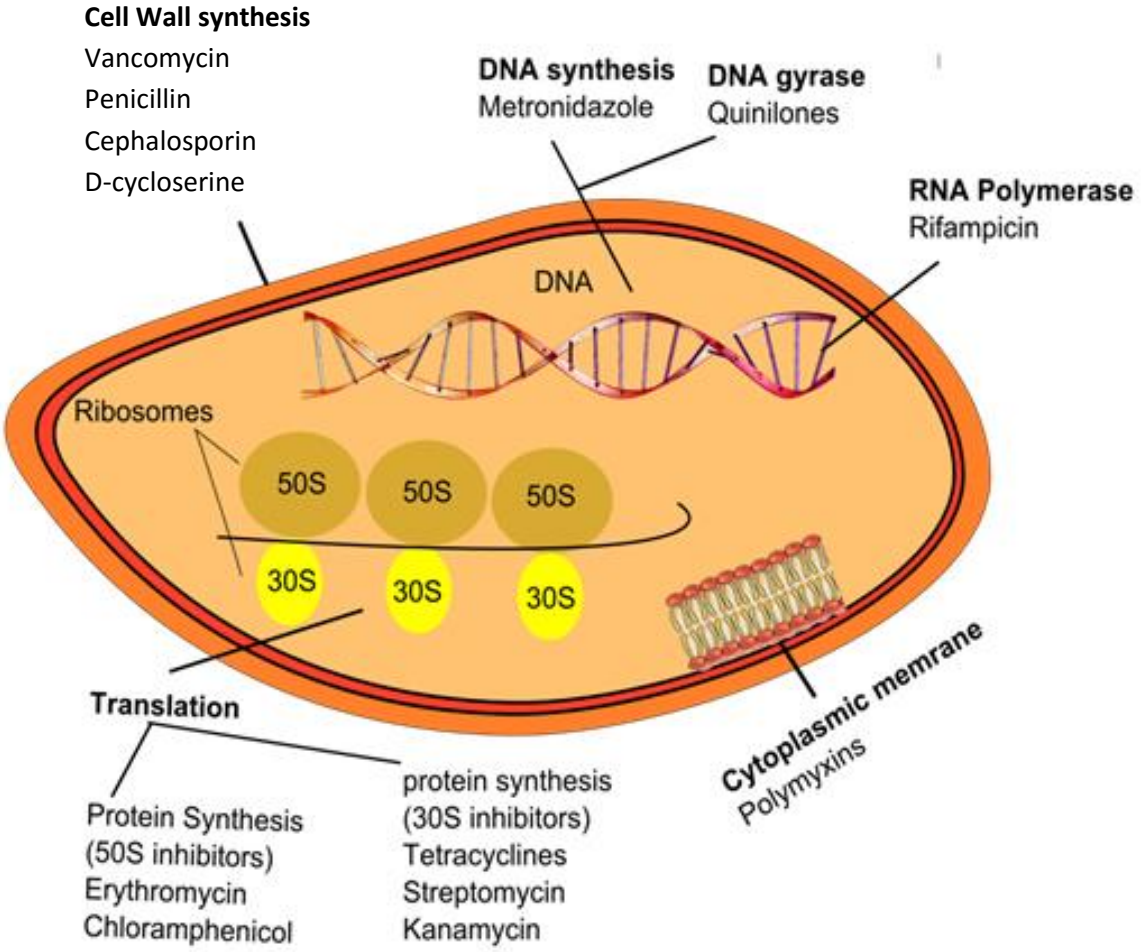

Figure 1.1 Principle targets of antibiotics. Drug target interactions can take different forms depending on which bacterial function is affected. Quinolones interfere with DNA supercoiling which leads to the formation of double stranded DNA breaks and eventually cell death. Tetracyclines inhibit protein synthesis by blocking the tRNA binding site. Chloramphenicol also interferes with protein synthesis but via different route - it interacts with the peptidyl-transferase centre in ribosomal 50S subunit and prevents binding to the A-site tRNA with the attachment of mRNA to the 50s ribosome, which consequently inhibits protein synthesis. β-lactams target cell wall synthesis binding to PBPs and decreasing peptidoglycan synthesis.

As antibiotic resistance is a growing threat, other antimicrobial targets are being explored in a bid to keep up with the evolutionary process of the bacterial resistance.

Acyldepsipeptidolactones are among the currently examined natural products with a novel antibacterial mode of action. With the acyldepsipeptide (ADEP) being the main component, this group of antibiotics work by disrupting the highly regulated protease activity of the ClpPs resulting in a fast degradation of the essential cellular proteins and eventually cell death (Clardy *et al*., 2006). Fatty acid biosynthesis is also becoming an interesting target for pharmaceutical companies. For example, Platensimycin was reported to be potentially active against *Staphylococcus aureus* by limiting the activity rate of FabF and was tested in mouse models infected with *S.aureus*, resulting in 10^4 to 10^5 fold reductions in bacterial counts (Clardy *et al*., 2006, Wang *et al*., 2006). However, despite the *in vivo* activity established in the mouse model, Platensimycin is not ready for clinical use due to its poor pharmacokinetic profile (Allahverdiyev *et al*., 2013).

1.1.2 Antibiotic resistance

The introduction of antibiotics is recognised as one of the most important medical achievements of the 20th century, and in the early days many believed that this would provide a permanent solution. By contrast, there is now great concern that without drastic action we may no longer be able to control many common infections due to the causative bacteria becoming resistant to all available antibiotics. However, while antibiotic resistance has been exacerbated by human use and misuse of antibiotics, most antibiotic biosynthesis pathways evolved millions of years ago suggesting that antibiotic resistance predates the clinical use of antibiotics. Therefore, while the introduction of antibiotics may be a factor, it is not the only cause for the acquisition of modern resistance genes (Wright and Poinar, 2012).

To study the evolution of resistance genes, DNA samples were collected from Late Pleistocene permafrost sediments. The samples were found to include genes for: the

ribosomal protection protein TetM, which confers tetracycline resistance, VanX a part of the Vancomycin resistance pathway, and a β-lactamase belonging to the TEM group of the β -lactamases. Several *tetM*-related genes were identified, most of them are very similar to the Actinomycetes ribosomal protection protein (Costa *et al*., 2011). Phylogenetic analysis of Vancomycin resistance genes confirmed that many of the ancient VanHAX operon sequences are statistically similar to the modern Vancomycin resistance genes. To confirm that the 30,000 years old Vancomycin resistance genes are actually related to the modern proteins, researchers used crystallography to determine the 3D structure of VanA (Brown and Balkwill, 2009, Costa *et al*., 2011). Results showed that the quaternary and tertiary structure of VanA contained the D-Ala-D-X ligase fold similar to the currently existing enzymes, including VanA from Vancomycin resistant *Enterococcus faecium.* There have also been reports of finding antibiotic resistance among bacteria in extreme environments like deep terrestrial subsurface and deep oceans. Since one of the critical factors in this kind of research is ensuring the absence of anthropogenic sources of antibiotics, studies were also conducted in isolated places such as Lechuguilla Cave in Mexico, which has been isolated for more than 4 million years and provides the perfect ecosystem to study the evolution of resistance genes. In this study 93 bacterial strains were tested for antimicrobial susceptibility, of the strains 70% were resistant to 3-4 different antibiotics, while 3 strains were resistant to 14 antibiotics (Bhullar *et al*., 2012). All these studies support the hypothesis that antibiotic resistance is an ancient and natural phenomenon and it is not a mere result of antibiotic introduction.

Bacterial resistance to antimicrobial agents can be manifested in several ways. The first way is that it can be innate or intrinsic, where species or genera of bacteria are inherently resistant to a particular class of antibiotics. For example, *Pseudomonas aeruginosa* exhibits low antibiotic susceptibility due to reduced permeability of its outer

membrane, in addition to the intrinsic presence of β-lactamase in the periplasm which inactivates β-lactams (Cox and Wright, 2013). Another element of intrinsic resistance is efflux pumps. In *E. coli* the AcrAB-TolC RND efflux system plays an important role in its resistance to a broad range of antibiotics such as tetracyclines, fluoroquinolones, ß-lactams and the macrolides. Bacteria can also acquire genes for a metabolic pathway that produces altered bacterial cell walls that do not contain the binding site for the antibiotic (Tenover, 2006). Mutations can also cause the bacterium to develop resistance by altering the target protein to which the antimicrobial agent binds to, as in the case of penicillin – binding protein (e.g., change in penicillin-binding protein 2b in pneumococci), through production of enzymes that inactivate the antibiotic such as the erythromycin ribosomal methylase in staphylococci, or by up-regulating pumps that expel the antibiotic from the bacterial cell (e.g., efflux of fluoroquinolones in *S.aureus*) (Livermore, 2003).While the previous means of acquiring resistance were through chromosomal mutations and selection, bacteria can also develop resistance through horizontal gene transfer, which is essentially exchanging with other bacteria the genetic elements that encode resistance (Tenover, 2006) (Figure 1.2). This can occur through conjugation, during which Gram negative bacteria (and some Gram positive bacteria) transfer a resistance plasmid via pili and Gram positive bacteria exchange DNA by producing pheromones that facilitate the clumping of the donor and recipient bacterium (Tenover, 2006). In transduction, the resistance plasmid or transposable element is transferred from one bacterium to another by a phage; while transformation allows the bacteria to acquire resistance by uptake and incorporation of naked DNA into the bacterial genome (Davies and Davies, 2010).

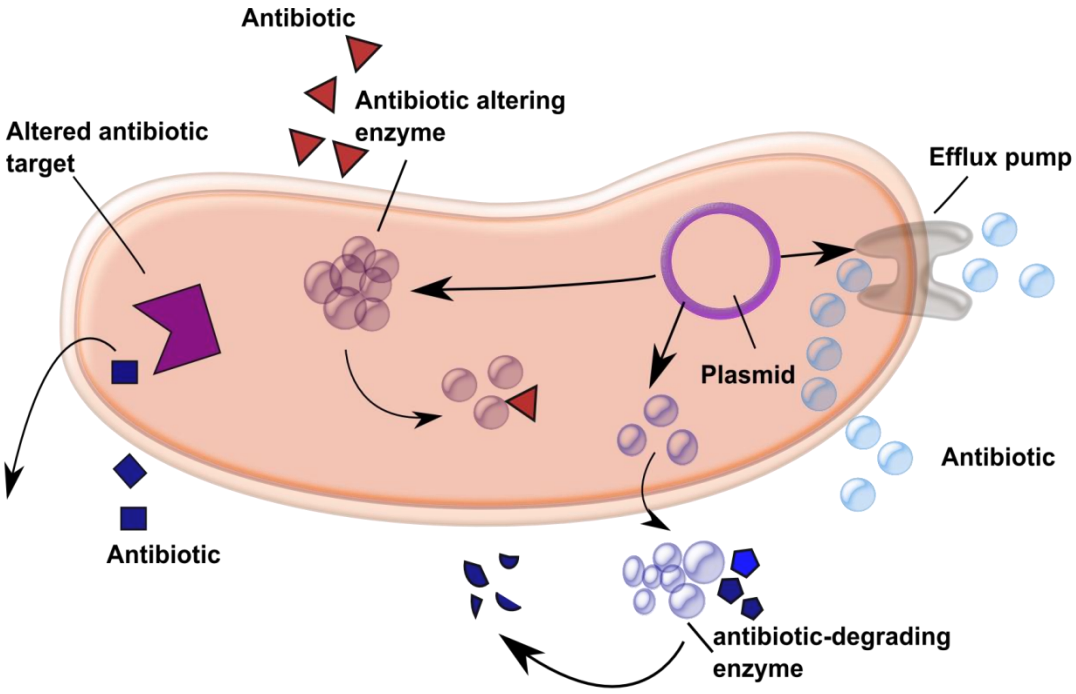

Figure 1.2 Mechanisms of antibiotic resistance. Bacteria can avoid antibiotic effects by: altering the antibiotic's target through mutation, the presence of efflux pumps, production of inactivating enzymes that interfere with the function of the antimicrobial agent.

1.1.3 Implication of antibiotic resistance

Antibiotics could be considered one of the greatest discoveries of the 20th century, however there is a threat of transition to a post antibiotic era, where increasing levels of antibiotic resistance may make a simple bacterial infection life threatening. When penicillin became available in 1940, almost all *Staphylococcus aureus* strains were susceptible to its antimicrobial effect, but shortly thereafter, *S. aureus* became capable of resisting penicillin by destroying it with β-lactamases (Neu, 1992). Today 95% of *S. aureus* worldwide is resistant to penicillin. Methicillin was introduced in 1959, but it was not long before resistance cases started to appear in several countries, The United Kingdom, Poland and Denmark at first and then it spread to the United States by the early

1980s. Methicillin Resistant *S. aureus* (MRSA) was resistant to all the main classes of antibiotics that were in circulation at that time, β-lactams, erythromycin, fusidic acid, streptomycin and tetracycline (Howden *et al*., 2010).

Now that MRSA has become a source of major concern, clinicians turned to vancomycin which was released in 1958 and was the only agent that is used successfully to treat MRSA (Howden *et al*., 2010). Unsurprisingly, the increased use of vancomycin has not only selected resistance against vancomycin in MRSA but also in *Enterococci faecium*, 61% of which are now resistant to vancomycin. As MRSA continued to pose a serious threat, the scientific community was again under pressure to come up with a new molecule in order to tackle the resistance problem. In the mid-1980s fluoroquinilones provided a solution, and initially they were able to inhibit MRSA growth at <2µg/ml (Howden *et al*., 2010). Today MRSA resistance to ciprofloxacin, a synthetic version of nalidixic acid, is greater than 80% and less than 20% of MRSA isolates are actually eradicated by the currently available antimicrobial agents (Neu, 1992, Fair and Tor, 2014).

Mupirocin was first introduced into clinical practice in the UK in 1985. It showed high efficacy against MRSA by targeting bacterial protein synthesis. However, within a short period of its introduction high levels of mupirocin resistance in *S. aureus* started to appear, especially in patients who had received long-term mupirocin treatment (Hardy *et al*., 2004). All the previously mentioned examples demonstrate the capability of bacteria to quickly develop resistance against virtually any antibiotic class, which makes it critical to find new antimicrobial classes to combat bacterial resistance. Despite this urgent need, there has been a lack of novel antimicrobial agents discovered. The number of newly approved antibiotics from 1998 – 2002 was 56% lower than in the period from 1983- 1987 (Figure 1.3). Since 2002, eight antibiotics have been approved, only two of which had a new mode of action: anidulafungin and linezolid (Spellberg *et al*., 2004). Another issue

with the development of new antibiotics is the lack of diversity. Approximately half of all antibiotics target the cell wall and although studies have recently started to identify novel molecular targets, their activity is usually insufficient to be carried into production stage without further modification (Projan, 2003; Fair and Tor, 2014).

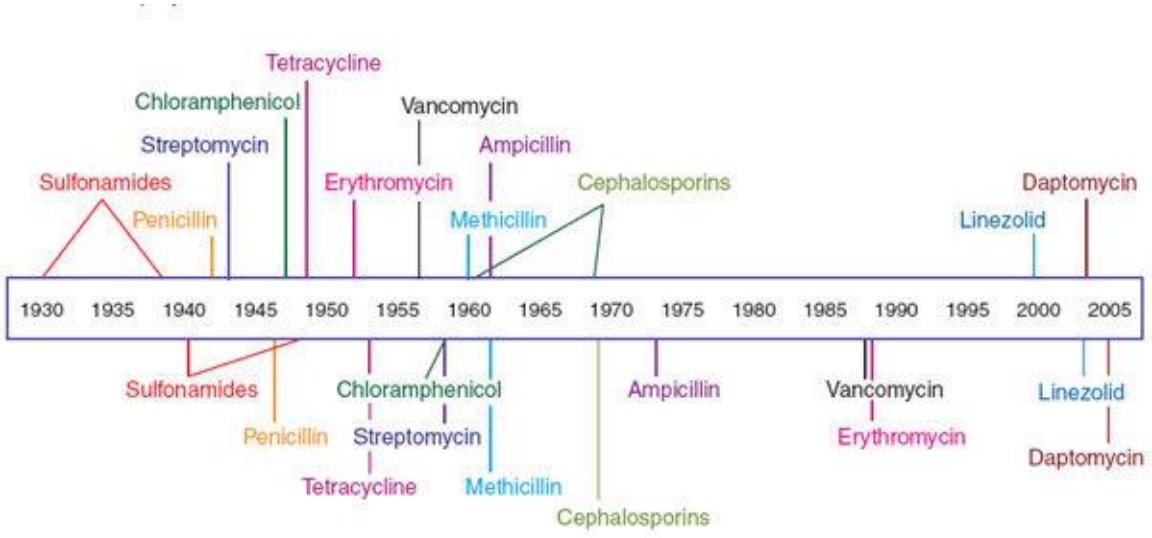

Figure 1.3 Antibiotics introduced into clinical practice. Antibiotics above the timeline indicate the year they were introduced in, while the antibiotics below the timeline show the year resistance was observed reproduced from (Clatworthy *et al*., 2007)

Another impact of the increase of antimicrobial resistance is the rise of "superbugs". These microbes not only have reduced therapeutic options available due to their multiple drug resistance (MDR), but they also have an economic impact as the period of hospital care is extended (Davies and Davies, 2010). In 2006, the term extensively drug resistant TB (XDR TB) was used to define TB strains with resistance to isoniazid and rifampicin, in addition to all the fluoroquinolones and at least one of the injectable tuberculosis drugs (Amaral *et al*., 2009). In 2007, Italy was the first country to report total drug resistant TB (TDR-TB), followed by 15 TDR TB cases in Iran in 2009 (Udwadia,

2012). According to the WHO 2 million people will develop MDR TB by 2015, and in most of the cases 50% of these infections will be XDR TB (Mishra *et al*., 2014).

Today 60% of hospital acquired infections are caused by MRSA (CDC, 2015), accounting for an estimated one million extra days of hospitalization in the EU alone, costing approximately $570 million. The infections caused by community acquired MRSA has reached the endemic stage in many European countries, US and parts of Asia, in addition to being the most frequent cause for emergency room visits in the United States (Chatterjee and Otto, 2013).

Enterococcus resistance is endemic in North America, while it is on the rise in Europe. Enterococcus species have been considered the second most common cause of wound and urinary tract infections, with 12% of the nosocomial infections in the USA being caused by *E. faecalis* (Arias and Murray, 2012). Recent studies showed that 60% of *E. faecium* is resistant to vancomycin, which are currently treated with either linezolid, to which resistance does occur but rarely, or daptomycin that until recently had a promising potential in circumventing vancomycin resistant *E. faecium* (VRE). However, clinical isolates of *E. faecium* showed that resistance can still arise by spontaneous mutations in the gene *liaF* and a second gene responsible for membrane phospholipid metabolism. This observation was also confirmed by comparative analysis which revealed that daptomycin is less effective in depolarizing the cell membrane in the resistant strains due to the alterations in the cell wall ultrastructure and cell membrane (Arias and Murray, 2012). MDR *P. aeruginosa* is also increasing worldwide with limited treatment options, as β-lactams, fluoroquinolones and aminoglycosides are no longer effective. Colistin was found to be active against *P. aeruginosa* with new reports suggesting that using it in combination with rifampin proved active *in vitro*. However, patients need to monitored to check for any toxicities associated with this agent (Obritsch *et al*., 2005).

Another concern is the NDM-1 (New Delhi metallo – beta lactamase 1), an enzyme which encodes resistance to β-lactams antibiotics, generally found on a plasmid that harbours many other resistance genes, which makes it resistant to a wide range of antimicrobial agents with the exception of colistin. Worryingly, it is found on a transmissible genetic element which means the resistance can easily disseminate to other bacterial strains. Given previous spread of resistant strains, we can already predict that NDM-1 is close to being a serious health threat and can turn any strain that contains it into a super bug (Moellering, 2010).

Despite the increasing resistance problems, international efforts to control the crisis have not been particularly successful, because of a lack of coordination and a little novel antibiotic development due to the lack of investment by pharmaceutical companies (Carlet *et al*., 2012). Without significant big pharmaceutical company contribution, most of the actual research in this regard is actually carried out in academic centres and small biotechnology companies.

As of September 2014, seven new antibiotics reached phase three, in addition two compounds are currently being reviewed by the FDA, which have the potential to be used against Gram negative bacilli (Hay *et al*., 2014). The fact that 75% of currently used antibiotic scaffolds are based on natural products tells us a great deal about the potential of complex environments to yield organisms with antimicrobial activities (Taylor, 2013). Enacyloxins were originally identified in *Frateuria* sp in 1982 (Watanabe *et al*., 1982), but they were recently back in the spot light when it was discovered that they can be also produced by *Burkholderia ambifaria.* The importance of this finding is not limited to the new producer, but also to the newly elucidated biosynthetic pathway, a hybrid of non-ribosomal peptide synthase and polyketide synthase. This concept of hybrid biosynthetic

pathways could open the door for more modifications and pathway engineering in order to produce a novel, more effective version of enacyloxins (Pidot *et al*., 2014).

Janthinocin A, B and C have been in use since the 1990s to treat infections by Gram positive bacteria including MRSA. Researchers are now trying to isolate an antifungal compound from the producer organism *Janthinobacterium lividum*, a known cause for soft rot. *J. lividum* is thought to produce the active antifungal compound only when in contact with the host plant. This research certainly highlights the importance of extending our antibiotic hunt to even virulent organisms and benefit from their toxins in human therapeutics (Pidot *et al*., 2014).

Predatory bacteria are also becoming an interesting alternative to antibiotics. Organisms like *Bdellovibrio bacteriovorus* are obligate predators of Gram–negative bacteria for energy and nutrients. The *Bdellovibrio* genome contains several hydrolases essential for prey digestion and more importantly for attacking bacterial biofilms (Allen *et al*., 2014). Screening of previously approved drugs can also be a useful approach to appease this urgent need for new antibiotics, as their known pharmacology and toxicology profiles will reduce the cost of developing an entirely new drug by almost 40%. This was demonstrated by the Wright group, where 30,000 compounds were screened from the Canadian compounds collection. Four compounds were identified and showed synergism with novobiocin against *E. coli*. Furthermore, these four compounds were found to affect the cell shape and bacterial membrane permeability, which provides a physical base for this synergy (Worthington and Melander, 2013). CRISPR (clustered regularly interspaced short palindromic repeats) have recently emerged as tools with a strong potential to target and destroy bacterial pathogens in a way that compensate for the drawbacks of most of the currently known antibiotics. CRISPR are used to create sequence–specific antimicrobials

that can be aimed exclusively towards resistant bacteria, unlike the traditional antibiotics which kill off both pathogenic and beneficial bacteria (Kahrstrom, 2014).

Many international organizations have joined forces to develop a strategy for combating antibiotic resistance. The European commission released a list of key actions to successfully fight antibiotic resistance. WHO issued a series of recommendations in 2001(WHO global strategy for containment of antimicrobial resistance), which was a culmination of expert workshops, consensus meetings and consultative groups to evaluate the situation (WHO, 2001). The American government put together a national strategy to control antibiotic resistance in collaboration with partners in healthcare public health, academic, industrial and federal research. In 2009, the EU-US summit agreed on establishing TATFAR (transatlantic task force on urgent antimicrobial resistance) with the objectives of promoting appropriate use of antibiotics, and increasing the US and the EU's mutual understanding relevant to the antibiotic problem, which includes exchange of information, coordination and cooperation (Antibiotic Action, 2011). Some developing countries are also contributing to the worldwide effort, through GARP (Global Antibiotic Resistance Partnership) which currently works in four countries: India, South Africa, Kenya and Vietnam intially. These policies and guidelines collectively led to a number of recommendations which can be summarized below:

- Optimizing prescribing practice and promoting appropriate use of antibiotics
- Improving infection prevention methods
- Encouraging and reinforcing research to develop new and effective antibiotics
- Providing better access to surveillance data
- Strengthening international collaboration

- Developing quick tests to be used in health care centres for distinguishing between a viral and a bacterial infection, and consequently the need for using antibiotics (CDC, 2014; Leung *et al*., 2011; Gottlieb and Nimmo, 2011)

1.2 Polyketides

Polyketides are an important class of natural products, with both diverse structures (Figure 1.4) and clinical functions, including antibiotics like erythromycin and tetracycline, anticancer drugs and immune-suppressants (Abe, Simpson, 1987, Zheng and Keatinge-Clay, 2012). Polyketides are synthesized by bacteria, fungi and some plants.

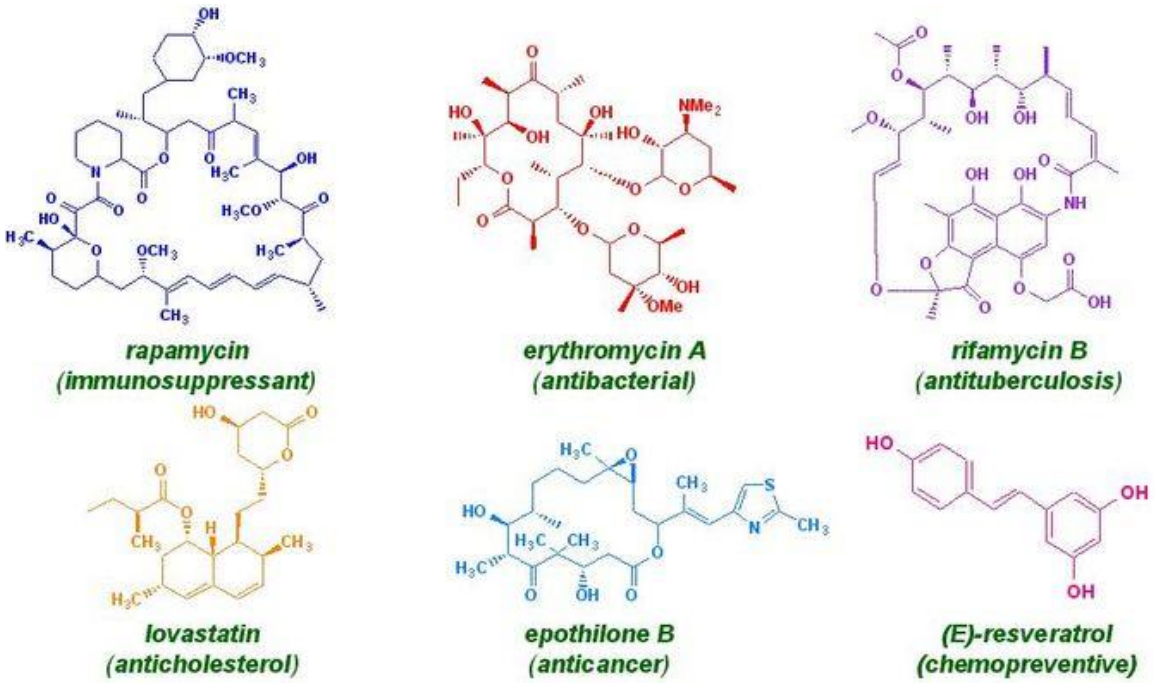

Figure 1.4 Examples of different polyketides.

Polyketides are produced *in vivo* by polyketide synthase enzymes (PKS). Three types of PKS have been identified so far, type I, type II that contain a single set of iteratively acting enzymes and type III. A characteristic feature of type I PKSs is the presence of multiple active sites within each polypeptide. In the iterative type I PKS a single multienzyme is used repeatedly for multiple condensation reactions. Whereas, the modular type I PKS incorporates a set of enzymatic domains for each catalytic cycle. They contain multifunctional polypeptide units grouped into modules, each module consists of at least three domains β-ketosynthase (KS), acyltransferase (AT) and acyl carrier protein (ACP), with the exception of trans-AT systems. Some modules also contain β-keto-processing domains, β-ketoreductase (KR), dehydratase (DH) and enoylreductase (ER). A thioesterase (TE) is often found at the end of the last module and it is responsible for releasing the product from the enzyme. Examples of polyketides produced by this type of synthase are erythromycin, rapamycin and avermectin (Hopwood, 1997, Hopwood and Sherman, 1990). Type II PKSs are multi-enzyme systems with each catalytic activity located on a separate protein subunit (McDaniel *et al*., 1995). Type III PKS systems differ from the previous two by having a single protein system that does not contain a domain or modular structure. Also type III PKS does not involve a carrier protein but instead it uses acyl-CoA as a substrate (Hertweck, 2009).

Polyketides have attracted much interest recently, especially in the metabolic engineering field due to their flexibility in substrate selectivity which results in the difference of reduction levels of the β-keto groups, the length of the polyketide chain and the degree of post-PKS modification, which all together allow the formation of a diverse product spectrum and make PKSs a very promising area for drug discovery (Piel, 2010) (Gao *et al*., 2010).

1.2.1 Fatty acids

Fatty acid biosynthesis is closely related to polyketide synthesis and is an important process in all living organisms. Many of the vital functions in bacteria depend on fatty acid synthase (FAS) pathways, including membrane biosynthesis and quorum sensing. As shown in (Figure 1.5), the fatty acid synthesis system can be divided into two groups, FAS type I and FAS type II. Whilst type II express all the proteins as individual polypetides from separate genes, FAS type I expresses large multi-enzyme complexes that carry all the necessary proteins for fatty acid synthesis on one or two polypetide chains. Mammalian (FAS II) consists of two identical polypeptide chains, each containing all the required domains for the biosynthesis process, including: β-ketoacyl synthase, malonyl acetyl transferase, dehydratase, enoyl reductase, β-ketoacyl reductase, ACP and thioesterase. The first step in the biosynthesis process is a condensation reaction between a malonyl group derived from malonyl-CoA, and an acetyl group from acetyl-CoA. This process results in the formation of a β-ketoacyl derivative which is then reduced in three steps: β-ketoacyl reduction, β-ketohydroxyacyl dehydration and finally enoyl reduction. The resulting saturated acyl derivative acts as a primer for further elongation and reduction cycles to yield a palmitoyl derivative, which is then hydrolysed by thioesterase and palmitate is released (Menendez *et al*., 2009).

In *E. coli* fatty acid biosynthesis falls into the FAS type II category. The growing chain is dependent on two coenzymes, coenzyme A and an ACP, which are responsible for supplying precursors for the condensation reaction (Campbell and Cronan, 2001, Magnuson *et al*., 1993). The starter unit (acyl) is attached to the cysteine thiol of the ketosynthase (KS), while the extender unit (malonyl) is attached to the phosphopantetheine thiol residue of the acyl carrier protein, ACP. The chain extends into a β-ketoester, which is reduced by ketoreductase (KR), dehydrated by a dehydratase (DH) and then a final

reduction by the enoyl reductase (ER). The extended chain is then transferred back to the KS to go through another cycle of successive steps, which is repeated until the chain reaches its designated length. The full length chain is finally passed to the thioesterase (TE), where it is released as a free acid or an acyl ester (Staunton and Weissman, 2001).

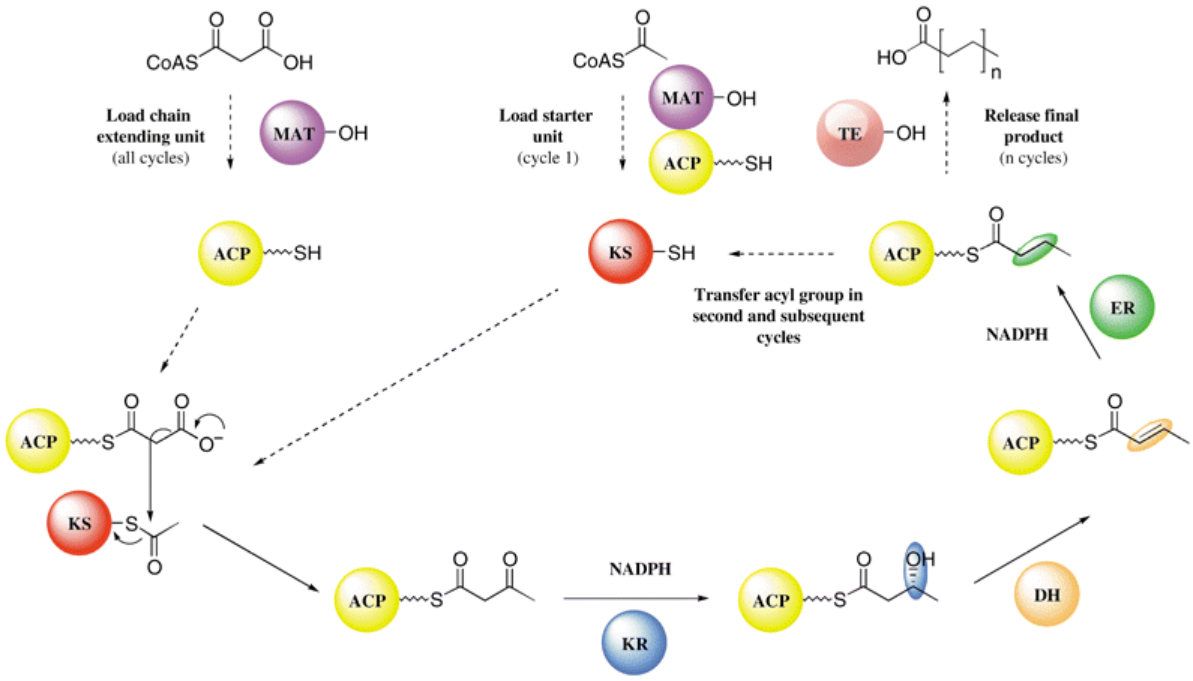

Figure 1.5. Fatty acid biosynthesis. Contrary to polyketide biosynthesis, the resulting β-ketoacyl is always completely reduced. MAT, malonyl-CoA-ACP transferase; AT, acyltransferase; ACP, acyl carrier protein; KS, ketosynthase; KR, Ketoreductase; DH, Dehydratase; ER, enoyl reductase. Reproduced from Staunton and Weissman (2001).

1.2.2 Type I polyketide synthases

Type I PKSs are large multifunctional enzymes usually > 300 KDa, arranged into modules each of which contain a set of domains responsible for catalysing one condensation reaction (Dittmann *et al.*, 2001). A type I PKS module needs at least three

enzymes to be functional: an acyl transferase (AT), an acyl carrier protein (ACP) and a ketosynthase (KS) (Cheng *et al*., 2009). Modules may also contain ketoreductase (KR), dehydratase (DH) or enoylreductase (ER), which are optional domains that give polyketides their structural diversity (Piel, 2010). Most of the types I PKSs have a thioesterase (TE) domain which is responsible for "off-loading" the resulting polyketide. Modular PKSs use every catalytic site once during a cycle, and usually in such systems the number of modules is an indication of the number of elongation and reduction cycles which makes it easy to predict the resulting polyketide structure (He and Hertweck, 2005). However, some polyketides are an exception to this co-linearity like the aureothin biosynthesis pathway where only four modules are required to catalyze five rounds of Claisen condensation (Busch and Hertweck, 2009). Polyketide biosynthetic pathways that breach this co-linearity include many other compounds, like borrelidin gene cluster which uses a single elongation module three times, or lankacidin in which iterative use of some of the modules is observed (August *et al*., 1998, He and Hertweck, 2005). Iterative pathways among PKSs are more common than we think, but the basis on which this iterative or non-iterative behaviour occurs is still a mystery to be solved.

1.2.2.1 Erythromycin biosynthesis pathway

The search for the erythromycin gene cluster progressed after Thompson *et al.*, (1982) discovered a clone derived from *Saccharopolyspora erythraea* that conferred erythromycin resistance to *Streptomyces lividans* implying that the clone contains *ermE* (the erythromycin resistance gene). This finding was then followed by (Tuan *et al*., 1990) who paved the way to identify the erythromycin gene cluster by sequencing upstream and downstream of *ermE* (Rawlings, 2001). Three genes, *eryAI*, *eryAII* and *eryAIII*, are large opening reading frames in the erythromycin biosynthetic pathway coding for three large

multifunctional proteins DEBS1, DEBS2 and DEBS3 respectively (Figure 1.6) (Staunton and Wilkinson, 1997; Weissman and Leadlay, 2005). Similar to other type I PKS systems, each module contains the essential three domains: ketosynthase (KS) that catalyses the decarboxylative condensation of the methylmalony–ACP building block with the starter unit or polyketide chain provided by the previous PKS module, acyl transferase (AT) that is responsible for loading the extender unit onto the phosphopantetheine arm of the ACP domain, and acyl carrier protein (ACP) that holds the growing polyketide chain and delivers the resulting polyketide chain to the KS domain in the next module (Cane, 2010). Optional domains are also present in the pathway and they perform reductive modification to the growing chain before the next round of chain elongation.

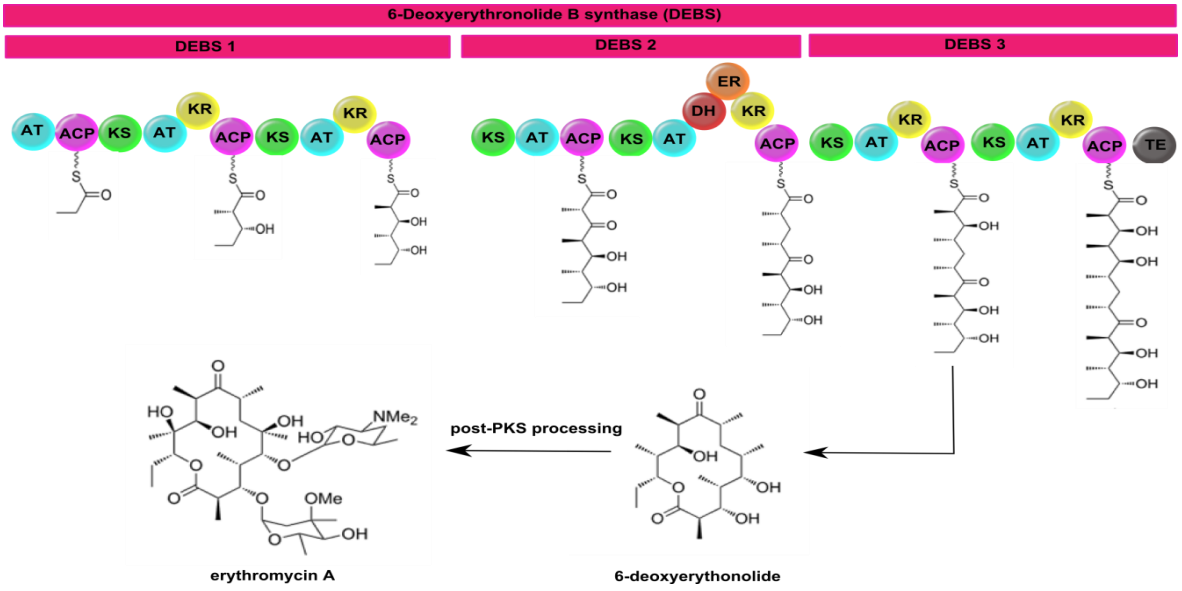

Figure 1.6 Erythromycin biosynthesis pathway. DEBS is the best studied PKS, it catalyses the key steps to erythromycin biosynthesis. The biosynthetic pathway involves six Claisen condensations and several reduction steps in order to release erythromycin A through a terminal esterase. Domains are acyltransferase (AT), acyl carrier protein (ACP), ketosynthase (KS), ketoreductase (KR), dehydratase (DH), enoyl reductase (ER), and thioesterase (TE) (Staunton and Wilkinson, 1997; Weissman and Leadlay, 2005).

The starter unit (propionate) is loaded by the AT and ACP which are linked together. Although *in vivo* the loading domain is able to accept only acetate or propionate,

in vitro studies showed that a variety of starter units can be accepted like butanoate and 2-methylpropanoate. Apart from module 3, all the other modules have reductive domains. Modules 1, 2, 5 and 6 all have a KR which catalyses reduction of keto group to a hydroxyl group, while module 4 contains all the reductive domains (KR, DH and ER) to produce a fully reduced alkane (Staunton and Weissman, 2001). The fully formed compound is released by the TE domain which catalyses the lactonization of the complete polyketide chain.

1.2.3 Type II polyketide synthases

Type II PKSs, found in bacteria and plants, assemble an iterative multienzyme complex by encoding distinct proteins (Lal *et al*., 2000; Moore and Hopke, 2001; Chopra *et al*., 2008). KS_{α}, KS_{β} (chain length factor) and ACP are the minimal set of modules needed to produce a basic polyketide backbone in the type II PKS. However, additional enzymes are required to fold and cyclise the polyketide chain into a polycyclic structure; these enzymes include cyclases and their equivalent aromatases (Staunton and Weissman, 2001). Additional tailoring of the polyketide chain is performed by oxygenase, glycosyl and methyl transferases. The chain assembly starts with the KS_{α} and KS_{β} (CLF) forming a heterodimer (Hertweck *et al*., 2007). The length of the resulting polyketide chain is determined by KS_{β} (CLF). According to Khosla and co-workers, the region responsible for the chain length is located at the interface of the dimer with certain residues in that region acting as gatekeepers in the polyketide tunnel, and so reducing the size of these residues elongates the channel, allowing two more elongation cycles (Seow *et al*., 1997). Unlike the tight association between KS_{α} and KS_{β} (CLF), the interaction between KS_{α} and ACP is specific but weak enough to give multiple exchanges of KSα-ACP during the biosynthetic process. Following the formation of each successive C-C bond, the growing chain is transferred back from the ACP to the KS before the protein detaches (Das and Khosla,

2009). Further enzymes are needed to convert the basic polyketide chain into a polycyclic aromatic product. These enzymes can be categorized as auxiliary PKS enzymes which recognize ACP bound substrates and tailoring enzymes. Once the chain reaches its full length, the ACP dissociates from the polyketide chain attached to it, by hydrolysis or cyclisation or by the activity of auxiliary PKS functions like KR, ARO/CYC. Tailoring enzymes then transform the polyketide chain into a fully decorated natural product as in the case of actinorhodin (Figure 1.7) (Das and Khosla, 2009, Hertweck *et al*., 2007).

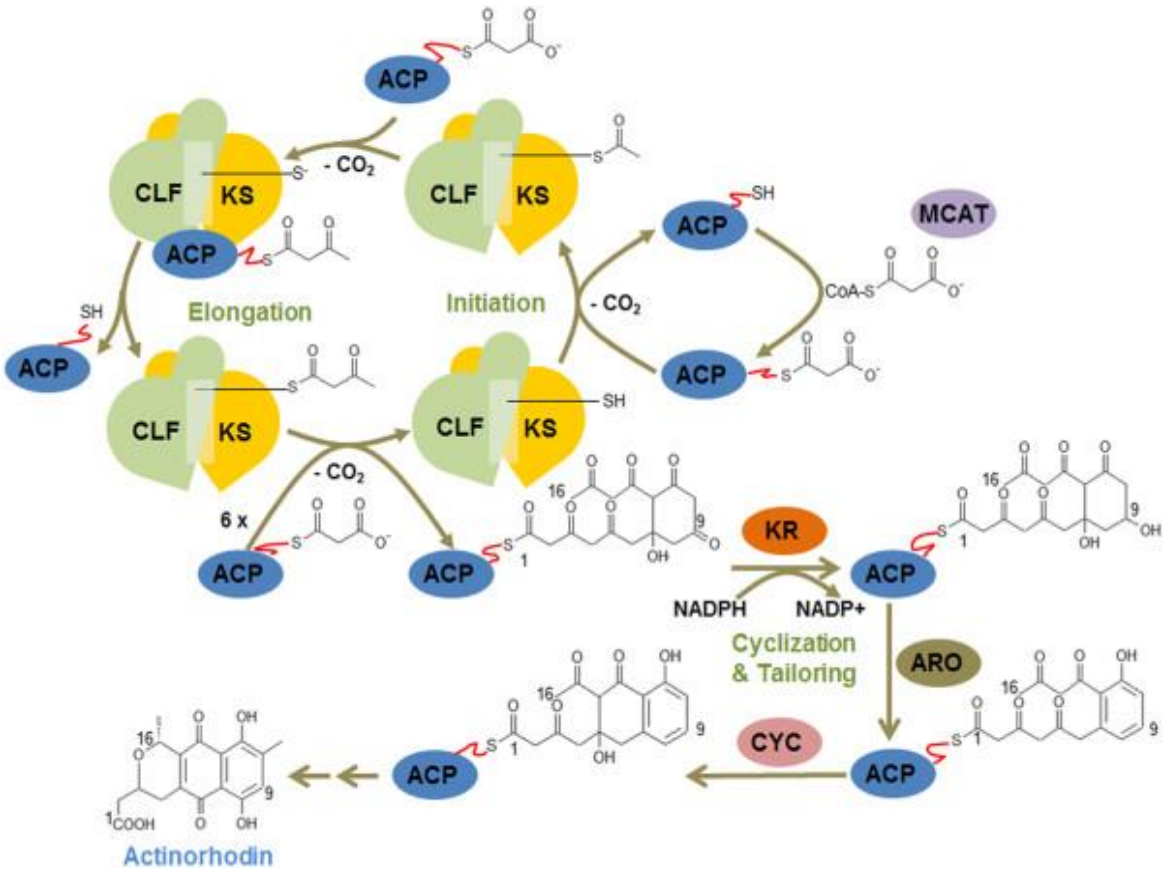

Figure 1.7 Biosynthesis by a PKSII system. KS and CLF domains have the function of catalysing chain initiation and elongation with malonyl as a building block. The resulting poly-β-keto intermediate is then modified by tailoring enzymes such as KR, CYC and ARO into actinorhodin. Reproduced from (Staunton and Weissman, 2001).

1.2.4 Type III polyketide synthases

Type III PKSs are homodimers, and the active site in each monomer catalyses iteratively the priming, extension and cyclization reactions to produce the final polyketide molecule. Until recently type III PKSs were thought to be specific to plants, and it was only in 1999 when the first bacterial type III PKS RppA was discovered amongst other putative compounds (Hashimoto *et al*., 2014, Agnes and Scott, 2007). To date five groups of bacterial type III PKSs are recognised based on the structure of the resulting molecule. RppA from *Streptomyces griseus*, is responsible for catalyzing production of 1,3,6,8-tetrahydroxynaphthalene. The others are: Ph1D from *Pseudomonas fluorescens* which is known for its broad substrate specificity, DpgA from *Amycolatopsis orientalis* which only uses malonyl-CoA as a substrate to synthesise 3,5-dihydroxyphenylacetyl-CoA, ArsB from *Azotobacter vinelandii*, and SrsA from *S. griseus* which catalyze the formation of alkylresorcinols (Yu *et al*., 2012). The interesting feature about the latter group of PKS type III systems is that the *ars* operon contains two genes which encode a putative type I FAS: ArsA and ArsD. These enzymes synthesize a fatty acid chain that is directly transferred onto the active site cysteine of ArsB, thus enabling ArsB to utilize the fatty acid from acyl-ArcAs as the starter substrate, followed by three rounds of condensation with the extender unit malonyl–CoA, to finally produce alkylresorcinols. Two different extender units, methylmalonyl-CoA and malonyl-CoA, are used by SrsA to eventually synthesise alkylresorcinols in a similar manner to ArsB. The final group of type III PKSs includes alkylpyrone synthases like ArsC from *A. vinelandii* and germicidin synthase Gcs from *S. coelicolor*. They are unusual in that they utilize unnatural acyl-CoAs and ACP linked acyl-CoAs as starter units (Chemler *et al*., 2012, Nakano *et al*., 2009, Yu *et al*., 2012). Type III PKSs are also present in fungi, with some promise in terms of discovering

new biosynthetic pathways, and the creation of novel unnatural/natural products (Hashimoto *et al*., 2014).

1.3 Mupirocin

Pseudomonas is a diverse genus of Gamma proteobacteria which can be found in wide range of environments including soil, water, plant surfaces and animals. They are well known for their capacity to utilize a variety of organic compounds as energy sources, their medical and agricultural importance, their resistance to many antimicrobial compounds, and also for their remarkable metabolic capacity. *Pseudomonas* spp. produce a large array of natural products that have a wide range of biological activities. Studying the structure and the biosynthetic pathway of these metabolites led to the discovery of many novel antimicrobial compounds and new biosynthetic mechanisms (Gross and Loper, 2009). Of particular interest is *Pseudomonas fluorescens*, more than 100 years ago Baader and Garre (1887) first noticed its antimicrobial activity when grown on gelatine. This antibacterial compound was able to inhibit the growth of *Staphylococcus aureus*, *Salmonella typhi*, and *Bacteroides friedlanderi* in addition to yeasts (Lewis, 1929, Pappa, 1990). An interesting observation was made by I. M. Lewis when he noticed that spore forming bacteria and micrococci were sensitive to the substance produced by *P. fluorescens*, in contrast to Gram negative and Gram positive bacilli which showed some resistance. In the 1960s Fuller and co-workers were able to make some progress in optimizing the growth conditions and culture media appropriate for the *P. fluorescens* growth. This yielded sufficient amounts of the antibiotic for further studies (Pappa, 1990, Fuller *et al*., 1971). Later on Chain and co-workers discovered that the antimicrobial activity exhibited by *P. fluorescens* is all due to pseudomonic acid, which was further characterized and divided into four groups of metabolites collectively named mupirocin. The four types are pseudomonic acid A, B, C and D, where pseudomonic acid A is the

major metabolite which accounts for 90% of mupirocin (Figure 1.8) (Sutherland *et al*., 1985, Chain and Mellows, 1977).

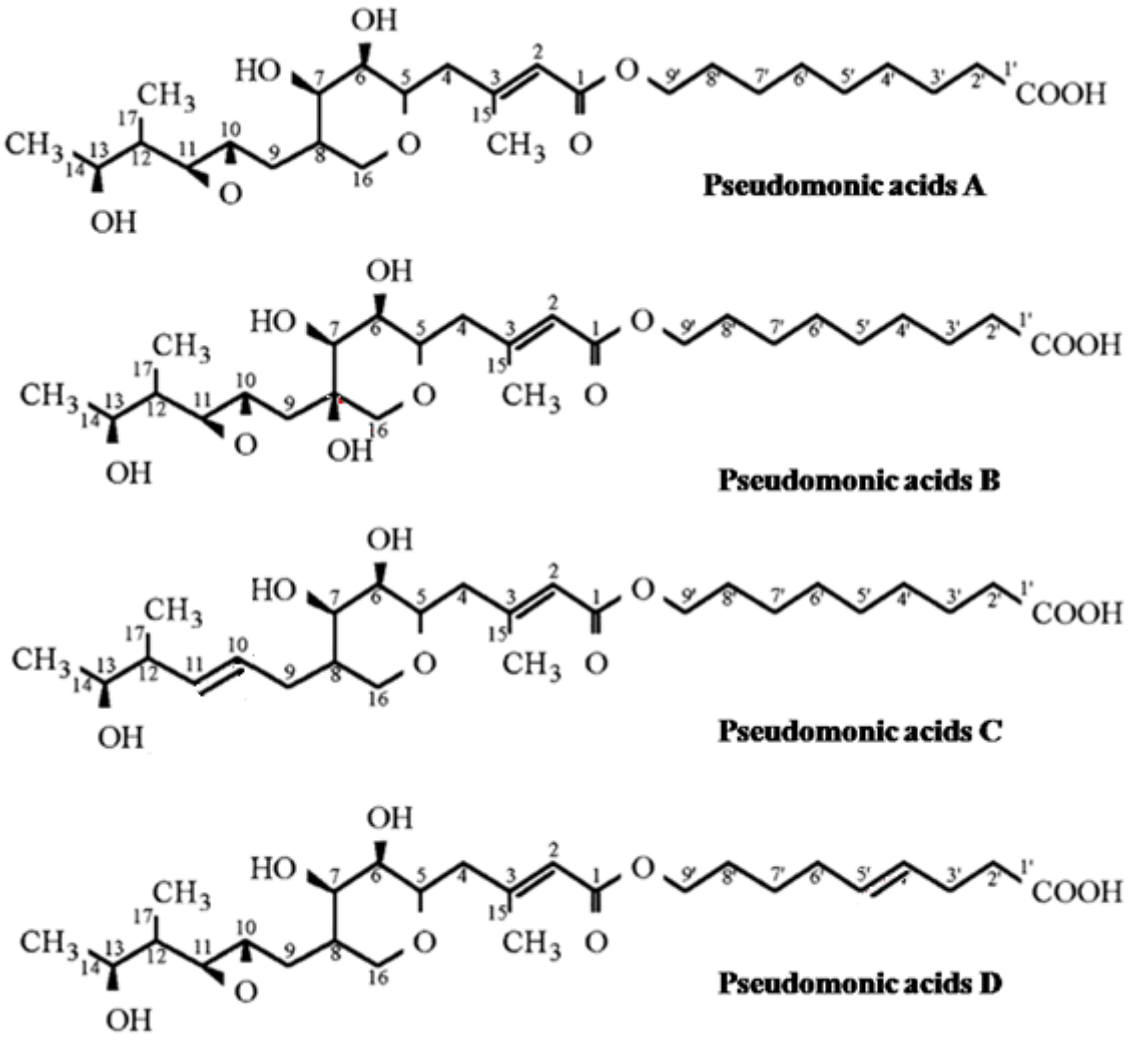

Figure 1.8 Mupirocin chemical structures. Mupirocin is a mixture of pseudomonic acids: pseudomonic acid A (90%), pseudomonic acid B (8%) has an extra hydroxyl group at C8, pseudomonic acid C (<2%) has a double bond in the position C10 to C11, and pseudomonoc acid D (<2%) contains an unsaturated fatty acid chain at C4' and C5'.

1.3.1 The mupirocin biosynthetic cluster

The mupirocin biosynthesis cluster is approximately 74 kb in size and encodes 35 ORFs. The cluster contains six multifunctional genes (*mmpA,B,C,D,E* and *F*) and various genes with individual functions, two of which are located in the first 40.5 kb of the cluster (*mupA* and *mupB*) (Figure 1.9). Some of the individual genes like *mupB*, *mupD*, *mupG* and *mupS* show similarity to type II PKSs, which suggests that, the *mup* cluster is a combination of both Type I and Type II PKSs, (Figure 1.9) (El-Sayed *et al*., 2003). The first four elongation modules for the monic acid backbone are encoded by *mmpD*, and the last two encoded by *mmpA*. These type I PKSs consist of KS, ACP, KR, DH and MT domains. The only two AT domains in the pathway are encoded by *mmpC*, which also encodes a putative ER. A type I iterative PKS with KS, KR, DH and triple ACP domains is encoded by *mmpB*, and is thought responsible for synthesis of 9HN moiety. The *mmpB* gene is proposed to encode the only TE in the system, which implies that it facilitates the final steps of the pathway and the release of the final product (Thomas *et al*., 2010).

Despite its similarity to type I PKSs, the *mup* cluster possesses some features that do not follow the typical modular pattern. As is the case in many PKS systems, loading modules are specifically designed to accept the starter unit in order to initiate the metabolic process. However, the *mup* cluster lacks an obvious loading module. So far the proposed theory on how such systems work includes a malonate residue, which is loaded to the first KS domain and then decarboxylated to provide acetate as a starter unit (El-Sayed *et al*., 2003, Thomas *et al*., 2010). AT domains in the *mup* cluster belong to a growing family of PKSs called the *trans* AT PKSs. This terminology refers to the AT domains are encoded by a separate gene in the pathway, as opposed to *cis* AT pathways, where the AT domain is present in each and every module. Despite being common amongst other *trans* AT

PKSs, the reason behind the unusual domain architecture seen in both MmpA and MmpB, which contain a tandem doublet and triplet ACPs respectively is still not fully understood. However, the fact that they are more closely related to each other than any other ACP in the cluster, suggests that they might be a result of a gene duplication event (Gurney and Thomas, 2011, Rahman *et al*., 2005)

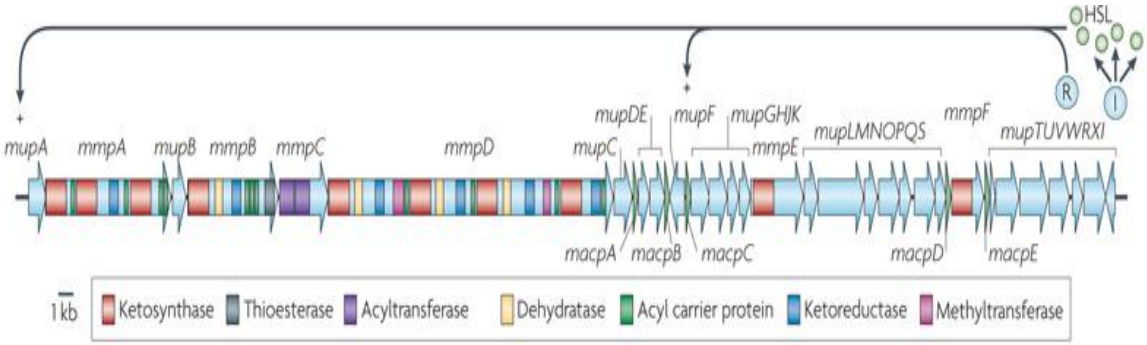

Figure 1.9 Organisation of mupirocin biosynthesis cluster. The *mup* cluster is localised to a 74 kb region of the *P. fluorescens* chromosome. Genes are shown as blue arrows; domains are coloured as indicated (El-Sayed *et al*., 2003, Thomas *et al*., 2010).

Table 1.1 Deduced functions of *mup* genes (El-Sayed *et al*., 2003, Thomas *et al*., 2010).

ORF	Deduced Function
mupA	Reduced flavin mononucleotide ($FMNH_2$) oxygenase
mmpA	Polyketide synthase (ketosynthase, acyl carrier protein and ketoreductase)
mupB	3-Oxo-acyl carrier protein synthase
mmpB	Polyketide synthase (ketosynthase, dehydratase, ketoreductase, acyl carrier protein and thioesterase)
mmpC	Acyltransferase and enoyl reductase
mmpD	Polyketide synthase (ketosynthase, dehydratase, ketoreductase, methyltransferase and acyl carrier protein)

mupC	Dienoyl CoA reductase
macpA	Acyl carrier protein
mupD	3-Oxo-acyl carrier protein reductase
mupE	Enoyl reductase
macpB	Acyl carrier protein
mupF	Ketoreductase
macpC	Acyl carrier protein
mupG	3-Oxo-acyl carrier protein synthase
mupH	β-hydroxyl-β-methyl glutarate CoA synthase
mupJ	Enoyl CoA hydratase
mupK	Enoyl CoA hydratase
mmpE	Polyketide synthase (ketosynthase and hydroxylase)
mupL	Hydrolase
mupM	Isoleucyl-tRNA synthetase
mupN	Phosphopantetheinyl transferase
mupO	Cytochrome P450
mupP	Unknown
mupQ	Acyl CoA synthase
mupS	3-Oxo-acyl carrier protein reductase
macpD	Acyl carrier protein
mmpF	Polyketide synthase (ketosynthase)
macpE	Acyl carrier protein
mupT	Ferrodoxin dioxygenase
mupU	Acyl CoA synthase
mupV	Oxidoreductase
mupW	Dioxygenase
mupR	Transcriptional activator
mupX	Amidase
mupI	*N*-Acyl homoserine lactone synthase

1.3.2 Mupirocin biosynthesis

The biosynthetic pathway starts with the activation of the substrates and the condensation of the carboxylic acid starter unit which is catalysed by the KS (Gurney and Thomas, 2011). The extender unit is then transferred on to the phosphopantetheine arm of the ACP, and at this stage the condensation reaction takes place between the starter and the extender unit, joining them together by the action of KS. The resulting product is either left unreduced, or is partially or completely reduced depending on the presence of optional reductive enzymes in the pathway: ketoreductase KR, dehydratase DH and enoyl reductase ER (Gurney and Thomas, 2011). This chain of events is repeated until the polyketide has reached the required length. Because the *mup* cluster lacks an obvious loading module, loading is proposed to happen through *mmpC* that encodes MmpC, which consists of two AT domains (AT1 and AT2). AT1 is thought to work as acyl hydrolase and AT2 exhibits malonyl tranferase activity. These two AT domains are proposed to catalyse the transfer of starter and extender unit (in-*trans*) to KS and ACP respectively via acyl-CoA activated intermediates between condensation modules (Figure 1.10) (El-Sayed *et al*., 2003).

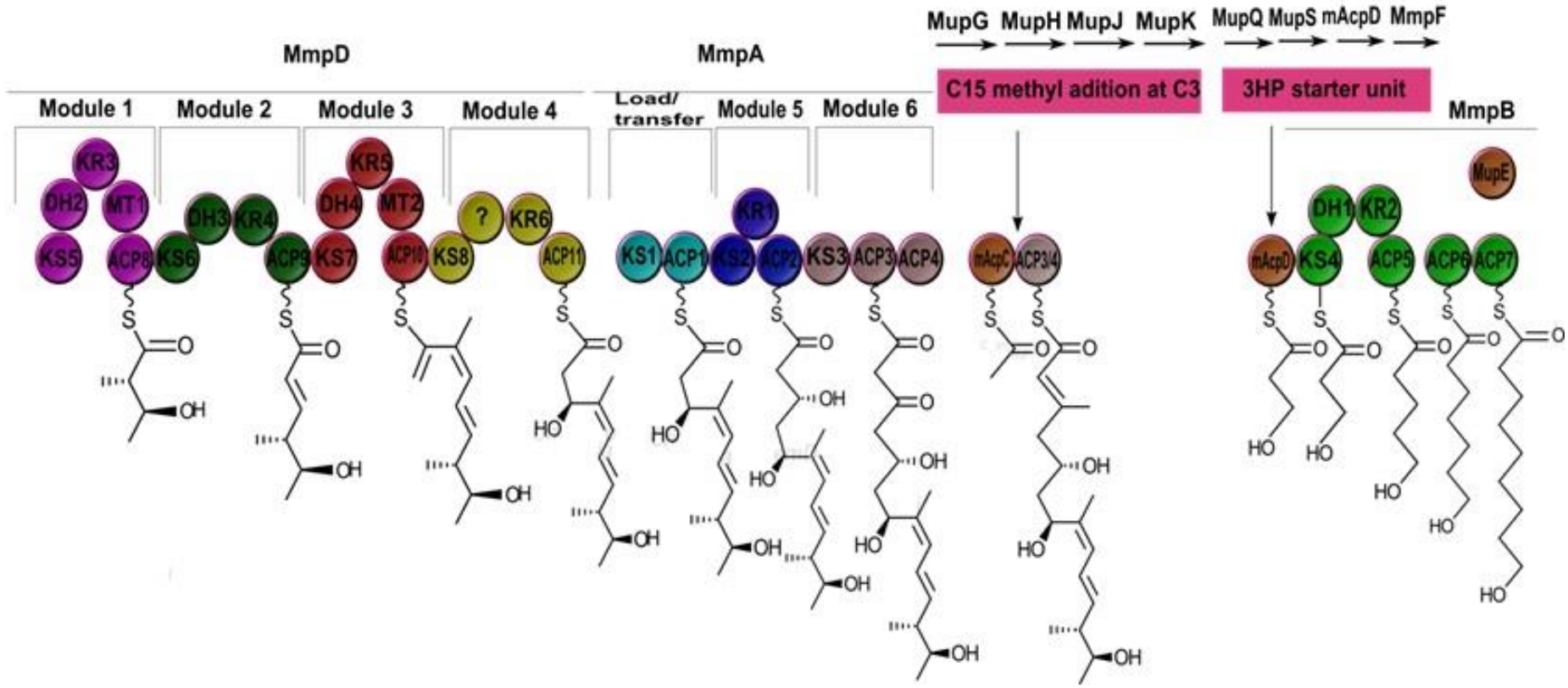

Figure 1.10 Proposed Mupirocin biosynthetic pathway modules. MmpD and MmpA are involved in the biosynthesis of the monic acid backbone, while the 9HN is synthesised via iterative condensations via the action of MmpB with additional ketoreduction and dehydration. Modification to the resulting polyketide chain (Monic acid) is carried out by the tailoring enzymes; MupW, T, O, U, V, C and F, these modifications include formation of pyran ring and addition of the epoxide group.

1.3.2.1 Biosynthesis of the monic acid backbone

The mupirocin biosynthetic pathway is not collinear with the gene sequence, since the first condensation modules are found on MmpD despite MmpA being the first gene to be transcribed. This was confirmed by mutation of the KR4 active site tyrosine to phenylalanine, which resulted in the mutated strain not producing any pseudomonic acid A but instead producing mupiric acid. Six condensations take place in order to synthesise the heptaketide chain that forms the monic acid skeleton (Thomas *et al*., 2010). A proposed set of steps for monic acid biosynthesis start with a *trans* AT located in MmpC transferring an activated starter unit (thought to be acetyl-coenzyme A) to the 4-phosphopantethine arm of ACP-D1. The chain is then moved to the thiol group of the active cysteine on KS-D1. Now that the ACP-D1 is vacant, the activated extender unit (malonyl-CoA) is transferred to the 4-phosphopantethine arm of ACP-D1, followed by Claisen condensation catalysed by KS-D1. Another possible scenario could be that the activated starter unit is directly transferred to KS-D1 or possibly that it is loaded onto one of the type II ACPs of the "tailoring region" and then transferred to KS-D1. This first module of MmpD creates the isoleucine-like side chain structure by the action of KR and α-methylation. To form the C12 unit the chain undergoes three rounds of condensation on the KSs and ACPs (modules 2 to 4) of MmpD and another α-methylation which takes place on MT in module 3. The intermediate is then thought to be transferred across from MmpD to the first module of MmpA, which is thought to be non-elongating due to its atypical domains (KS^0 and ACP). Although the KS^0 has Gln instead of His which could mean that it is not functioning in a normal way, mutation of KS^0 results in a Mup^- phenotype (El-Sayed *et al*., 2003). It could be that the KS^0 is a pseudo-loading module that aids the chain transfer from MmpD to MmpA. Two more elongations plus the final beta-branching are performed to extend the chain to produce the C17 which is a precursor to the monic acid.

1.3.2.2 Tailoring the monic acid backbone

Post PKS tailoring is a significant part of the polyketide biosynthetic pathway as it is one of the factors that make polyketides such a diverse group in terms of structure or activity. Post PKS modifications may include addition of moieties like sugars units, halogenation, methylation or cyclisation, while further oxidative or reductive steps might also occur in order to produce the complete metabolite. The tailoring region in the *mup* cluster comprises 26 ORFs (*mupC-X, and macpA-E*), in addition to *mmpE* and *mmpF*. The tailoring activities might take place either before or after esterification of the monic acid and 9-hydroxynonanoic acid. Initially the epoxide ring is created by oxidation of the C-10,11 double bond (Cooper *et al*., 2005a, El-Sayed *et al*., 2003). Reduction of C-8,9 double bond and oxidation of C-16 creates the tetrahydropyran ring, in addition the hydroxylation of C-6 and addition of the C-15 methyl group. Although it appears that the number of tailoring enzymes exceeds that of the predicted steps needed for the formation of the complete polyketide, it has been proven that they are indeed all essential for the synthesis of the main metabolite pseudomonic acid A. Mutagenesis of *mupT* and *mupW,* which are putative dioxygenases, produced a novel pseudomonic acid (mupirocin W) that lacks the tetrahydropyran ring, but has the 9-hydroxynonanoic acid chain attached. Therefore, it seems like *mupW* and *mupT* have the function of catalysing the epoxidation of C-8,16 double bond which is proposed to be essential for the tetrahydropyran ring formation. This confirmed their role in mupirocin biosynthesis, but without a clear indication as to when this step normally occurs (Cooper *et al*., 2005a, El-Sayed *et al*., 2003). To test the significance of other tailoring genes, mutagenesis studies were carried out to include mutations in *mupQ, S, T, R, X* and *I*. The results showed that all the genes are required for normal pseudomonic acid production, but that they might differ in the level of impact their deletion would have on pseudomonic acid production (Cooper *et al*.,

2005b). In order to produce pseudomonic acid A it is proposed that MupU facilitates the transfer to mAcpE, prior to MupO catalysing the oxidation of the C-7 hydroxyl to ketone. This is followed by C8-9 dehydration by MupV to create the enoyl bond. The final steps before formation of pseudomonic acid A is the reduction of C-8-9 by MupC and ketoreduction at C-7 by MupF. When *mupO*, *mupU*, *mupV*, or *macpE* were deleted pseudomonic acid A production was not only abolished, but the pathway was shifted to produce pseudomonic acid B (80%, 87%, 137% and 60% compared to the wild type respectively). This finding might imply that the protein product of these genes are all involved in the same biosynthetic step, which could explain why there appear to be more tailoring genes than should be needed for the additional modification steps to produce a completed functional polyketide chain (Cooper *et al*., 2005b). Other modifications to the mupirocin backbone includes the incorporation of β-methyl group at C-15, this is catalysed by the genes in the HCS cassette (Haines *et al*., 2013).

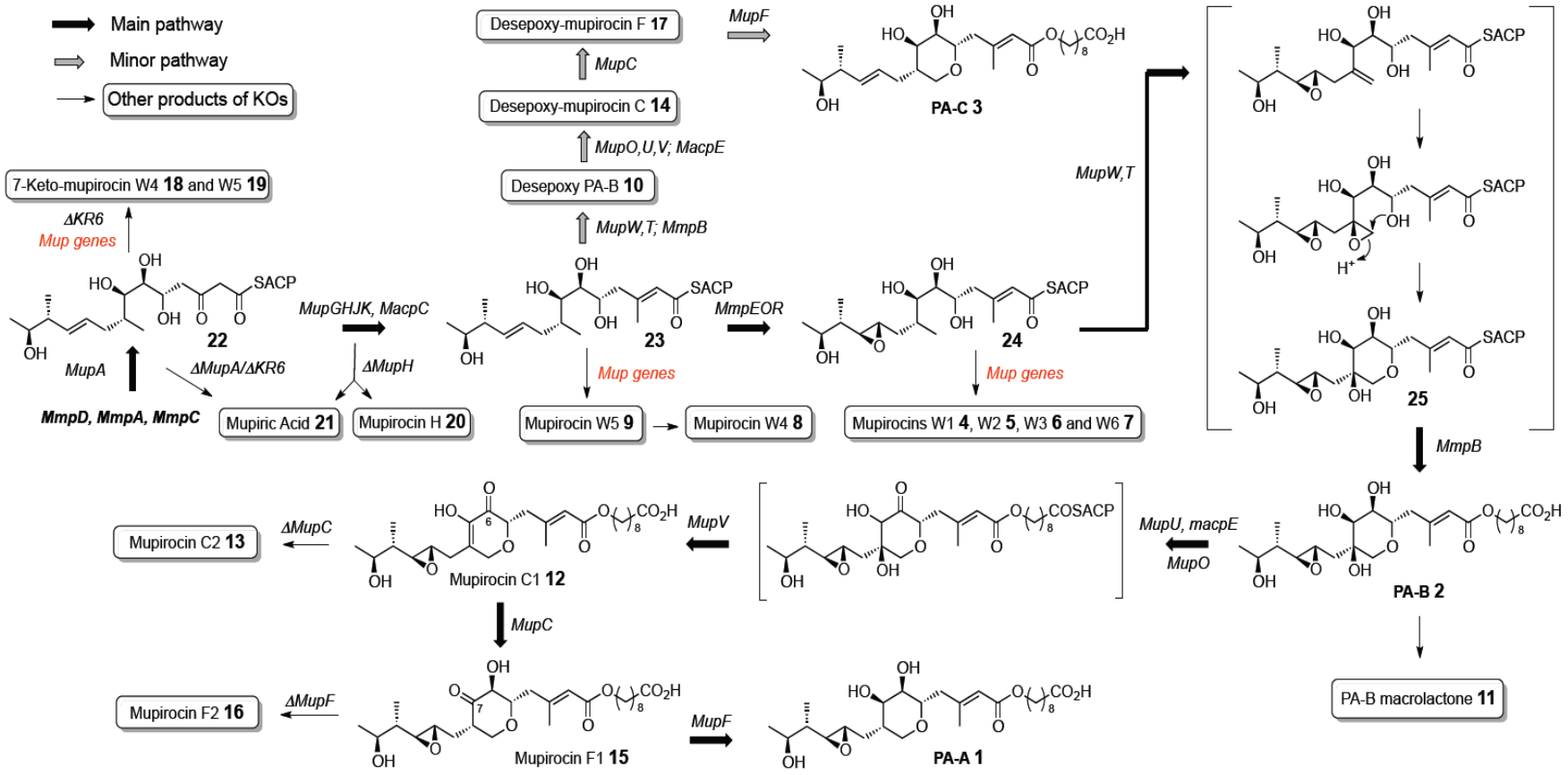

Figure 1.11 Overview of the biosynthesis pathway of mupirocin and related metabolites.The PKSs MmpD, MmpA and MmpB together with MmpC catalyse the condensations that generate the polyketide backbone. Further tailoring of the polyketide is required for the formation of the active pseudomonic acid A (Gao *et al*., 2014).

1.3.2.3 9-hydroxynonanoic acid biosynthesis

The current hypothesis for the 9-hydroxynonanoic acid biosynthesis is that the starter unit is 3-hydroxypropionic acid. This process involves three iterative condensation reactions, and a complete reduction of the keto groups by the action of ketoreductase, dehydratase and enoyl reductase. Previous studies have identified MmpB as a likely candidate for the three iterative condensations using malonate as an extender unit. Although MmpB lacks an obvious ER domain, the enoyl reduction step might be carried out by MupE, which shows a high degree of sequence similarity to known enoyl reductases (El-Sayed *et al*., 2003, Gurney and Thomas, 2011, Thomas *et al*., 2010). Being the last enzymatic reaction involved in the 9-hydroxynonanoic acid reduction it was expected that the absence or inactivity of MupE (enoyl reductase) would result in a fully unsaturated fatty acid, if it were the only enzyme involved. However, this was not observed when *mupE* was mutated suggesting that there is an additional enzyme involved in this process (El-Sayed *et al*., 2003). Further investigation revealed a third domain in MmpC that could participate in the formation of 9- hydroxynonanoic acid, because it also shows similarity to enoyl reductases. The presence of the three tandem ACPs could also indicate that MmpB is associated with 9-hydroxynonanoic production as they could be used successively to complete the three rounds of condensation (Cooper *et al*., 2005b, El-Sayed *et al*., 2003). Experiments conducted to find out more about how this ACP triplet works have shown that point mutations in the active site of *acp5S>A* abolished mupirocin production, while point mutation in each of *acp6* and *acp7* had much less effect on mupirocin levels. On the other hand, while deleting one of the ACPs in *mmpB* slightly reduces mupirocin production, pairwise deletions e.g. (Δ*macp5*/*6*, Δ*macp6*/*7*, Δ*macp5*/*7*) significantly decreased mupirocin production. Therefore, it seems that any one of the doublet and the triplet ACPs is sufficient for the formation of the polyketide chain, but that

reduction of the triplet cluster to a single mACP does have a quantitative effect on production (Rahman, 2005).

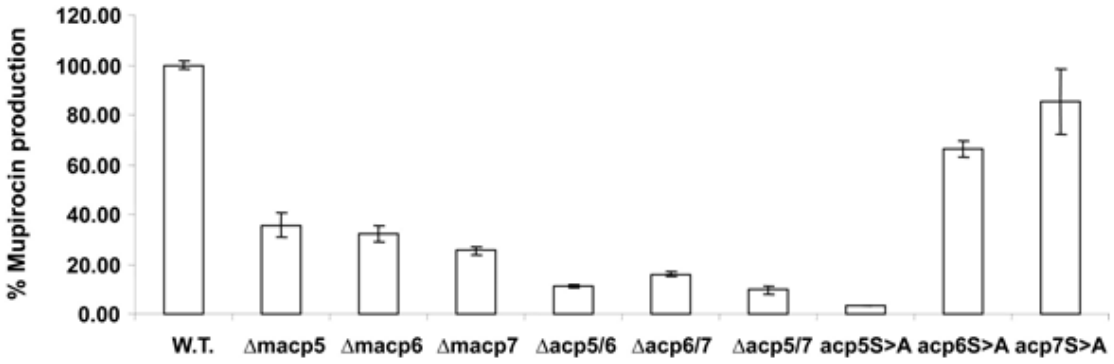

Figure 1.12 Quantitative HPLC analysis of PA-A production in each of the ACP mutants (Rahman, 2005).

The final polyketide product is either released by the only TE in the pathway located in MmpB or it is possible the TE might play a role in the esterification of 9-hydroxynonanoic acid. It is still not clear whether 9-hydroxynonanoic acid is produced first and then joined to monic acid or 9- hydroxynonanoic acid is elongated on C_3 starter unit 3-hydroxypropionate esterified with the monic acid produced by MmpD/MmpA (El-Sayed *et al*., 2003, Hothersall *et al*., 2007) (Cooper *et al*., 2005b).

1.3.3 Regulation of Mupirocin production

Quorum sensing is a mechanism that allows bacteria to control gene expression through constitutive production of autoinducers, which once a critical population density is reached accumulates to a sufficient concentration to trigger the required response (Kuo *et al*., 1994). In the case of mupirocin, quorum sensing involves the production of N-acyl homoserine lactones (NAHL) that build up to induce enough mupirocin production to kill

surrounding bacteria (El-Sayed *et al*., 2001). In this regard, *Vibrio fischeri* is a typical representative of this kind of gene expression, where the autoinduction of the *lux* regulon is responsible for bioluminescence (Miyashiro and Ruby, 2012). In the mupirocin system, MupI and MupR sequences show similarity to LuxI and LuxR which mediate the response to homoserine lactones (Thomas *et al*., 2010). It is predicted that the NAHL produced by MupI binds to MupR in order for the latter to bind to the promoter and activate 3-oxo-C10 N-acyl homoserine lactone (El-Sayed *et al*., 2001, Thomas *et al*., 2010). To test if the *mup* cluster was regulated by quorum sensing mechanism, the *xylE* gene encoding catechol 2, 3-dioxygenase was used as a reporter gene at different places in the *mup* cluster. While deletion of *mupI* abolished synthesis of homoserine lactone in *P. fluorescens*, providing 3-oxo-C10 N-acyl homoserine lactone exogenously restored the function proving that *mup* cluster is controlled by quorum signal. Since MupR controls the putative regulatory region upstream of *mupA* and the region between *mupF* and *macpC*, it is plausible that the *mup* cluster might be transcribed as one long unit through the MupR/MupI system binding to the promoter regions upstream of *mupA*, *macpC* and *mupF*. The *mup* cluster might also be regulated by *mupX*, as it appears that inactivating it reduces mupirocin production by about 40%. Inactivation of *mupX* does not have any effect on the product profile, but it might be required for the expression of other genes in the *mup* cluster (El-Sayed *et al*., 2001, Hothersall *et al*., 2011). Expressing *mupR* in-*trans* resulted in an almost fivefold increase in mupirocin production, in addition to some early intermediates like mupiric acid, mupirocin H and truncated products of PA-A and PA-B. (Hothersall *et al*., 2011).

1.3.4 Clinical significance

Mupirocin works by binding to the bacterial isoleucyl-tRNA synthetase, which consequently leads to competitive inhibition of protein synthesis in the bacterial cell. The C12 to C14 terminus of the monic acid resembles the hydrophobic side chain of isoleucine; the pyran ring interacts with the ATP-binding pocket of IleRS. It is proposed that the 9-hydroxynonanoic acid would fit into a hydrophobic groove to help in the binding process, and stabilise the complex (Figure 1.13) (Thomas *et al*., 2010). To prevent protein synthesis, mupirocin thus acts as an analogue of lle-AMP, and blocks the binding of the activated amino acid to the catalytic cleft of the Rossman fold domain of lleRS. This in turn mimics the effect of isoleucine starvation, triggering the stringent response, which down-regulates many functions in the bacterial cell including protein synthesis (Thomas *et al*., 2010) (Cassels *et al*., 1995).

Mupirocin was discovered in 1971 and it was first introduced into clinical practice in the UK in 1985 (Fuller *et al*., 1971). Since the early stages of its introduction mupirocin has demonstrated many properties that are advantageous for a topical antibiotic, such as low resistance rate in common cutaneous pathogens, and a lack of cross resistance to other agents (Cookson, 1990). In a study to determine the effectiveness of mupirocin in clinical settings, it was found that mupirocin provides protection against *S. aureus* infection, especially in dialysis patients and ICU populations (Nair *et al*., 2015). Mupirocin is also successfully used as a nasal ointment to decolonize nasal passages to control asymptomatic MRSA carriage (van Rijen *et al*., 2008). Mupirocin is widely used outside healthcare settings to manage community-acquired MRSA. However, although considered an ideal topical antibiotic, studies have shown that the long term use of mupirocin can promote *S. aureus* resistance, rendering it unsuitable for prolonged treatments (Thomas *et al*., 2010).

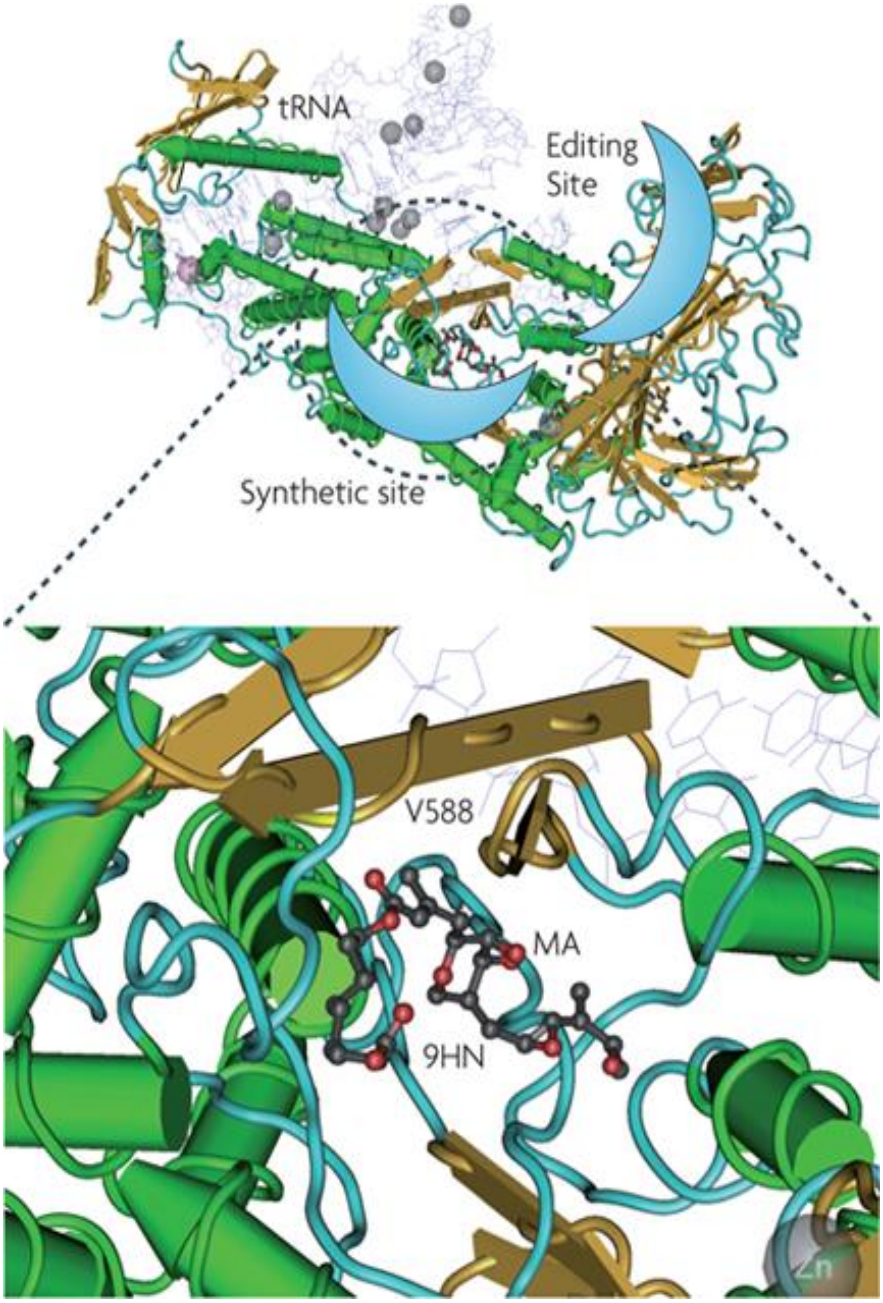

Figure 1.13 Mupirocin mode of action. Mupirocin bound in the synthetic site of isoleucyl-tRNA synthetase (from Thomas et al., 2010) (Hurdle et al., 2004, Silvian et al., 1999).

1.3.5 Resistance to mupirocin

In 1987, two years after the introduction of mupirocin, resistance began to emerge. Two phenotypes of mupirocin resistance have been identified: low level mupirocin resistance (8-256mg/L) and high level mupirocin resistance (>256mg/L) (Patel *et al*., 2009). High level mupirocin resistance is usually associated with mupirocin decolonization failure. Strains with high level mupirocin resistance are the result of the presence of IleRS proteins which are similar to eukaryotic IleRS that are naturally resistant to much higher levels of mupirocin acquired by horizontal gene transfer (Thomas *et al*., 2010). In *S. aureus* eukaryotic-like IleRS is encoded by *mupA* on conjugative plasmids that confer high level mupirocin resistance, as well as other antimicrobial agents like macrolides, tetracycline, gentamicin and trimethoprim (McNeil *et al*., 2011, Oliveira *et al*., 2009). Two distinct IleRS enzymes are responsible for *S. aureus* strains with high level mupirocin resistance. One is a mupirocin resistant enzyme encoded by the plasmid *ileS-2* and the mupirocin sensitive enzyme encoded by the chromosomal wild type *ileS-1*. Recent studies have also identified an additional gene responsible for high-level mupirocin resistance (*mupB*), which contains conserved motifs found in class I tRNA synthetases (Seah *et al*., 2012) (Ramsey *et al*., 1998). On the other hand, spontaneous point mutations in the chromosomal *ileS* result in low level mupirocin resistance. These mutations occur in the Rossman fold and close to the conserved motif KMSKS, which is involved in determining the binding of the 9-hydroxynonanoic acid moiety and ATP. The most common mutations associated with low level mupirocin resistance are the Val to Phe substitutions, especially the V588F and V631F (Silvian *et al*., 1999, Hurdle *et al*., 2004). The crystal structure of the IleS, tRNA and mupirocin complex revealed that when valine is substituted with phenylalanine, the much bulkier benzyl side chain of the latter disrupts

the hydrophobic pocket inside the Rossman fold, which is critical for mupirocin binding (Antonio *et al*., 2002).

1.3.6 Non-ribosomal peptide synthases

Similar to the PKS system, NRPSs contain modules, which are responsible for incorporating building blocks into the growing polypeptide chain. The size of the resulting product varies, but they can reach remarkably large sizes like the 1.6 MDa cyclosporin NRPS, which comprises 11 modules all synthesised by a single NRPS protein in *Tolypocladium niveum*. In bacteria on the other hand, modules are distributed over several NRPSs, which are usually arranged into operons. *Pseudomonas syringae* has one of the largest bacterial NRPS systems, containing 8 modules (Evans *et al*., 2011). A minimum of three domains is required to achieve a functional NRPS, an Adenylation (A) domain, a Peptidyl Carrier Protein (PCP) and a Condensation (C) domain for the peptide bond formation. A-domains are responsible for activating carboxy acid substrate to amino acyl adenylate while ATP is being consumed. The PCP-domain acts as a transport unit that accepts the activated amino acid that is covalently tethered to its 4´-phoshopantetheine cofactor as thioester. This cofactor is post-translationally transferred to a conserved serine residue of the carrier protein (CP), and acts as a flexible arm to allow the bound amino acyl and peptidyl substrate to travel between different catalytic centres. The next step in NRPS synthesis is carried out by the condensation domain, which is responsible for the peptide bond formation. This is achieved by catalysing the nucleophilic attack of the amino group of the activated amino acid bound to downstream module, onto the acyl group of the amino acid attached to the upstream module. During synthesis, the growing peptide chain is handed over from one module to the next until it reaches the final module in PCP-domain. This module contains in most cases a TE-domain that is important for product release (Figure 1.14).

TE-independent termination has also been observed in some NRPS systems like in myxochelin biosynthetic pathway, in which an aldehyde is produced through the action of the reductase that catalyses the thioester reduction. The final product can be either released as a macrocyclic product such as in surfactin, or a linear peptide as in pyochelin.

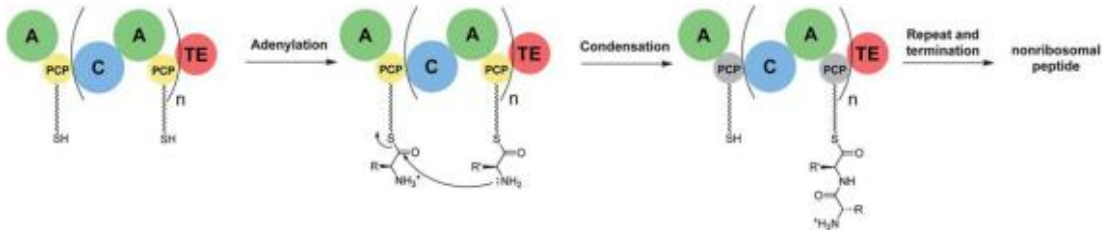

Figure 1.13 Nonribosomal peptide synthetase (NRPS) assembly line. The peptidyl carrier domain (PCP) has a phosphopantetheine prosthetic group terminated with a thiol. The adenylation (A) domain activates amino acids and the condensation (C) domain makes the amide linkages. Termination is frequently catalyzed by a thioesterase (TE) domain (from Condurso & Bruner, 2012).

1.3.7 Thiomarinols

Thiomarinols are antibiotics produced by marine bacteria *Pseudoalteromonas rava* sp and *Pseudoalteromonas luteoviolacea*. Structurally, thiomarinol is a combination of two separate classes of antibiotics, pseudomonic acids and pyrrothines (Shiozawa *et al*., 1993). From a biosynthetic point of view, thiomarinols are considered to have three elements: a functionalised polyketide acid, linked by ester to a hydroxyl fatty acid, in turn linked by amide to pyrrothine. Thiomarinols are active against both Gram positive and Gram negative bacteria (Murphy *et al*., 2014), and importantly they are potent against *Staphylococcus aureus* (MRSA). It is thought that its additional potency against Gram negative bacteria is due to either increased uptake, as Gram negative bacteria are protected by the outer membrane, or because of the holomycin part which inhibits RNA synthesis, and provides a second target besides the isoleucyl-tRNA synthetase (Fukuda *et al*., 2011,

Murphy *et al*., 2011). It is worth mentioning that at least in Gram negative bacteria resistance is conferred by a single gene, *tmlM* which encodes an IleS, suggesting that the potency is not the result of attacking more than one target. Previous work on the thiomarinol biosynthetic pathway showed that thiomarinol was more active in terms of inhibiting MRSA growth than the pyrrothine amides. Marinolic acid (produced by the *trans*-AT PKS part and the equivalent to pseudomonic acid or mupirocin) showed less activity than mupirocin which suggests that the addition of the pyrrothine (produced by the NRPS part) is the reason for thiomarinol's increased potency (Fukuda *et al*., 2011). Thiomarinol differs from mupirocin in having 8-hydroxyoctanoate instead of the 9-hydroxynonanoic acid, the presence of an extra 4-hydroxyl group, pyrrothine and the lack of the 10,11 epoxide ring. All of which may contribute to the differences in activity (Fukuda *et al*., 2011).

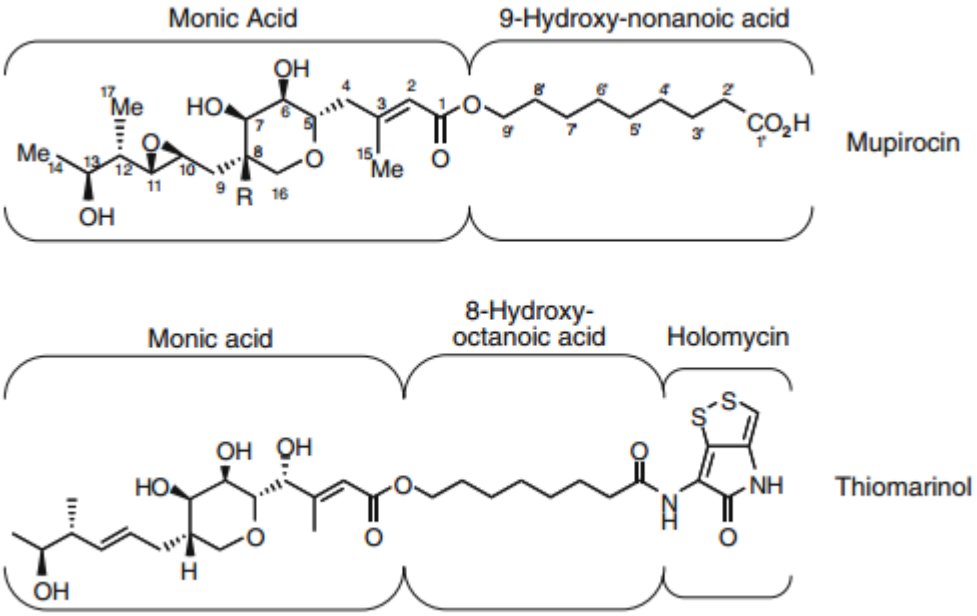

Figure 1.14 Chemical structures of mupirocin and thiomarinol. The structures highlight the differences between these two compounds. Monic acid and the 8-hydroxyoctanoic acid combined are the equivalent to pseudomonic acid/mupirocin.

The thiomarinol biosynthetic pathway appears to be entirely encoded on a 97,600 bp plasmid (pTML1) that includes 27 ORFs, with *trans*-AT PKSs (*tmpA to tmpD*) responsible for the marinolic acid part (Fukuda *et al*., 2011). The other part of the plasmid encodes the 7 NRPS-encoding ORFs that are thought to be responsible for pyrrothine production. Sequencing data showed a great similarity to the *mup* cluster, but also some intriguing differences between the two systems. One difference is the absence of an *macpE* equivalent in thiomarinol cluster. In the mupirocin pathway, the protein mAcpE is thought to accept the polyketide intermediate from MupU, which is then processed by MupO, V, C and F (Fukuda *et al*., 2011). In thiomarinol biosynthesis, there is instead an extra module consisting of a KS and ACP in TmpB, which might be involved in the equivalent final tailoring steps in marinolic acid biosynthesis. Extra ACP domains can be seen in several modules like the third module of TmpD and the last module of TmpA, a possible function could be increasing the pathway's throughput (Figure 1.15). It is worth mentioning that SANK73390-Δ*tmpD* mutants produced only yellow pigmented pyrrothine material, while SANK73390-Δ*holA* mutants produced only marinolic acid. This observation indicates that marinolic acid and pyrrothine are produced separately and then joined together by the action of TmlU, which activates the pseudomonic acid as a thioesterase, and HolE which catalyses the amidation as an acyltransferase (Figure 1.16) (Fukuda *et al*., 2011) (Dunn *et al*., 2015).

Although no obvious regulatory protein was found in pTML1, four of the five transcriptional units have likely operator sequences through which the genes are regulated (Fukuda *et al*., 2011). Mutasynthesis studies on the Thiomarinol cluster yielded a number of different metabolites, which can provide more clues into how to genetically engineer SANK73390 in order to produce new antimicrobial compounds active against MRSA (Murphy *et al*., 2011, Murphy *et al*., 2014, Fukuda *et al*., 2011).

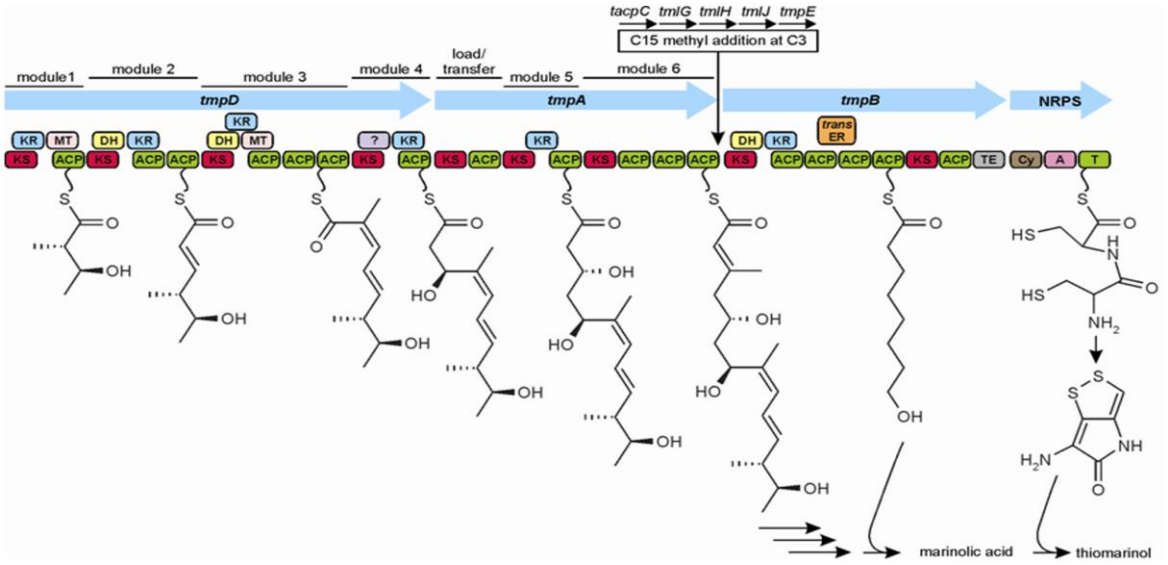

Figure 1.15 Predicted scheme for thiomarinol biosynthesis showing the roles of TmpD (modules 1 to 4)/TmpA (modules 5 and 6) for monic acid, TmpB for 8-hydroxyoctanoic acid and HolA/NRPS for pyrrothine. Cy, Condensation domain; A, Aminoacyl Adenylation Domain; T, Thiolation Domain or Peptidyl Carrier Protein (from Fukuda *et al*., 2011).

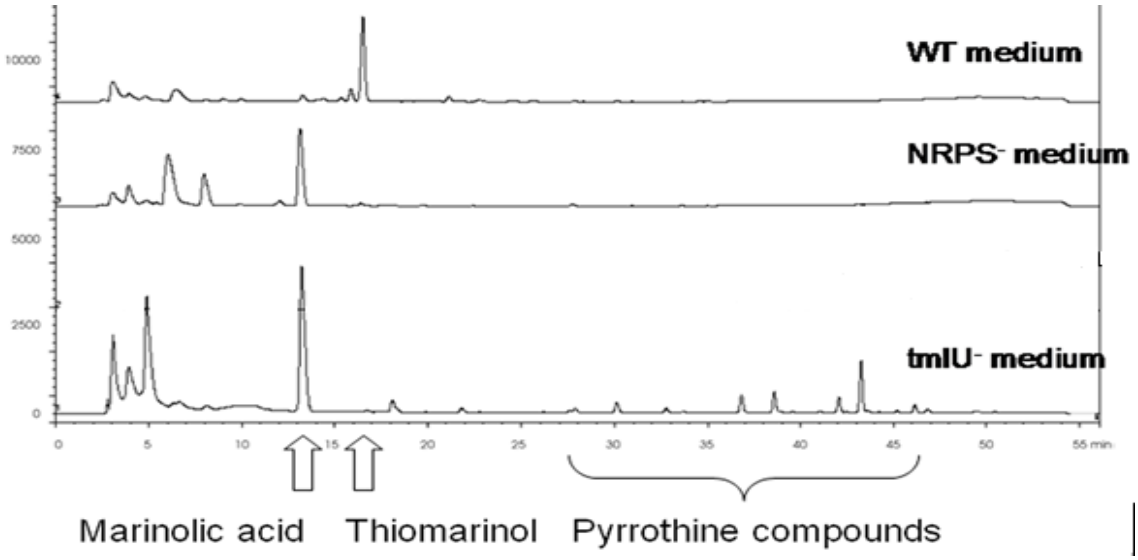

Figure 1.16 HPLC analysis of products from wild type *Pseudoalteromonas rava* SANK 73390 and mutant derivatives. In the absence of TmlU, the amide bond between marinolic acid and pyrrothine is not formed (from Fukuda *et al*., 2011).

Table 1.2 Predicted gene products on pTML1 (Fukuda *et al*., 2011)

Gene name	Predicted function
tmlN	Phosphopantetheinyl transferase
tmlT	Ferredoxin dioxygenase
intA	similar to phage integrase
orfA	N-terminal of transposase
repA	Plasmid replication initiator
parA	ATPase, partitioning
parB	DNA binding, partitioning
tacpB	Acyl carrier protein
tmpF	Ketosynthase domain
tacpD	Acyl carrier protein
tmlS	3-oxoacyl-ACP reductase
tmlQ	Acyl-CoA synthase
tmlM	Isoleucyl tRNA synthase
tmlA	FMNH(2)-dependent oxygenase
tmpA	Multifunctional PKS
tacpC	Acyl carrier protein
tmlG	3-oxoacyl-ACP synthase
tmlH	HMG-CoA synthase
tmlJ	Enoyl-CoA hydratase
tmpE	Enoyl-CoA hydratase and ketosynthase
tmlL	Putative hydrolase
tmpB	Multifunctional PKS
tmpC	*Trans* acyl-transferase plus putative enoyl reductase
tmpD	Multifunctional PKS
tmlB	3-oxoacyl-ACP synthase
tmlC	NADH: flavin oxidoreductase
tmlF	Ketoreductase
tmlP	Unknown
tmlO	Cytochrome P450
tmlU	Acyl-CoA synthase
tmuA	Membrane protein / Permease
tmlY	Unknown
tacpA	Acyl carrier protein
tmuB	Putative dioxygenase
tmlW	Dioxygenase (Rieske 2Fe-2S protein)
tmlZ	Chromosomal replication initiation protein
holA	Non-Ribosomal Peptide Synthase
holB	Oxidoreductase
holC	Thioesterase
holD	Acyl-CoA dehydrogenase
holE	Acetyltransferase
holF	Truncated Globin/ Monooxygenase
holG	Decarboxylase; flavoprotein

1.4 Aminocoumarin

The aminocoumarin class of antibiotics, produced by different strains of *Streptomyces*, consists of compounds structurally similar to each other. These possess the same unique feature, the 3-amino-4,7-dihydroxycoumarin moiety; examples include novobiocin, chlorobiocin, coumermycin A1 and simocyclinone (Heide, 2009a). The biosynthetic gene clusters for each have been sequenced, and several genes encoding important enzymes have been identified. These include the amide synthetases NovL, CloL, CouL and SimL, which are responsible for creating an amide bond during biosynthesis of aminocoumarin antibiotics. Interestingly, a similar gene (*tmlU*) was found in the biosynthetic gene cluster of thiomarinol. This finding suggested the possibility that SimL (the most similar of these amide synthetases) or others of this group might be able to replace TmlU in SANK73390 (Fukuda *et al*., 2011). Aminocoumarins are produced by different strains of *Streptomyces* and they target bacterial gyrase, which is an essential enzyme for DNA replication and transcription in bacteria (Luft *et al*., 2005). Aminocoumarin antibiotics are a successful example of generating a hybrid antibiotic using the mutasynthesis procedure. Heide and coworkers were able to demonstrate that by feeding a synthetic precursor (Ring A), necessary for the biosynthesis of the prenylated 4-hydroxybenoate moiety of clorobiocin, to a strain with an engineered novobiocin biosynthetic gene cluster, they could produce analogs of the novobiocin glycon (novobiocin acid) (Heide, 2009). The next step was the addition of the culture extract from the first feeding to another strain unable to produce clorobiocin, and this formed the deoxysugar, the 4-methyl group and the 5-methylpyrrolle-2-carbonyl moiety, which is characteristic of clorobiocin, and attached them to the novobiocin acid analog. Thus, this procedure led to the generation of a hybrid antibiotic that possessed the structural features of both novobiocin and clorobiocin (Anderle *et al*., 2007b).

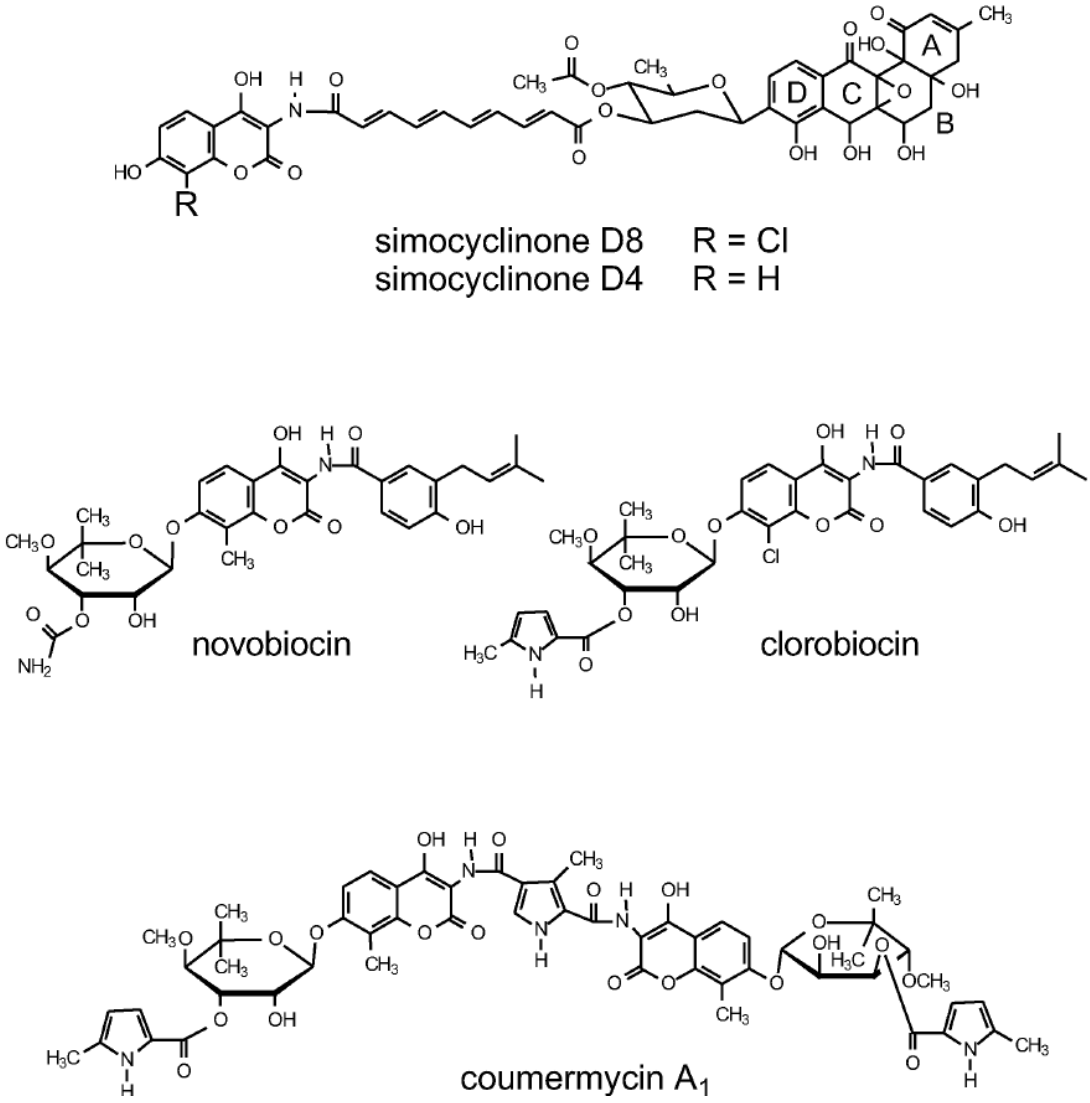

Figure 1.17 Structures of the aminocoumarin antibiotics. clorobiocin, novobiocin, coumermycin A1, simocyclinone D8 and simocyclinone D4 (from Heide, 2009b).

1.5 Statement of objectives

With antibiotic resistance on the rise, different approaches have been utilized to tackle this problem, most of which depend on creating semi-synthetic molecules using existing antibiotics as a scaffold. As genomic sequencing has become cheaper and faster, and sequences of many antibiotic-producing bacteria are readily accessible, combinatorial biosynthesis approaches became more popular as a means to produce novel antimicrobial molecules. This was achieved by genetically manipulating the biosynthetic pathways of different systems and creating hybrid compounds with new and more efficient properties. Examples of hybrids that might be useful include, mupirocin derivatives lacking the ester bond that could be used systemically, or a hybrid of thiomarinol and mupirocin, where thiomarinol activity is not toxic to the eukaryotic cells but still has the antimicrobial activity of both of the molecules combined. Research in the Thomas lab at the University of Birmingham has been focused on understanding the biosynthetic pathway of Mupirocin to underpin development of such derivatives. Although most of the biosynthetic pathway has been elucidated, there are still some aspects that need to be further investigated in order to rationally design hybrid pathways producing novel antimicrobial compounds.

The initial objective of this project (chapter 3) was to investigate the possibility of incorporating amide synthases from different polyketide pathways into the mupirocin biosynthetic pathway. The background for this is derived from the role that these amide synthetases play in their native systems. SimL for example, is an essential enzyme that assembles simocyclinone, which bears a structural resemblance to both mupirocin and thiomarinol. Likewise, in the thiomarinol pathway TmlU is one of the enzymes involved in linking pseudomonic acid to holomycin creating thiomarinol. The hypothesis investigated in chapter 3 is whether SimL and other similar amide synthetases can catalyse the attachment of parts of mupirocin to thiomarinol. To test this, several amide synthetases

were identified, and cloned into an expression vector to be provided in-*vivo* in-*trans* to the mupirocin and thiomarinol producing strains. Effects of in-*trans* expression of these proteins could then be detected by HPLC analysis.

Expression of TmlU in the mupirocin producer was observed to inhibit normal production of pseudomonic acid A (chapter 3). This was of interest, as understanding the mechanism of this inhibition could yield insight into how TmlU functions in thiomarinol biosynthesis, and how it interacts with different elements of the mupirocin pathway. When TmlU was expressed in the mupirocin producer, truncation of the fatty acid produced by MmpB was observed. This lead to the hypothesis that TmlU inhibits mupirocin production through interaction with MmpB. In chapter 4, this hypothesis is investigated through testing the effect of mutations of both MmpB and TmlU on pseudomonic acid A production. These mutations would allow insight into the mechanism by which TmlU inhibits mupirocin biosynthesis, and allow identification of the specific region of MmpB putatively responsible for interaction with TmlU. This interaction would then be tested using the bacterial two hybrid system to look for protein-protein interactions.

In thiomarinol biosynthesis, holomycin is produced by a set of NRPS genes, the *hol* genes. It would be desirable to generate holomycin in-*vivo* in the mupirocin producing strain, as this could facilitate generation of a mupirocin-holomycin hybrid in the future. The hypothesis of chapter 5 is to demonstrate whether plasmid encoded holomycin biosynthesis can occur in the mupirocin producer. To test this, the holomycin operon would be cloned into a vector and expressed in-*trans* in the mupirocin producer. Any new compounds produced could be detected by HPLC, and their bioactivity identified by bioassay. Holomycin production may also be detectable through a phenotypic shift, due to the yellow colour of the compound.

While most of the steps in the mupirocin pathway have been elucidated, some of the tailoring genes have not yet been assigned a function, and the timing of some steps is not yet certain. One function without an assigned gene is the 6-hydroxylation of monic acid. Deletion of *mupA* in the mupirocin producer yielded only mupiric acid, which lacks the α-hydroxyl. This suggested the intermediate could not proceed beyond MmpD. One hypothesis that could explain this is that the KS2 of MmpA has gatekeeper activity, where it demonstrates selectivity for the 6-OH group. Further to this, a loop was identified on homology models that could be responsible for this specificity. This led to a second hypothesis, can the KS2 be re-engineered to relax this specificity, therefore allowing condensation of the non 6-OH intermediate through MmpA. To test these hypotheses, chromosomal mutations would be made to swap regions of other MmpA KS domains into KS2. These mutant strains would be analysed by HPLC, LC-MS, and NMR where necessary, to identify compounds produced. Identification of a full length product lacking the 6-OH would indicate both that KS2 has the described gatekeeper activity, and which specific region of the protein is responsible for this specificity.

CHAPTER 2

2 MATERIALS AND METHODS

2.1 Bacterial strains, culture conditions and plasmids

All the bacterial strains used in this study are listed in Table 2.1. L-broth and L-agar, (Bertani, 1951) were used to grow *P. fluorescens* NCIMB10586 at 30°C supplemented with 50µg/ml ampicillin; antibiotics used in this study are listed in Table 2.2. Chemical reagents used in this study were purchased from Sigma-Aldrich. Recombinant DNA was transformed initially into *Escherichia coli* DH5α for plasmid propagation and sequencing. *E. coli* S17-1 was used to mobilise vectors/plasmids into *P. fluorescens* NCIMB10586 by conjugation. The conjugants were then plated on M9 minimal media: 200ml salt solution containing NA_2HPO_4 (6g/l), KH2PO4(3g/l), NH4Cl (1g/l), MgSO4(1mM), thiamine HCl (1mM), CaCl2(0.1mM), glucose (0.2%) added to 200ml 50% H_2O agar) and left for 2-3 days to grow at 30°C. Bioassays for mupirocin production were performed using *Bacillus subtilis* 1064 as an indicator strain, which was grown at 37°C in L broth overnight. To introduce changes into the chromosomal DNA the plasmid pAKE604 was utilised as a suicide vector. Plasmid pET28 was used in site-directed mutagenesis to introduce deletions and mutations into plasmids. *Pseudoalteromonas* spp. SANK 73390 is the producer of thiomarinol and was grown in marine agar or marine broth at 23°C. Marine broth contains 33.33g of sea salt in 1 L distilled water, 5g bacteriological peptone, 0.1g ferrous sulphate and 0.89g yeast extract (Shiozawa *et al*., 1993). For marine agar 15g of agar powder is added to the previous mix.

Table 2.1 Bacterial strains used in this study

Bacterial strain	Genotype/phenotype	source
E. coli DH5α	Φ80lacZΔM15, *recA1, endA1, gyrA86, thi-1, HsdR17(r $_{k^-}$, m $_{k^+}$), supE44, relA1, deoR,* Δ*(lacZYA-ArgF)U169*	Gibco BRL
P. fluorescens NCIMB10586	Wild type (W.T) strain which produces mupirocin	G. T Banks
Escherichia coli S17-1	*recA pro hsdR RP4-2-Tc::Mu-km::TAN7*	Simon *et al*., 1983
Pseudoalteromonas SANK73390	Wild type (W.T) strain which produces Thiomarinol	Daiichi Sankyo Co., Ltd
B. subtillis	*rpC2amyE::(spec P xyl-gfp-lacI) chr::pSG1196 (rrnD-lacO cat*	Moir *et al*., 1979
P. fluorescens NCIMB10586ΔACP5 (ACP-Ba)(mmpB)	*P. fluorescens* with ACP5(mmpB) deletion	Rahman *et al*., 2005 (C.M. Thomas lab)
P. fluorescens NCIMB10586ΔACP6 (ACP-Ba)(mmpB)	*P. fluorescens* with ACP6(mmpB) deletion	Rahman *et al*., 2005 (C.M. Thomas lab)
P. fluorescens NCIMB10586ΔACP7 (ACP-Ba)(mmpB)	*P. fluorescens* with ACP7(mmpB) deletion	Rahman *et al*., 2005 (C.M. Thomas lab)
P. fluorescens NCIMB10586ΔmupA	*P. fluorescens* strain with mupA deletion	Joanne Hothersall (C.M. Thomas lab)

Table 2.2 Antibiotics used in this study

Antibiotic	Working concentration (µg/ml)	Solvent
Ampicillin	50	H_2O
Chloramphenicol	50	70% (v/v) Ethanol
Kanamycin sulphate	50	H_2O
Tetracycline hydrochloride	15	70% (v/v) Ethanol

Table 2.3 Plasmids used in Chapter 3.

Plasmid	Size (kb)	Properties	Source
pJH10	13.76	IncQ replicon,multiple cloning site (*EcoRI-SacI*),Tet^R	El-sayed *et al.*, 2011
pJH10-Xho1-linker	14.5	IncQ replicon, multiple cloning site (*EcoRI-SacI)*, Tet^R with Xho1-linker	Hothersall *et al*., 2007
pGEM-T-Easy	3.0	Amp^R , tac promoter, N-terminus GST.TAG	G.E. Healthcare
pAMH1	16.4	1.96 kb *EcoRI-SalI* fragment containing *tmlU* cloned into pJH10-*Xho*1-linker	Omer-Bali thesis 2013
pSIML	15.26	1.5 kb *EcoRI-XbaI* fragment of *simL* cloned into *pJH10*	This study
pNOVL	15.30	1.54 kb *EcoRI-XbaI* fragment of *novL* cloned into *pJH10*	This study
pCLOL	15.27	1.51 kb *MfeI-XbaI* fragment of *cloL* cloned into *pJH10*	This study
pCOUL	15.27	1.51 kb *MfeI-XbaI* fragment of *couL* cloned into *pJH10*	This study
pGEMSM	4.5	1.5 kb *EcoRI-XbaI* fragment of *simL* cloned into *pGEM-T-Easy*	This study

pGEMNV	4.54	1.54 kb *EcoRI-XbaI* fragment of *novL* cloned into *pGEM-T-Easy*	This study
pGEMCL	4.51	1.51 kb *EcoRI-XbaI* fragment of *cloL* cloned into *pGEM-T-Easy*	This study
pGEMCO	4.51	1.51 kb *EcoRI-XbaI* fragment of *couL* cloned into *pGEM-T-Easy*	This study

Table 2.4 Plasmids used in Chapter 4.

Plasmid	Size (kb)	Properties	Source
pJH10	13.76	IncQ replicon,multiple cloning site (*EcoRI-SacI*),Tet^R	El-sayed *et al.*, 2011
pJH10-Xho1-linker	14.5	IncQ replicon, multiple cloning site (EcoRI-*SacI)*, Tet^R with Xho1-linker	Hothersall *et al.*, 2007
pAMH1	16.4	1.96 kb EcoRI-*SalI* fragment containing *tmlU* cloned into pJH10-*Xho*1-linker	Omer-Bali (2013)
pET28a	5.3	kan^R, His-Tag,*T7p,lacI*	Novagen
pAKE604	7.2	pMB1 replicon. Amp^R, Km^R , *oriT, lacZα, sacB*	El-Sayed *et al.*, 2001
pUT18	3.23	Amp^R, CyaA (225- 399), *lacI*	Euromedex
pKT25	3.442	Kan^R , CyaA (1-224), *lacI*	Euromedex
pET28a-tmlU	7.2	1.96 kb *EcoRI-SalI* fragment containing *tmlU* cloned into pET28a	Fukuda *et al.*, 2011
pTmlUM1	16.4	1.96 kb *EcoRI-SacI* fragment containing *tmlU* with the mutation A>C cloned into pJH10-Xho1-linker.	This study
pTmlUM2	16.4	1.96 kb *EcoRI-SacI* fragment containing *tmlU* with the mutation GA>GT Cloned into pJH10-Xho1-linker	This study
pTmlUM3	16.4	1.96 kb *EcoRI-SacI* fragment containing *tmlU* with the mutation AAG>AGG Cloned into pJH10-Xho1-linker	This study
pTEMD	8.219	1kb *BhamH1-HindIII* fragment containing TE with the mutation A>C cloned into pAKE604	This study
pMMH4	19.5	5kb *KpnI-XbaI* fragment containing *mupO*, *macpE* and *mupUV* cloned into pJH10 vector.	M.Macioszek thesis 2009

pUT18tmlU	5.19	1.96 kb *EcoRI-XbaI* fragment containing TE cloned into pUT18	This study
pKT25TE	4.204	0.762 kb *EcoRI-XbaI* fragment containing TE cloned into pKT25	This study

Table 2.5 Plasmids used in Chapter 5

Plasmid	Size (kb)	Properties	Source
pJH10	13.76	IncQ replicon,multiple cloning site (*EcoRI-SacI*),Tet^R	El-sayed *et al.*, 2011
pGEM-T-Easy	3.0	Amp^R , tac promoter, N-terminus GST.TAG	G.E. Healthcare
pGEMHol1	8.77	5.77 kb *XhoI-AgeI* fragment containing part of the hol genes cloned into pGEM-T-Easy	This study
pGEMHol2	6.0	3 kb *AgeI – SbfI* fragment containing part of the hol genes cloned into pGEM-T-Easy	This study
pGEMHol3	6.0	3 kb *AvrII – SbfI* fragment containing part of the hol genes cloned into pGEM-T-Easy	This study
pGMTHol	14.77	11.77 XhoI-BstbI fragment containing the complete *hol* genes cloned into pGEM-T-Easy	This study
pHolA-H	24.76	11 kb *XhoI-ClaI* fragment containing the *hol* genes from A to H cloned into pJH10	This study
pHolA-HtmlU	26.72	1.96kb *XbaI-SacI* fragment containing *tmlU* cloned into pHolA-H	This study

Table 2.6 plasmids used in Chapter 6

Plasmid	Size (kb)	Properties	Source
pAKE604	7.2	pMB1 replicon. Amp^R, Km^R , *oriT, lacZα, sacB*	El-Sayed *et al*., 2001
pAKEKS1	3.0	1 kb *EcoRI-HindIII* fragment containing KS1 loop in KS2 cloned into pAKE604	This study
pAKEKS3	8.77	1 kb *EcoRI-HindIII* fragment containing KS3 loop in KS2 cloned into pAKE604	This study

2.2 Polymerase chain reaction (PCR)

PCR was used to amplify fragments of DNA. Bacterial template DNA was prepared by suspending one bacterial colony in 50µl of sdH_2O, and then heating at 90°C for 6 minutes before centrifugation. The supernatant was transferred into a clean microcentrifuge tube and used as a template. Primers were synthesised by **Abingdon Health Laboratory Services** of the University of Birmingham and were used at a concentration of 100pmol/µl. Velocity DNA polymerase from Bioline was used to amplify DNA segments for cloning purposes, while *Taq* polymerase from Invitrogen was used for screening. The melting temperature of each primer was calculated using the equation: Tm = 4 (G + C) + 2 (A + T) °C and the annealing temperature was calculated accordingly.

Table 2.7 Primers used in Chapter 3

Name	Template DNA	Sequence	Purpose	Restriction sites
SIMLF	pET28-*simL*	GCCGAATTCATGAAACACCACCACCACCACCACC	Clone *simL* into pJH10	EcoRI - XbaI
SIMLR		GTGTCTAGATCA TTC GCC ATG CGT GGC CTC CC		
NOVLF	pET28-*novL*	GCCGAATTCGTGGCGAACAAGGATCACGC	Clone *novL* into pJH10	EcoRI - XbaI
NOVLR		GTGTCTAGATCACCTGTCCACCAGGACGTC		
CLOLF	pET28-*cloL*	GCCCAATTGGTGGCGAACAAGGACCACG	Clone *cloL* into pJH10	MfeI- XbaI
CLOLR		GTGTCTAGATCACCTGTCCACCAGCACGTC		
COUL	pET28-*couL*	GACCAATTGGTGGCGAACAGGGACCACG	Clone *couL* into pJH10	MfeI- XbaI
		5’ GTGTCTAGATCACCTGTCCACCAGCACGTC 3’		

Table 2.8 Primers used in Chapter 4 (mutated nucleotides are highlighted in RED)

Name	Template DNA	Sequence	Purpose	Restriction sites
a1379cF	pET28-*tmlU*	GTTGGTTAAATACCGGAGCTC TTGGCAAGTTCGATGC	Introduce a point mutation in *tmlU*	N/A
a1379cR		GCATCGAACTTGCCAAGAGCT CCGGTATTTAACCAAC		
g1378a_a1379g F	pET28-*tmlU*	AGAACCAGGTTGGTTAAATAC CGGAAGTCTTGGCAAGTTCGA T	Introduce a point mutation in *tmlU*	N/A
g1378a_a1379g R		ATCGAACTTGCCAAGACTTCC GGTATTTAACCAACCTGGTTC T		
a698gF	pET28-*tmlU*	AACCACGGGAACACCAAGGA TTGCAAGACATACAC	Introduce a point mutation in *tmlU*	N/A
a698gR		GTGTATGTCTTGCAATCCTTG GTGTTCCCGTGGTT		
dTEaF (arm1)	*P. fluorescens NCIMB10586*	GCCGGATCCCTGGTC GATCAAGTGC AGGGCTGGCT	Introduce mutation to TE in *P. fluorescens* 10586	BamHI -HindII
dTEaR (arm1)		GAGGCACATAGAAAAAGCTG GCGAGCATGAACAAC		
dTEaF (arm2)		GTTGTTCATGCTCGCCAGCTTT TTCTATGTGCCTC		
dTEaR (arm2)		GGCAAGCTTCCGCTCCACCTT CAGAATTCGCCTGC		
hTEaF (arm1)	*P. fluorescens NCIMB10586*	GCCGGATCCTGGATACGCAGG CACCGCCAGATCTG	Introduce mutation to TE in *P. fluorescens* 10586	BamHI -HindII
hTEaR (arm1)		TAGCGCGCCAGGGTGGCGGG AAGACTGCTTGC		
hTEaF (arm2)		GCAAGCAGTCTTCCCGCCACC CTGGCGCGCTA		
hTEaR (arm2)		GGCAAGCTTCTCGATCAGCGA CTGCGCCAACGCATA		
tmlUF	SANK73390	GGCTCTAGAGATGAATGAGTC AGCCCTTAACCC	Clone *tmlU* into pUT18	XbaI-EcorI
tmlUR		GCGGAATTCGATGACTCCAGT ACAGTTTGCTCA		
TEF	SANK73390	GGCTCTAGAGTCGCTGGCGGG CGCGGACTCGCC	Clone TE into pUT18	XbaI-EcorI
TER		GCGGAATTCT**TTA**ATGGGGGC TCGCGGTCAGG		

Table 2.9 Primers used in Chapter 5

Name	Template DNA	Sequence	Purpose	Restriction sites
HOL1F	SANK73390	GCGCTCGAGGGAGTTATATTA TGAACATGGATGCATTTAAG	Clone the HOL1 fragment into pGEM-T-easy	XhoI-AgeI
HOL1R		CCGACCGGTCCCTCGGTTTTC TAATATACCGGC		
HOL2F	SANK73390	CGAGGGACCGGTAGTGAGTA AAGAAGCTG	Clone the HOL2 fragment into pGEM-T-easy	AgeI-AvrII
HOL2R		CGCCCTAGGGCTATGCCCACT AAGTTGG		
HOL3F	SANK73390	CCGCCTAGGTTGGTTTTCACA ATAAC	Clone the HOL3 fragment into pGEM-T-easy	AvrII-BstbI
HOL3R		GCGTTCGAACTATGGCCCTTT TGTCTTAGTAG		
tmlUHF	SANK73390	GGAGAGCTCATGAATGAGTC AGCCCTTAACCC	Clone couL into pJH10	MfeI- XbaI
tmlUHR		GGCTCTAGATCATGACTCCAG TACAGTTTGC		

Table 2.10 Primers used in Chapter 6

Name	Template DNA	Sequence	Purpose	Restriction sites
KS2/KS1F (arm1)	*P. fluorescens10 586*	CGCAAGCTTCATATGCGCGA CCAGGACATCGTGGTCGAG CCAGCGGTACTGTTCGAGCA CGCTAC	Replacing KS2 loop with the KS1 loop	HindIII EcoRI-
KS2/KS1 R (arm1)		CATACTGGCCGCCTGGTCCA GCCCTTCGCCGGGATCAATC TGGGCCTGGAGTAGGTTGA GGTGGTATTCGTTACGCTCG GCGGCCACGAATACGCCGA CCTTCTCC		
KS2/KS1F (arm2)		CTGGACCAGGCGGCCAGTA TGATCGCCAACCGCGTGTCT TATC		
KS2/KS1 R (arm2)		GGCGAATTCGATGGGATCG CCCAGCGCCGTAC		
KS2/KS3F (arm1)	*P. fluorescens10 586*	CGCAAGCTTCATATGCGCG ACCAGGACATCGTGGTCGA GCCAGCGGTACTGTTCGAGC ACGCTACGCC	Replacing KS2 loop with the KS3 loop	HindIII EcoRI-
KS2/KS3 R (arm1)		CGACGATGGGCTCATGGAC AGCACCAGCGGCCGCCCCT CGGCAGTCTGTTGCGCCCCA TACAGTTGGTACTCTTCGTA CGTTACGCCCACGAATACGC CGACCTTCTCC		
KS2/KS3 R (arm2)		GCTGTCCATGAGCCCATCGT CGATCGCCAACCGCGTGTCT TATC		
KS2/KS3 R (arm2)		GGCGAATTCGATGGGATCG CCCAGCGCCGTAC		
tmlUHR		GGCTCTAGATCATGACTCCA GTACAGTTTGC		

2.2.1 Velocity DNA polymerase kit

Velocity polymerase possesses 3´-5´ proofreading exonuclease activity which makes it suitable for high fidelity PCR. Velocity DNA has been developed to reduce extension time remarkably to 10s/kb, as opposed to 2 minutes for *Taq* polymerase. Also, velocity polymerase can be used to amplify fragments as large as 9kb from genomic DNA with high yield due to its processivity. Details of the reaction mixture are outlined in Table 2.11. A Sensoquest labcycler was used to carry out PCR using the program in Table 2.12.

Table 2.11 Velocity DNA polymerase reaction conditions

Reagents	Volume/Reaction µl
5x Hi-Fi reaction buffer (contains 10 mM Mg^{+2})	10
dNTPs (2.5 mM)	5
Forward primer (10 µM)	2
Reverse primer (10 µM)	2
DMSO	1.5
ddH_2O	27.7
Velocity DNA polymerase	0.5

Table 2.12 Velocity PCR program details

Description	Length	Temp (C°)	Cycles
Initial denaturation	2.00 min	98	1
Denaturation	30 sec	98	25-35
Annealing	30 sec	50-68	
Extension	15-30s/kb	72	
Final extension	4-10 min	72	1

2.2.2 Invitrogen *Taq* polymerase

Taq DNA polymerase is isolated from *Thermus aquaticus*. It is a heat stable enzyme but it does not have a 3-5 exonuclease activity and consequently no proofreading function. For this reason, *Taq* was only used for PCR screening following the protocol detailed in Table 2.13. PCR conditions are listed in Table 2.14

Table 2.13 Taq DNA polymerase reaction conditions

Reagents	Volume/Reaction µl
10x Buffer DNA	5
dNTPs (2.5 mM)	4
Forward primer (100 µM)	0.3
Reverse primer (100 µM)	0.3
50% glycerol	1.5
ddH_2O	27.8
MgCL (50mM)	1
Taq DNA polymerase	0.6

Table 2.14 PCR program for Taq DNA polymerase

Description	Length	Temp (C°)	Cycles
Initial denaturation	2.00 min	94	1
Denaturation	15 sec	94	30
Annealing	30 sec	(T_m — 4)	
Extension	1.00 min	72	
Final extension	7.00 min	72	1

2.2.3 QuickChange site directed mutagenesis

For site directed mutagenesis; the QuikChange Lightning Multi Site-Directed Mutagenesis Kit from Agilent Technologies was used, and amplification of the mutated fragments was done according to the manufacturer's protocol. The desired point mutation was designed to be close to the middle of the primer with ~10–15 bases of template-complementary sequence on both sides. Details of the protocol and PCR conditions are shown in Table 2.15 and Table 2.16 respectively.

Table 2.15 QuickChange site directed mutagenesis reaction conditions

Reagents	Volume/Reaction µl
10x Buffer DNA	5
dNTPs (2.5 mM)	1
Forward primer (10 µM)	1
Reverse primer (10 µM)	1
QuickSolution reagent	1.5
ddH_2O	To a final volume of 50
DsDNA template	10-100 ng

Table 2.16 PCR parameters for the QuickChange Lightning Site-Directed Mutagenesis

Segment	Length	Temp (C°)	Cycles
1	2.00 min	95	1
2	20 sec	95	18
	10 sec	60	
	30 sec /kb	68	
3	5.00 min	68	1

2.3 DNA manipulation

2.3.1 Plasmid extraction

Plasmid extraction was performed using Bioneer Accuprep® plasmid mini extraction kit or ISOLATEII plasmid mini kit from Bioline.

2.3.1.1 ISOLATEII plasmid mini kit from Bioline

Plasmid isolation was carried out using the solution provided by Bioline and according to the manufacturer's protocol. *E. coli* LB culture, 5ml, was harvested by centrifugation for 2 min at 11,000xg. The supernatant was then discarded and 500µl of the Buffer P1 was added to the pellet which was then resuspended by vortexing or pipetting up and down. The cells were lysed by adding Buffer P2 and gently inverting the tubes 6-8 times to avoid shearing of genomic DNA. The mix was incubated at room temperature for 5 min or until the lysate appears clear. 600µl of the neutralization buffer P3 was added and the tube was again thoroughly mixed by inverting. To clarify the lysate cells were spun for 10 minutes at 11,000 xg at room temperature. Binding of the DNA was achieved by pipetting 750µl of the clear lysate into ISOLATEII plasmid mini spin column and centrifuged for 1 minute at 11,000 x g. The flow-through was discarded and 500µl of wash buffer PW1 (preheated to 50°C) was added to the filter and centrifuged for 1 minute at 11,000 xg/11336.52 rpm 600µl of washing buffer PW2 was also added to the filter and centrifuged for 1 minute at 11,000 xg. After discarding the flow-through, the sample was centrifuged for another 2 minutes to remove residual ethanol. To elute, the spin column was placed in a 1.5 ml microcentrifuge tube and 50µl buffer P (preheated to 70°C) was directly added to the centre of the silica membrane and incubated for 2 minutes before it was spun down for 1 minute at 11,000 xg.

2.3.1.2 Bioneer Accuprep® plasmid mini extraction kit

5 ml of *E. coli* LB culture was collected by centrifugation at >8,000 rpm for 2 minutes. The supernatant was completely removed by pipetting and the cells were resuspended in 250 µl of Buffer 1. 250µl of buffer 2 was added to the previous mix. In order to get a clear lysate, 350µl of buffer 3 was added and the tubes were gently inverted 3-4 times to thoroughly mix the contents. The samples were then centrifuged at 16,600 x g at 4°C for 10 min or until white protein aggregation could be seen on the bottom of the tube leaving a clear lysate. Plasmid purification process involved transferring the cleared lysate to the DNA binding column, centrifugation at 16,600 x g for 1 minute and adding 500µl of buffer D (incubation for 5 minutes) the purpose of which is to inactivate any endonucleases that might degrade the plasmid DNA. To remove salts and other soluble debris, 700µl of buffer 4 was added to the DNA binding column and centrifuged for 1 minute at 16,600 x g. The flow-through was discarded and the samples were centrifuged again for 1 minute at 16,600 x g to remove any residual ethanol. The DNA binding column was transferred into a new microcentrifuge tube and DNA was eluted by adding 50 - 100µl of buffer 5 to the DNA binding filter. This was incubated for 1 minute and then centrifuged for 1 minute at 16,600 x g.

2.3.2 Restriction digest

Restriction digestion was carried out using enzymes purchased from New England Biolabs (NEB). Reaction volume was 50 µl for the purpose of cloning and 20µl for insert detection. The amount of enzymes added to the reaction did not exceed 2 µl. 4-5µl of the (10x) appropriate buffer was added which also includes the Bovine serum albumin (BSA). 5 -30µl of DNA was added to the reaction and the final volume was made up by adding sterile distilled H_2O. The samples were incubated at 37°C for two hours.

2.3.3 Agarose gel electrophoresis

Gels with a concentration of 1% (w/v) agarose were used to analyse PCR and restriction digest products. Agarose (1g) was suspended in 100ml of TAE buffer (40mM tris-acetate, 1mM EDTA pH8.0). The mixture was microwaved for 2 minutes and then cooled down at room temperature before adding 2µl of ethidium bromide solution (10mg ml^{-1}). The gel was poured into a tray, combs were inserted and then the gel allowed to set at room temperature. DNA samples to be loaded were prepared by adding 2µl of loading buffer (bottom: 0.25% w/v bromophenol blue, 15% w/v ficoll; top: 0.25% w/v xylene cyanol, 15% w/v ficoll) to 5µl DNA and 5µl H_2O. The samples were run on a gel alongside 1kb DNA molecular ladder (Fermentas) at 100V/500mA for 40 minutes. DNA was then visualised using a UV transilluminator.

2.3.4 DNA extraction from TAE *(*Tris-acetate-EDTA) agarose gel

Extracting DNA samples from agarose gel was carried out using the Illustra GFX PCR DNA and gel band purification kit from GE healthcare. The purification procedure was performed according to GE healthcare instructions with the solutions provided by the manufacturer. After the DNA samples were cut out of the agarose gel, gel bands were weighed and placed in a 1.5 ml microcentrifuge tube and capture buffer 3 was added (10µl/10mg). Samples were incubated in a 55°C water bath and inverted every 3 minutes until the gel bands were completely dissolved. Up to 800µl of capture buffer 3 was transferred to the GFX microspin column, incubated at room temperature for 1 minute and then centrifuged at 16,000x g for 30 seconds. The flow-through was removed and the filter was washed by adding 500µl of wash buffer type 1 to the GFX microspin column and centrifuging at 16,000x g for 30 seconds. The GFX microspin column was then transferred to a new 1.5 ml microcentrifuge tube and DNA was eluted by adding 10-50 µl elution buffer type 4, incubating for 1 minute at room temperature and spinning the samples at 16,000x g for 1 minute to recover the purified DNA. The purified DNA samples were stored at -20 ^{o}C degrees.

2.3.5 A-tailing blunt-ended PCR products

PCR products were A-tailed in order to ligate them to pGEM-T-Easy, a linearized vector with a single 3′-terminal thymidine at both ends which makes it necessary to add an A tail to the insert. The components detailed in Table 2.17 were all mixed in a microcentrifuge tube and incubated at 70°C for 30 minute prior to ligation to pGEM-T-Easy.

Table 2.17 A-tailing blunt ended PCR products

Reagents	Volume/Reaction µl
Purified PCR fragment	6
Invitrogen *Taq* MgCl2	1
dATP (2mM)	1
10 x Invitrogen Taq buffer	1
Invitrogen Taq DNA polymerase	1

2.3.6 DNA ligation

Ligations were performed either by using pGEM-T-Easy vector system which provides the blue/white screening option for inserts, or using the T4 DNA ligase kit from (Invitrogen). The DNA concentration of both the vector and the insert were determined using a Nano-drop machine (ND-100) or run on an agarose gel alongside known quantities of molecular weight standards. The following method was used to calculate 3:1 ratio for ligation reactions:

$$\text{Ratio unit} = \frac{size\ of\ vector}{size\ of\ insert}$$

$$\text{Ratio factor} = \frac{3}{ratio\ unit}$$

Molecular weight in ng of vector and insert required for the ligation

50ng (vector) x ratio factor = ng of insert

Ligation reactions were usually made up in 20µl volume and incubated overnight at 4°C.

2.3.7 Splicing by overlap extension (gene SOEing)

SOEing PCR was used to introduce site specific mutations, deletions or generating recombinant gene constructs. This was achieved by designing specific primers that include in their sequence the desired changes and also have terminal complementarity; two overlapping fragments can be attached together by a subsequent extension reaction (Figure 2.1). This method can be applied to fuse together two or more DNA fragments from different genes to produce the desired recombinant.

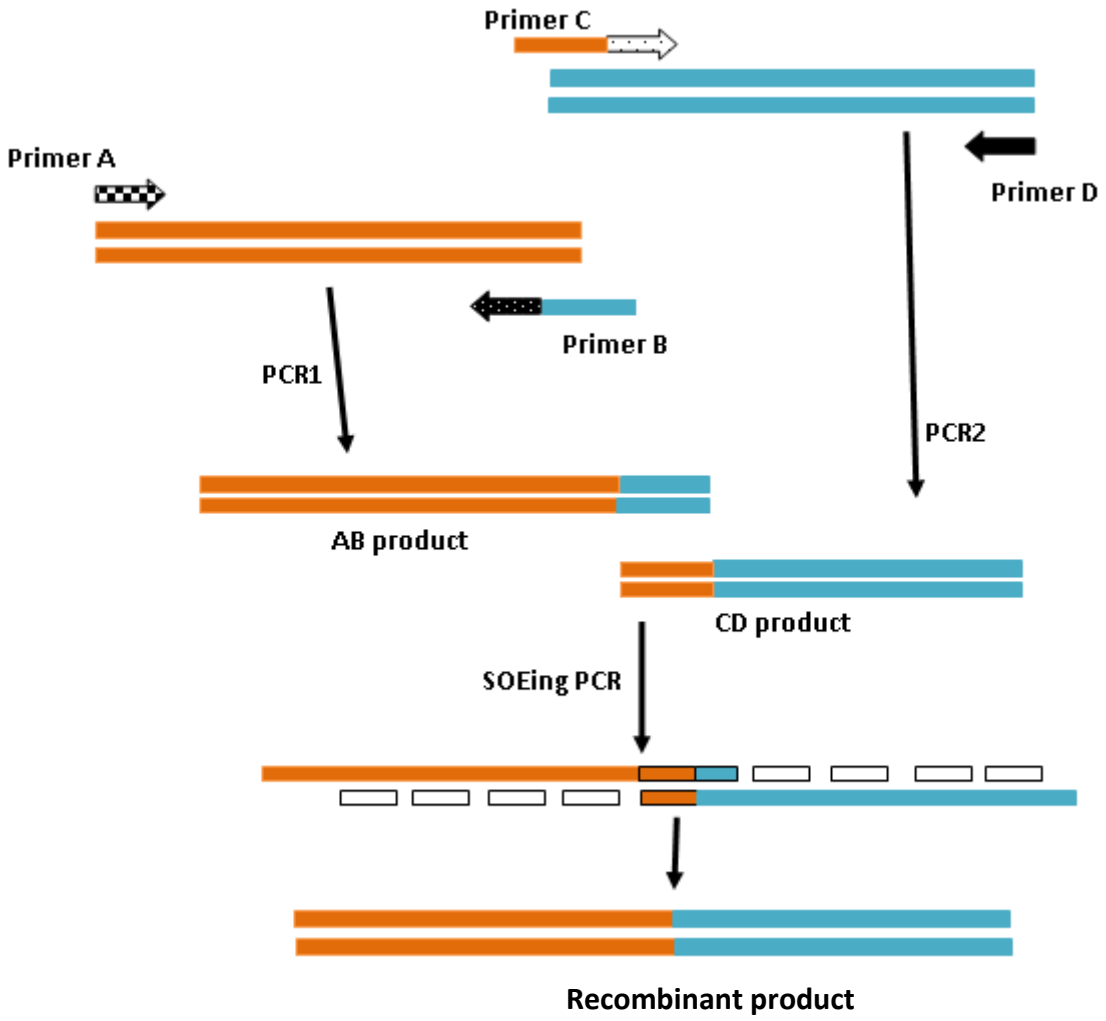

Figure 2.1 Splicing by overlap extension. Fragment AB is amplified using primers A and B, while fragment CD is amplified using primers C and D. For site directed mutagenesis pieces AB and CD are adjacent parts of the same gene where the mutation will be introduced. Primers B and C are chimeric, and are designed in a way that that the 3' ends complement fragment AB and fragment CD respectively. The PCR products (AB and CD) are gel purified and mixed together with all the required PCR components except the primers. AB and CD act as primers in this situation and allow the DNA to extend using the sequence complementarity between the two DNA pieces. A final PCR is carried out, this time with the primers A and D to produce the recombinant product.

2.3.8 DNA transformation

E. coli competent cells of S17-1 and DH5α were made according to (Cohen *et al*., 1972). An overnight culture of *E. coli* was diluted 1:100 in fresh L broth and grown at 37°C, 200 rpm until the OD_{600} reached 0.4-0.6. The cells were centrifuged at 11,000xg, 7 minutes and 4°C. The supernatant was removed and the cells resuspended in pre-chilled 100mM $CaCl_2$ (2ml per 5ml of culture). Cells were incubated on ice for 20 minutes, spun down for another 7 minutes at 4°C and 11,000xg. The supernatant was discarded and the pellet was resuspended in pre-chilled 100 mM $CaCl_2$ (0.5 ml per 5ml culture). At this stage the cells should be competent but were left on ice for several hours to improve their competency. Competent cells were stored at 4°C for up to two weeks. Transformation was achieved by adding 5µl of DNA to 100µl of competent cells. The mixture was left on ice for 30 minutes after which the cells were heat shocked by placing them in a 42°C water bath for 2 minutes. 1ml of L broth was added and the tubes were incubated at 37°C, 200 rpm for 1 hour. Cells were then plated out on selective plates and incubated overnight at 37°C.

2.3.9 DNA sequencing

For the clone to be sequenced, plasmid DNA was first extracted, of which 200-500ng was added to 3-4pmoles of the appropriate primers and the volume made up to 10µl with sterile distilled H_2O. Sequencing services were provided by the functional genomics laboratory at the University of Birmingham using an ABI 3700 analyser. Chromas Lite was used to analyse the generated sequences.

2.3.10 Sequencing analysis

Alignments of DNA and amino acid sequences were performed using the BLAST function (http://blast.ncbi.nlm.nih.gov/Blast.cgi). Alignments for multiple amino acid and

protein sequences were generated using COBALT (http://www.ncbi.nlm.nih.gov/tools/cobalt/cobalt.cgi) or ClustalW (http://www.ebi.ac.uk/Tools/msa/clustalw2/).

2.3.11 Conjugation and suicide vector excision

Conjugation was used to mobilize expression vectors and suicide plasmid derivatives from *E. coli* S17-1 to *P. fluorescens*. The process starts with mixing 1 ml of *E. coli* S17-1 containing the desired plasmid with 1 ml of *P. fluorescens*. The bacterial mating mixture was then collected by filtering onto a sterile 0.45µM Millipore filter which was then placed on an L agar plate at 30°C and left overnight to allow conjugation. The filter was washed with 1 ml sterile saline solution (0.85%) and serial dilutions were made ranging from 10^{-1} to 10^{-5}. 100µl aliquots from each dilution was plated on selective plates or M9 minimal media: 200ml salt solution containing NA_2HPO_4 (6g/l), KH2PO4(3g/l), NH4Cl (1g/l),MgSO4(1mM), thiamine HCl (1mM), CaCl2(0.1mM),glucose (0.2%) added to 200ml 50% H_2O agar) and left for 2-3 days to grow at 30°C. In the case of M9 minimal medium, single colonies were restreaked on selective M9 plates and incubated at 30°C for 2-3 days. Single colonies of the transconjugants were then streaked on selective L agar plates, while for chromosomal integration purposes the plates were supplemented with kanamycin. Overnight cultures were made out of the co-integrant colonies; serial dilutions were made and plated on L agar with 5% (w/v) sucrose to select for bacteria in which the integrated suicide vector has excised and been lost. To check for integration, colonies were patched onto an ampicillin plate followed by a kanamycin plate simultaneously and then incubated at 30°C for 2 days. Colonies were screened for the correct genotype by colony PCR.

2.4 Bioassay for Mupirocin production

The OD_{600} of overnight cultures of both wild type and mutant *P. fluorescens* was measured and the cultures were diluted to the OD_{600} of the least dense culture. Culture (10µl) was spotted on 20ml L agar plates which were incubated at 30°C overnight. The spots were then over-laid with L agar containing 40µl ml^{-1} *B. subtillis* overnight cultures and 2,3,5-triphenyltetrazolium chloride TTC (0.25mg ml^{-1}) and incubated overnight at 37°C. TTC is a commonly used redox indicator to signify cellular respiration since it acts as an alternative electron acceptor. Therefore, the agar turns red due to the actively growing *B. subtillis*, while where there is no growth the agar remains colourless. Mupirocin production was estimated by measuring the clearing zone where *B. subtillis* did not grow. Assays were done in triplicate and analysed statistically by calculating standard errors.

2.5 Bacterial two hybrid system

The bacterial two hybrid system (BACTH) exploits the fact that the catalytic domain of adenylate cyclase (CyaA) from *Bordetella pertussis* consists of two complementary fragments, T25 and T18, (Figure 2.2) that are not active when physically separated. When these two fragments are fused to interacting polypeptides, X and Y, heterodimerization of these hybrid proteins results in functional complementation between T25 and T18 fragments and therefore cAMP synthesis. Cyclic AMP produced by the reconstituted chimeric enzyme binds to the catabolite activator protein, CAP. The cAMP/CAP complex is a regulator of gene transcription in *E. coli* and it is involved in turning on the gene expression of, for example, the *lac* and *mal* operons involved in lactose and maltose catabolism. As a result, bacteria become able to utilize lactose or maltose as the unique carbon source and can be easily distinguished on indicator media. As a positive control, the reporter strain BTH101 were co-transformed with pUT18-zip and pKT25-zip while the

negative control was BTH101 transformed with the empty vectors pUT18 and pKT25 (Battesti and Bouveret, 2012). The genes encoding the proteins of interest were amplified by PCR and cloned into the vectors PKT25 and pUT18 in frame with the T25 and T18 fragments. The constructs were then transferred into DH5α strain and the plasmid DNA purified as described in section 2.3.1. The reporter cell BTH101 strain was then co-transformed with the two recombinant plasmids and incubated on indicator plates containing X-Gal (40 µg/ml) and 0.5 mM IPTG at 30°C for 24-72 hours.

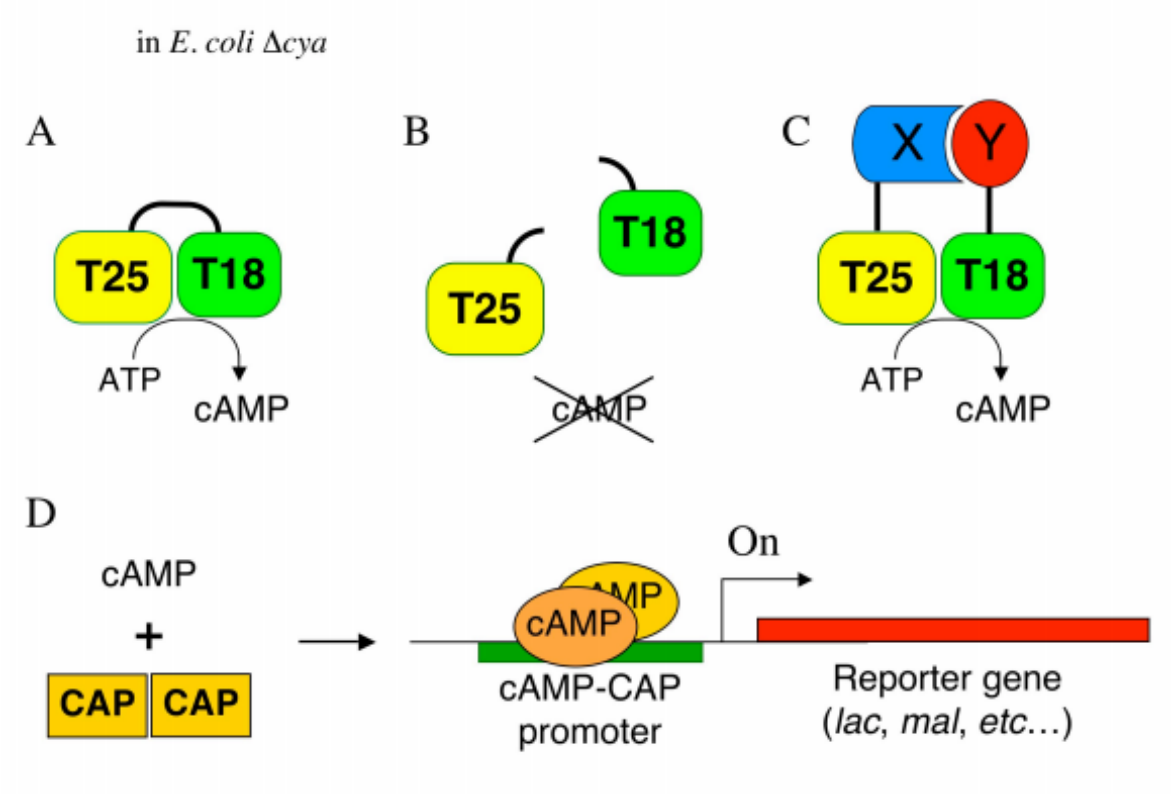

Figure 2.2 Principle of bacterial two hybrid system (Battesti and Bouveret, 2012). A) When the T25 and T18 fragments are co-localised they catalyse cAMP synthesis. B) When not co-localised, the fragments do not catalyse cAMP synthesis. C) When the T25 and T18 tags are fused to proteins that interact, the interaction can be detected by the co-localisation of T25 and T18 and the subsequent cAMP synthesis. D) Increased cAMP concentration leads to increased binding of cAMP to CAP, which is a regulator of several reporter genes.

2.6 High performance liquid chromatography

2.6.1 Mupirocin detection

Seed cultures of the tested strains were prepared by inoculating one colony into 25ml LB in a 250ml flask and incubating at 25°C and 200 rpm for 16 hours. 25ml of SSM medium (25g.$L^{-1,}$ soya flour, 2.5 spray dried corn liquor, 5 $(NH_4)_2$, 0.5 $MgSO_4.7H_2O$, 1 Na_2HPO_4, 1.5KH_2PO_4, 1 KCL, 6.25 $CaCO_3$, 4% Glucose) was inoculated with 1.25ml of the seed culture and incubated at 22°C, 200 rpm for approximately 40 hours. Samples were then centrifuged at 29,000xg for 10 minutes and the supernatant pH was adjusted to 4.5 with HCL. Prior to running the samples, supernatants were filtered using 0.2µm filters. HPLC was performed on a Gilson system using a reverse phase C18 column (15cm x 4.6mm) with a mobile phase of water/acetonitrile gradient (5-70% acetonitrile trifuoroacetic acid (0.01%)) over 60min at 1ml min^{-1} flow rate. Compounds were detected by UV absorption at 233nm and data was analysed using Unipoint LC system software.

2.6.2 Thiomarinol detection

Thiomarinol was extracted from 2ml SANK73390 culture. The culture pH was adjusted to pH6 and an equal volume of acetone was added to each culture. The mixture was vortexed for about 5 minutes and left for at least an hour at 4°C. The acetone was then removed using a speed vacuum pump for approximately 1 hour prior to adding an equal volume of ethyl acetate. The mix was left to settle until it had separated into two clear phases, the yellow layer at the top containing Thiomarinol and ethyl acetate and the bottom layer containing all the cell debris. The upper phase was transferred into a 2 ml microcentrifuge tube and the ethyl acetate was completely removed by the speed vacuum pump after which Thiomarinol was resuspended in 200µl methanol and analysed by HPLC with UV detection at 385nm.

2.7 β-galactosidase assay

Bacterial cells to be tested for their β-galactosidase activity were grown in 5 ml of LB broth in the presence of 0.5 mM IPTG and appropriate antibiotic at 30°C and 200 rpm for 4-6 hours or overnight. The cultures were then diluted 1-5 with 1x M63 medium which was prepared from autoclaved x5 M63 (10 g (NH4)2SO4**,** 68 gKH2PO4, 2.5 mg FeSO4.7H2O, 5 mg vitamin B1, and deionized H2O to a final volume of 1 L, pH adjusted to 7.0 with KOH) and the OD_{600} was measured. For the purpose of permeablizing bacterial cells 30µl of both toluene and 0.1% SDS solution were added to 2.5 ml of the diluted cell suspension. The cells were vortexed for 10 seconds and left at 37°C for 30-40 minutes to allow the toluene to evaporate. In a test tube 100 µl of the permealized cells were added to 900 µl of PM2 buffer (70 mM Na_2HPO_4**.**$12H_20$, 30 mM NaH_2PO_4 H_20, 1 mM $MgSO_4$,0.2 mM $MnSO_4$, pH 7.0, plus 100mM of β-mercaptoethanol added just before use) the tubes were then left in a 28°C water bath for 5 minutes.

To start the enzymatic reaction 250 µl of the ONPG substrate solution (0.4% ONPG in PM2 buffer without the β-mercaptoethanol) preheated to 30°C was added to the previous mix of permeablized cells and PM2 buffer. The reaction was stopped after 10 minutes by adding 500 µl of 1M of Na_2CO_3. The OD_{420} was measured and the enzymatic activity was calculated based on the following equation: A (units/ml) = 200 x (OD_{420} – OD_{420} in control tube) / min of incubation) x dilution factor.

Chapter 3

3 The effect of the amide synthetases NovL, CloL, CouL and SimL on production of pseudomonic acids

3.1 Introduction

The concept of mutasynthesis was first introduced by Birch (1963) as a way to generate analogues of different antibiotics from different classes, by utilizing genetically modified organisms in combination with feeding of chemical precursors. However, the term itself was coined by Rinehart in 1977 (Rinehart, 1977). Although very similar to the precursor directed biosynthesis (PDB), the mutasynthesis approach was able to eliminate competing natural precursors. Therefore, a less complex mixture of metabolites is produced, which makes purification of compounds simpler, yields higher and also increases the chances of successful incorporation of more diverse precursor analogues (Kennedy, 2008).

Mutasynthesis initially involved random mutagenesis, which was then followed by isolation and characterisation of the non-producing strains. One of the first mutasynthesis studies was conducted using the strain *Streptomyces fradiae* that produces neomycin B2 (Shier *et al*., 1969). The strain was subjected to random mutagenesis, which resulted in mutants that can only produce neomycin B2 when supplemented with the aminocyclitol precursor deoxystreptamine. When this mutant strain was supplemented with the aminocyclitols streptamine and epistreptamine, these unnatural precursors were utilised by the biosynthetic machinery to produce the novel neomycin analogues, hybrimycin A1 6 and hybrimycin B2 7 respectively (Kennedy, 2008).

Following the successful generation of neomycin analogues, this method was applied to many different biosynthetic pathways in order to create a wide range of

analogues, which included macrolide antibiotics such as erythromycin and platenolides in addition to β-lactams antibiotics (Daum and Lemke, 1979). Combinatorial biosynthesis was also amongst the approaches developed to achieve diversity in natural products. This technique combines genes from different biosynthetic pathways in order to generate novel compounds. In this respect, the aminocoumarins have been the perfect example of creating new structural variants through utilizing synthetic chemistry and genetic engineering (Heide, 2009b) (Figure 3.1).

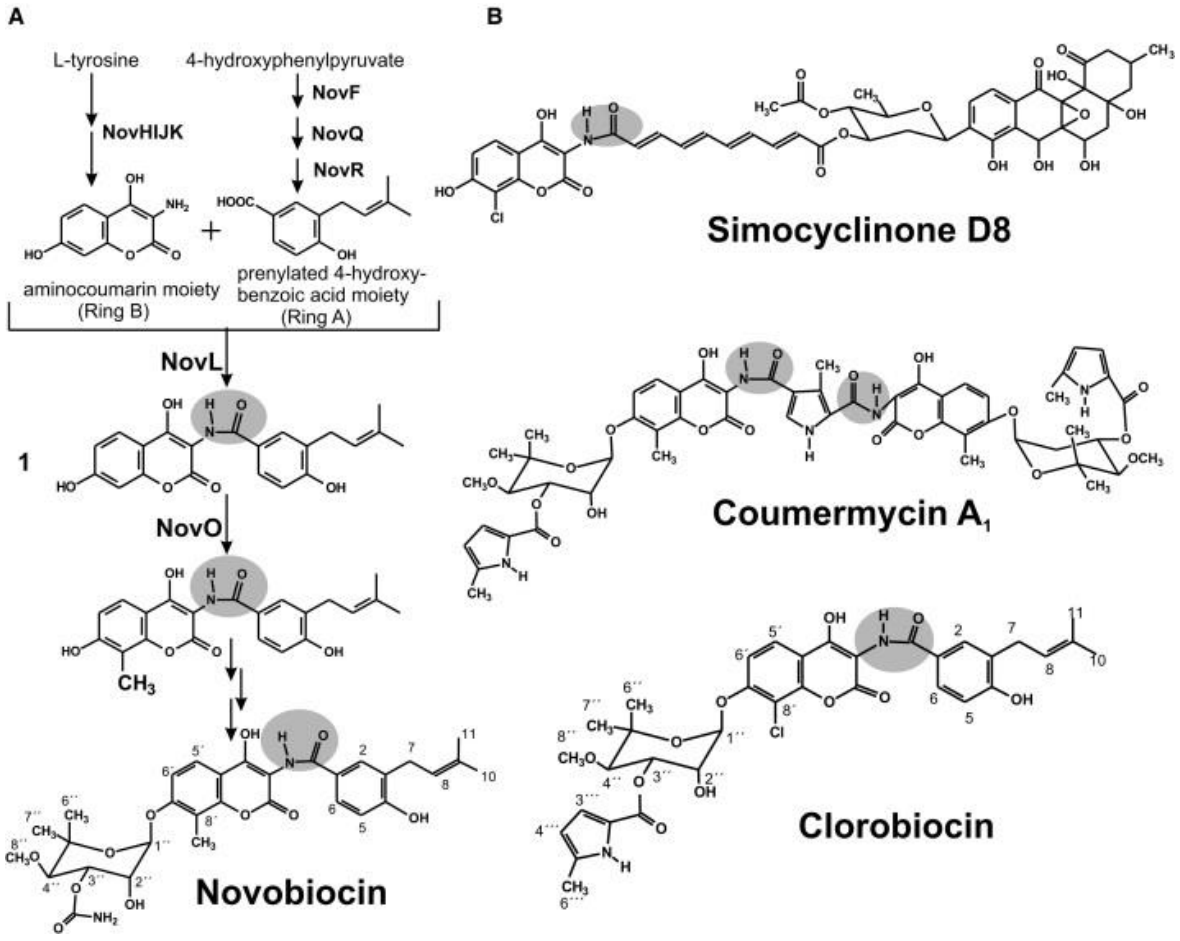

Figure 3.1 Aminocoumarin antibiotics and the biosynthesis of novobiocin (reproduced from Anderle *et al*., 2007b).

A prenyalated 4-hydroxybenzoyl moiety is the starter molecule in the clorobiocin biosynthetic pathway. It is formed from 4-hydroxyphenylpyruvate and dimethylallyl diphosphate and catalyzed by CloQ and CloR. Studies in the Lutz Heide lab confirmed that inactivation of either CloQ or CloR abolishes prenyalated 4-hydroxybenzoyl production and consequently antibiotic production (Pojer *et al*., 2003). To overcome this hurdle, synthetic analogues of the 4-hydroxybenzoyl moiety were added to the mutant strain lacking CloQ/ CloR, which resulted in formation of different clorobiocin analogues. This demonstrated the successful incorporation of these synthetic analogues into the clorobiocin skeleton. Although this was a very encouraging finding, substrate specificity appeared to prevent efficient incorporation of the synthetic substrate analogue (Heide, 2009b). This was overcome by using amide synthetases from other aminocoumarin pathways to replace CloL, and test their specificity in accepting different precursors. In the case of clorobiocin, it was found that the amide synthetase SimL and CouL from coumermycin and simocyclinone clusters respectively, were the most promiscuous in accepting a variety of precursors which were not accepted by CloL (Anderle *et al*., 2007b, Heide, 2009b).

NovL, CloL, CouL and SimL are all amide ligases essential for the assembly of novobiocin, clorobiocin, coumermycin and simocyclinone, respectively. Whereas TmlU is a CoA - ligase in the Thiomarinol biosynthesis cluster (see section 1.3.7), and together with HolE, has been demonstrated responsible for catalysing the attachment of the marinolic acid part to the holomycin part of the pathway (Figure 1.17) (Dunn *et al*., 2015). Given the role they play in their native systems, these enzymes might be able to act as a linking agent between two molecules from different pathways.

In this chapter we aimed to develop a combinatorial biosynthesis and mutasynthesis-based approach for the development of new bioactive molecules centered on the Mupirocin, Thiomarinol and Aminocoumarins. We aimed to test the hypothesis –

can TmlU, SimL and their homologues catalyse the linkage of mupirocin to other compounds, initially thiomarinol and aminocoumarin.

3.2 Results

3.2.1 Constructing pSIML, pCLOL, pNOVL and pCOUL

The genes *simL*, *cloL*, *novL* and *couL* from *Streptomyces* species were cloned into the broad host expression vector pJH10 using the primers listed in (Table 2.7). PCR products for *simL* and *novL* were digested with *Eco*RI and *Xba*I, while *cloL* and *couL* were digested with *Mfe*I (which recognises C^{v}AATTG and produces sticky ends identical to those produced by *Eco*RI) and *Xba*I. All were inserted into the expression vector pJH10 digested with *Eco*RI and *Xba*I. The resulting plasmids were designated pSIML, pCLOL, pNOVL and pCOUL, and only the sequenced clones were used in the downstream applications.

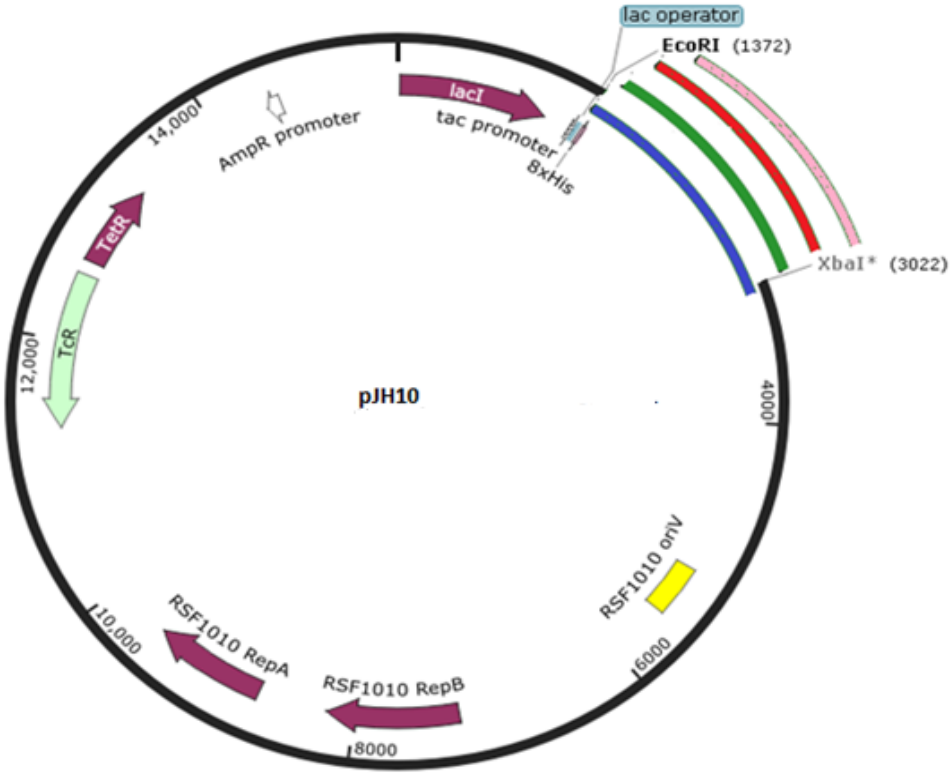

Figure 3.2 Cloning *simL, novL, couL* and *cloL*. The map of the vector pJH10 showing the insertion of *simL* (red arc), *novL* (blue arc), *couL* (green arc) and *cloL* (magenta arc). pSIML (**15.26kb**), pCLOL (**15.27kb**), pCOUL (**15.27kb**) and pNOVL (**15.30kb**).

3.2.2 HPLC analysis of pseudomonic acids produced by *P. fluorescens* WT NCIMB10586, NCIMB10586 (pSIML), NCIMB10586 (pNOVL), NCIMB10586 (pCLOL), NCIMB10586 (pCOUL)

Following the method described in section (2.6.1), pseudomonic acids produced were detected using HPLC for *P. fluorescens* NCIMB10586 with each of the amide synthetases expressed in-*trans*. NCIMB10586 WT and NCIMB10586-pJH10 were used as controls, and all the samples were tested in biological triplicates. Unlike when TmlU (the CoA-ligase in the thiomarinol biosynthesis cluster which interfered with mupirocin biosynthesis) was introduced, mupirocin was still produced. No significant difference in pseudomonic acid A production was observed with expression of each homolog in-*trans* (Figure 3.3), integration of peaks is recorded in Appendix A.

As these homologues were not inhibitory to mupirocin biosynthesis like TmlU, they proved good candidates for mutasynthetic experiments.

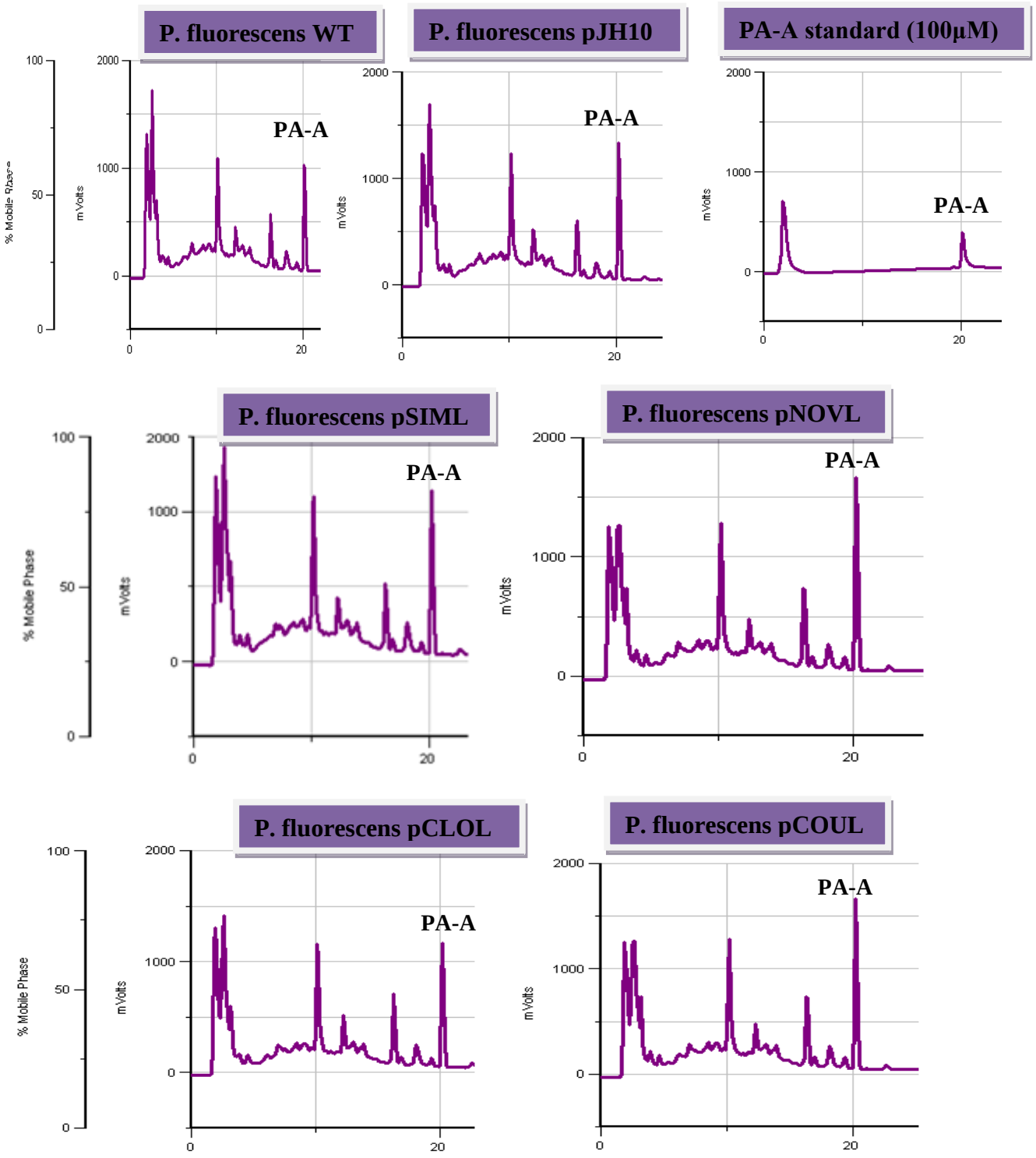

Figure 3.3 HPLC chromatograms of NCIMB10586 WT, NCIMB10586 pJH10, 100µM pseudomonic acid A standard, NCIMB10586 pSIML, NCIMB10586 pNOVL, NCIMB10586 pCLOL and NCIMB10586 pCOUL. UV of (233nm).

3.2.3 Effect of the amide synthetases on thiomarinol production and attempts to complement a Δ*tmlU* mutant

When *tmlU* (section 1.3.7) was deleted in pTML1 (thiomarinol cluster), marinolic acid and pyrrothine were produced separately, implying that TmlU plays a role in attaching these two parts together (Fukuda *et al*., 2011). In the aminocoumarin system several amide synthetases play a similar role, these include SimL, CloL, CouL and NovL (section 1.4). The aims of this experiment were to investigate whether it is possible to complement *Pseudoalteromonas spp.* SANK73390Δ*tmlU* with *tmlU* expressed *in trans*, and furthermore whether the amide ligases from the aminocoumarin pathways complement. The outcome of this study should be beneficial in deciding to what extent these amide synthetases can be exploited to make hybrid biosynthetic pathways.

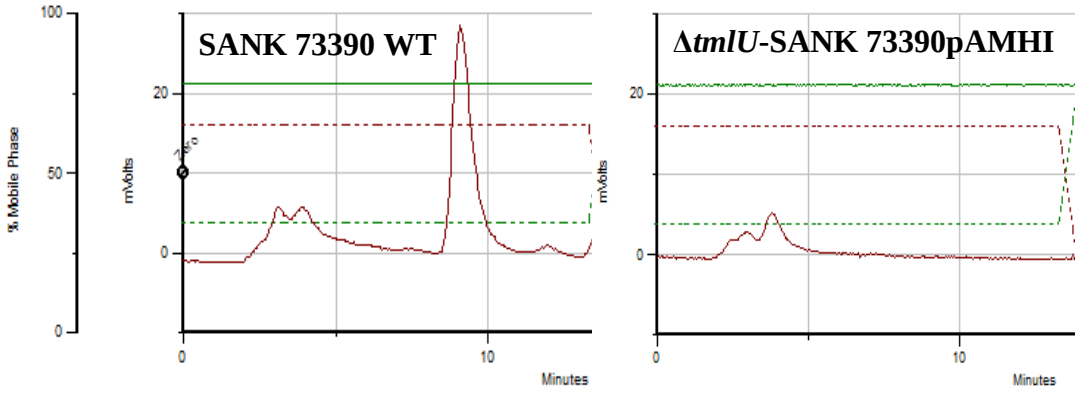

Figure 3.4 HPLC chromatograms of *tmlU* complementation experiment. *tmlU* was expressed *in trans* in Δ*tmlU*SANK73390. The green line represents the mobile phase

For this purpose, the amide synthetases were expressed *in trans* in SANK73390*ΔtmlU*. SANK73390 WT and SANK73390Δ*tmlU* were used as controls. thiomarinol was extracted from the transconjugant SANK73390 strains as described in (section 2.6.2) and detection of thiomarinol plus any new products was carried out by HPLC. Expression of *tmlU* in-*trans* from pJH10-*tmlU* in SANK73390Δt*mlU* did not restore thiomarinol production (Figure 3.4). No complementation was observed for SimL, NovL, CloL or CouL as well (data not shown).

Introducing SimL, NovL, CloL and CouL to a wild type SANK73390 did not have any effect on Thiomarinol production and a clear peak of Thiomarinol was observed at a retention time of 10 minutes (Figure 3.5). As these aminocoumarin amide synthetases had no detectable inhibitory effect on both mupirocin and thiomarinol production, they showed potential for mutasynthetic feeding experiments.

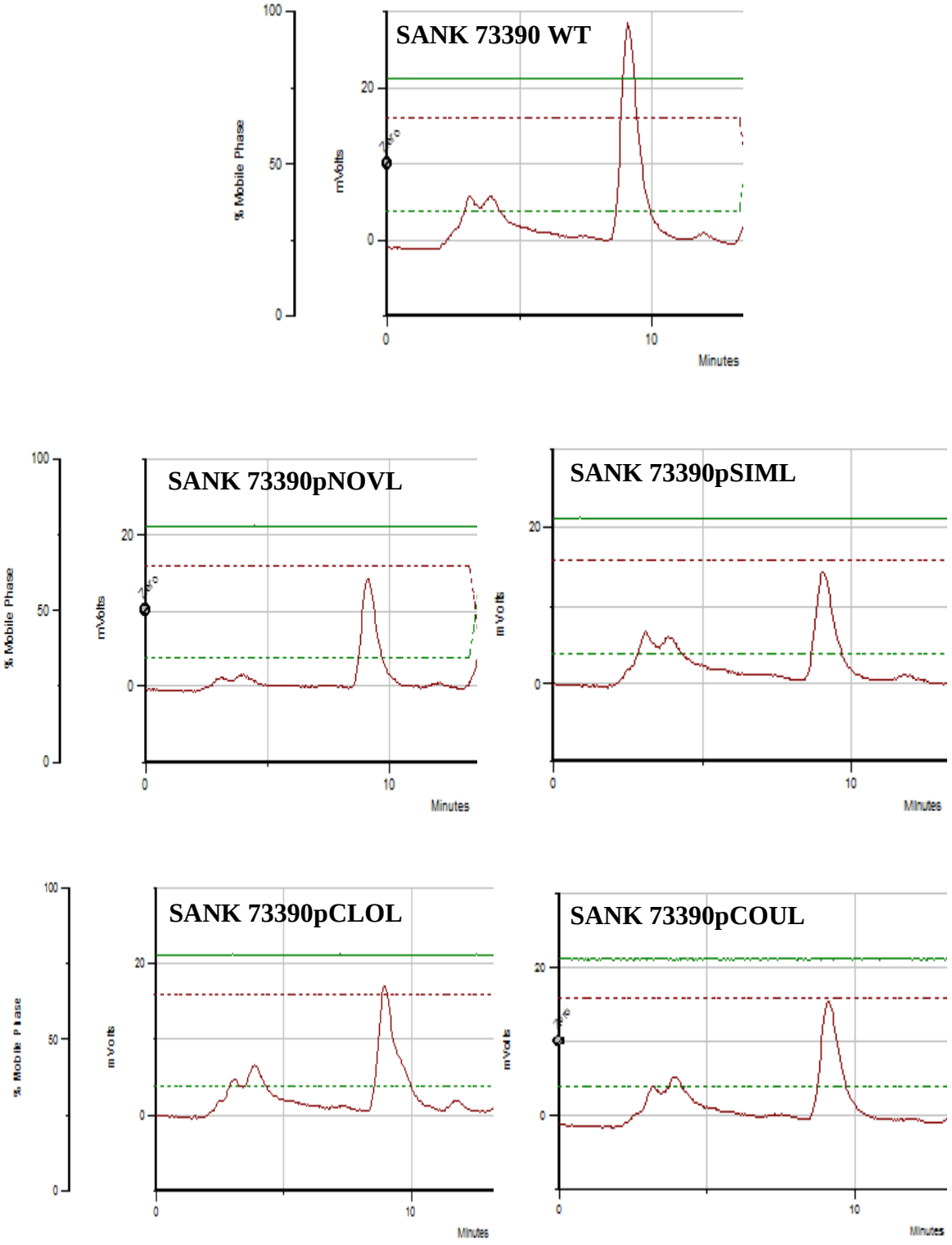

Figure 3.5 HPLC chromatograms showing the effect of *simL*, *novL*, *cloL* and *couL* on thiomarinol production. Production cultures and HPLC analysis was performed in triplicate, and integrated peak areas are listed in Appendix A.

3.2.4 Feeding studies

Of the substrates for these four amide ligases, those for SimL can arguably be regarded as the most similar to those for TmlU, since they can be divided into a fatty acid chain on one side and the aminocoumarin moiety on the other (Figure 3.6). There are similarities to the 8-hydroxyoctanoic acid in the thiomarinol pathway and the 9-hydroxynonanoic acid in mupirocin pathway. This similarity led us to design an experiment in which aminocoumarin is fed to *P. fluorescens* NCIMB10586 expressing SimL and see whether SimL can catalyse the joining of the aminocourmarin to the pseudomonic acid. For the same purpose the other amide synthetases NovL, CloL, CouL were tested.

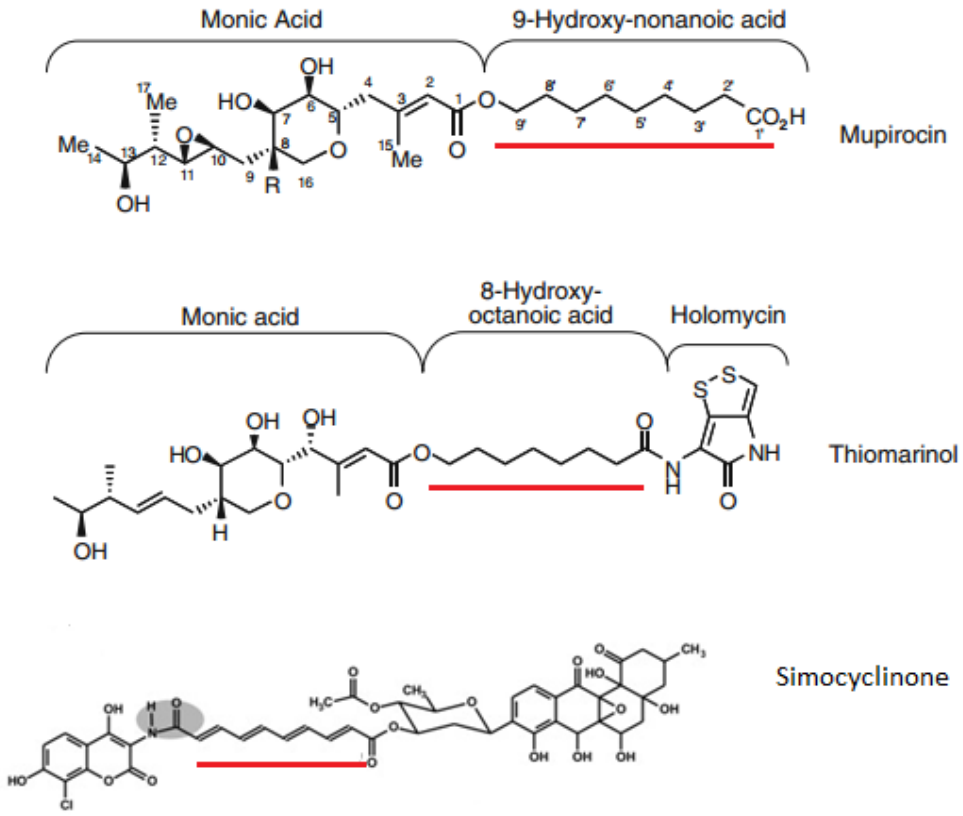

Figure 3.6 The structural similarities between mupirocin, thiomarinol and simocyclinone. The fatty acid chain is underlined in red (Gurney and Thomas, 2011) (Pacholec *et al*., 2005).

In order to investigate how SimL, NovL, CloL and CouL could assist in the process of creating a hybrid compound, different concentrations of aminocoumarin-3 were fed to *P. fluorescens* with each of the amide ligases genes expressed *in trans*. Aminocoumarin was dissolved in DMSO, filtered-sterilised, and fed to the fermentation media at the same time as inoculation. Aminocoumarin concentrations ranged from 10µg/ml to 2560µg/ml, each concentration was repeated in triplicate. The culture was then incubated at 22 ºC and 200 rpm for 48 hours. The cells were separated from the media by centrifugation 11000 xg for 10 minutes, and the supernatant analysed by HPLC. *P. fluorescens* pSIML was fed with aminocoumarin in the concentration range 10-160 µg/ml. PA-A production started to decline with >80µg/ml aminocoumarin until it was completely abolished at 320µg/ml (Figure 3.7). No new compounds were observed at any of the concentrations (Figure 3.8).

P. fluorescens (pNOVL), *P. fluorescens* (pCLOL) and *P. fluorescens* (pCOUL) were fed with aminocoumarin at concentrations 20, 40 and 80 µg/ml, which also did not result in any noticeable new products, (Figure 3.8). IPTG induction did not show any additional evidence for incorporation (data not shown).

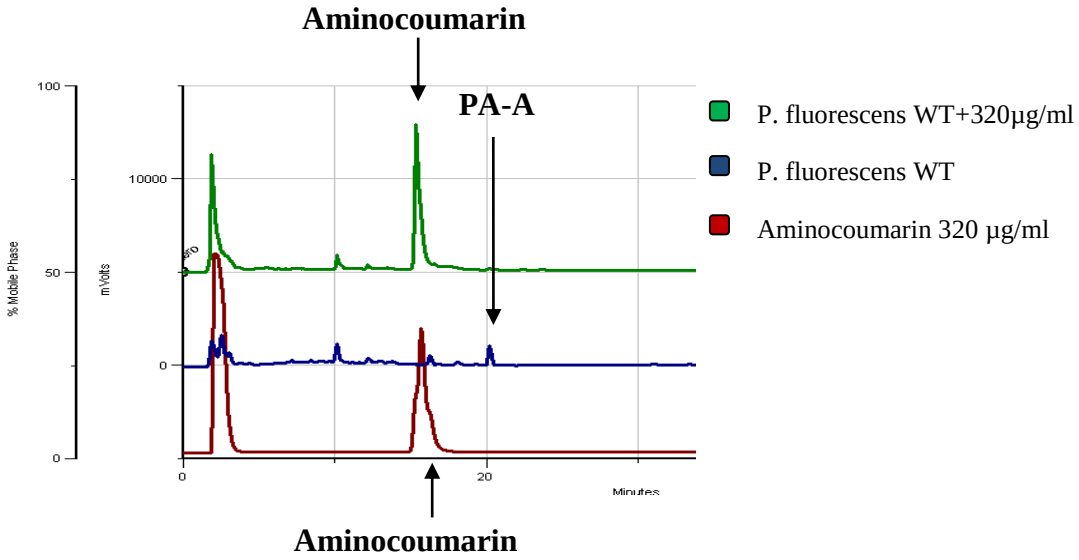

Figure 3.7 HPLC chromatograms for feeding *P. fluorescens* WT with 320 µg/ml of aminocoumarin.

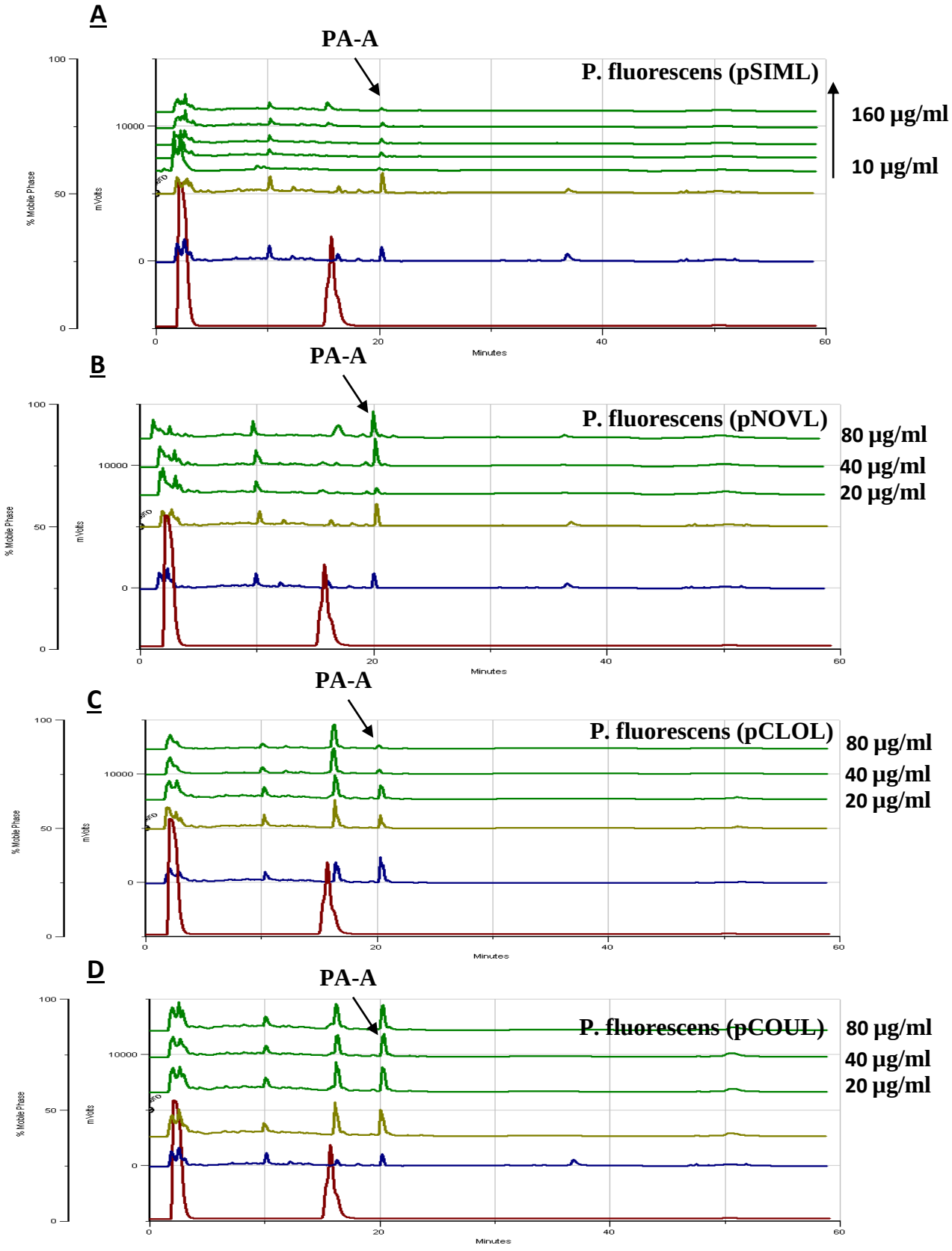

Figure 3.8 HPLC chromatograms of *P. fluorescens* expressing different amide ligases with feeding of aminocoumarin. The RED line represents 230 µg/ml of aminocoumarin as a control; the BLUE line represents *P. fluorescens* WT, while the YELLOW line represents *P. fluorscens* with the chosen amide ligase expressed *in trans*. Integration of peak areas is presented in Figure 3.9.

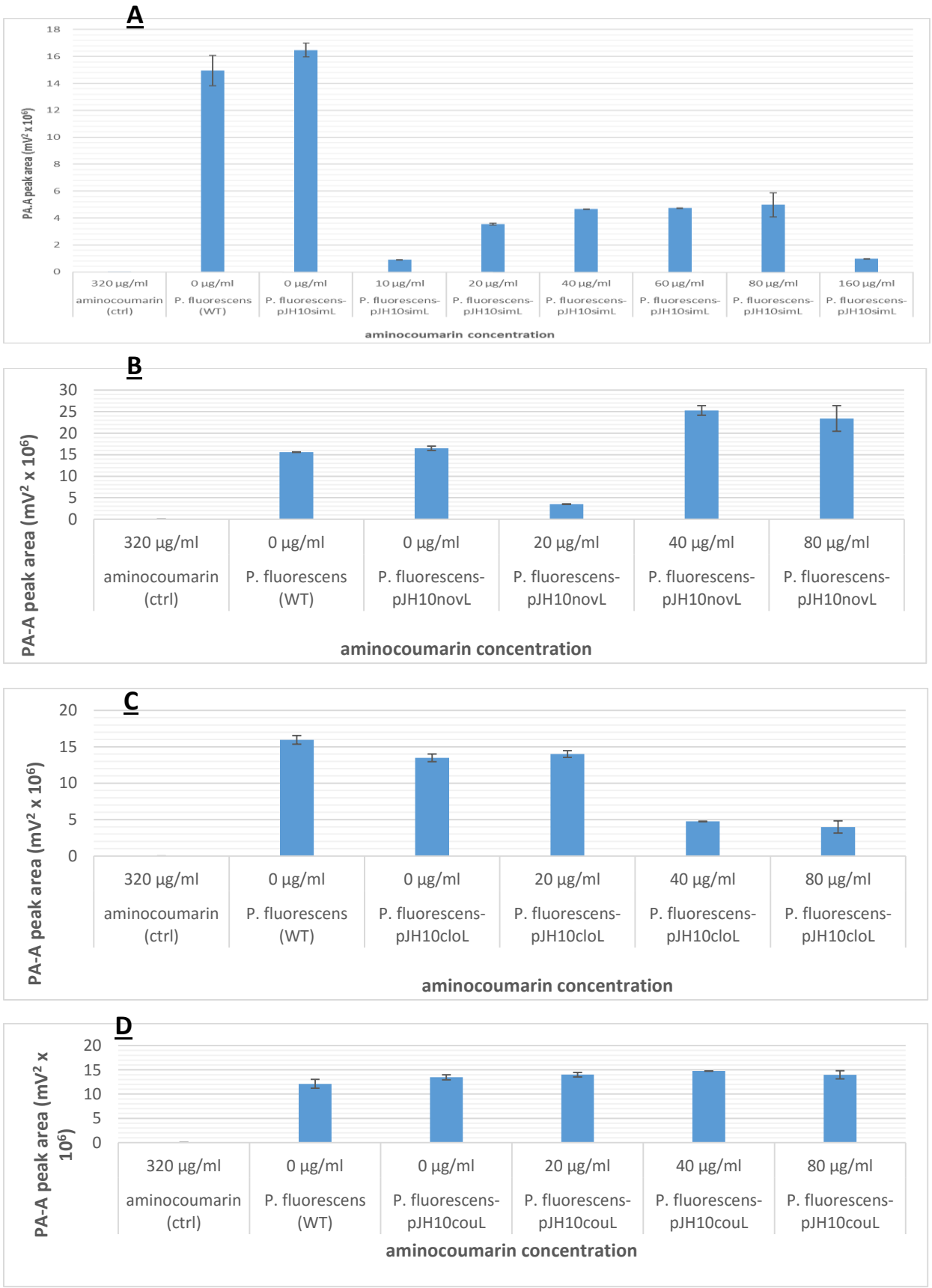

Figure 3.9 Quantitative analysis of the aminocoumarin effect on PA-A production. Production cultures and HPLC analysis were performed in triplicate. Error bars represent the standard error of the mean.

3.2.5 Discussion

Studies conducted on SimL so far showed that it is flexible in terms of accepting precursors (Luft *et al*., 2005). It was found that in addition to its natural substrate simocyclinone C4, SimL would accept a number of cinnamic and benzoic acid derivatives (Luft *et al*., 2005). These findings make SimL and other aminocoumarin amide ligases very attractive tools for creating new hybrid compounds with potential antibacterial activity. As such this part of the project was designed to investigate the possibility of creating new products derived from the pseudomonic acid or pyrrothine moieties of mupirocin or thiomarinol with antimicrobial activity.

No significant inhibition of mupirocin or thiomarinol production was observed with in-*trans* expression of the aminocoumarin amide synthetases (sections 3.2.2 and 3.2.3). This allowed them to be suitable candidates for the creation of hybrid compounds based on mupirocin and thiomarinol, potentially linking molecules from the different pathways such as pseudomonic acid and holomycin, as well as aminocoumarins. Especially since the latter compounds are a successful example of generating a hybrid antibiotic using mutasynthesis procedures (Anderle *et al*., 2007a).

Whilst no restoration of thiomarinol production was observed in *Pseudoalteromonas spp.* SANK73390*ΔtmlU* expressing aminocoumarin amide synthetases in-*trans*, no complementation was also observed by pJH10*tmlU*. One potential explanation is that the mutation has had a polar effect on genes in the vicinity of *tmlU*, preventing complementation. Another explanation is that the level of expression of TmlU from pJH10 is either too high or too low for complementation.

HPLC analysis showed that adding aminocoumarin seems to decrease PA-A production, although no new compounds were detected. As the aminocoumarin

concentration was increased, the amount of PA-A produced was observed to decrease (Figures 3.8 and 3.9), with the exception where *couL* was expressed. Adding aminocoumarin to *P. fluorescens* (pCOUL) did not seem to affect PA-A production.

Amongst the tested amide synthetases, SimL was the most promising due to its structural resemblance to both thiomarinol and mupirocin, (Figure 3.6). However, previous mutasynthetic approaches to create new compounds in aminocoumarins showed that although these amide synthetases come from the same class of antibiotics, they do not necessarily respond in the same way when it comes to accepting different substrates. This is evident when CloL, the amide synthetase of clorobiocin did not accept prenyalated 4-hydroxybenzoyl analogues, while CouL, which shares 91% sequence identity with CloL, proved more flexible and accepted several precursors (Anderle *et al*., 2007a). Although SimL and CouL were the most accepting of different substrates in the studies carried out by the Heide group, this flexibility did not result in success being observed with the heterologous expression of these proteins when introduced to the mupirocin pathway studied here, where no new compounds were observed.

When introduced to the Mupirocin pathway, TmlU abolished Mupirocin production (section 1.3.7). This effect is not seen in the rest of the amide synthetases. SimL on the other hand, though it does not interfere with Mupirocin production is certainly not able to capture the required intermediate, and use it as a substrate and facilitate the formation of a new analogue. There is recent biochemical evidence which indicated that TmlU does not act alone but needs HolE to complete the amidation process in the thiomarinol cluster (Dunn *et al*., 2015). A potential explanation why SimL, and possibly the rest of the amide ligases presented here, were not observed to incorporate new

substrates is because they need to pair up with another enzyme in order to complete their action.

Chapter 4

4 Investigating the inhibitory effect on of TmlU on Mupirocin biosynthesis

4.1 Introduction

TmlU has previously been identified as a putative amide ligase, an enzyme in the thiomarinol biosynthesis pathway responsible for creating the amide bond between the monic acid and the holomycin moiety (Fukuda *et al*., 2011, Murphy *et al*., 2011). It has been recently discovered that TmlU is not the only enzyme that is responsible for this amidation, but instead it works alongside another enzyme, HolE, which is an acyltranferase (Dunn *et al*., 2015). Nonetheless, TmlU is still an essential part of the thiomarinol biosynthesis process and could be of great potential for creating diverse hybrid compounds, and generating new families of antibiotics.

Attempts to create hybrid antibiotics by incorporating a range of different substrates using a general approach called mutasynthesis have been encouraging. For example, feeding a range of substrates like anhydrornithine and anhydrolysine into *P. fluorescens* strains defective in *holA* resulted in production of a number of pseudomonic acid derivatives (Murphy *et al*., 2011). However, to further exploit TmlU and its potential in such studies, more research is needed to understand its substrate specificity, what other roles TmlU is involved in within thiomarinol biosynthesis, and possibly its action when introduced to other biosynthetic pathways.

Previous studies on TmlU have demonstrated that expressing *tmlU* in-*trans* in *P. fluorescens* resulted in a reduced yield of PA-A and accumulation of truncated C_5 of PA-B (Omer-Bali, 2013). This implies that TmlU interferes with biosynthesis of 9-Hydroxynonanoic acid.

As discussed in section 1.3.2.3, MmpB is believed to be responsible for the biosynthesis of 9-hydroxynonoic acid. However, to date there is no direct evidence that this is the case. In combination with the knowledge that MmpB is capable of functioning with only one ACP (Shields *et al*., 2010), there might be more to the process of creating 9-hydroxynonanoic acid than what we currently understand regarding the iterative condensations. One hypothesis that was proposed by (Omer-Bali, 2013) was that TmlU targets the active site of one of the ACPs in MmpB. This is the first hypothesis to be addressed in this chapter, through investigation of the effect of expression of TmlU in-*trans* in *P. fluorescens* NCIMB 10586 carrying point mutations and deletions to the three ACP domains of MmpB. Omer-Bali reported that deletion of either ACP5 or ACP7 with TmlU expression yielded the C5 version of pseudomonic acid B (Figure 4.2). However, with deletion of ACP6, a small peak of pseudomonic acid A was observed. This suggested that deleting ACP6 reduces the negative impact of TmlU on mupirocin production. However, after the Omer-Bali observation proved un-reproducible, it was necessary to explore alternative hypotheses.

As truncation of the 9-HN was observed with TmlU expression (Figure 4.2), it may be possible that TmlU interacts with the thioesterase domain of MmpB, somehow causing premature release. Therefore, several further hypotheses are explored in this chapter, firstly is enzymatic activity of TmlU required for its inhibitory impact. This was investigated through point mutations to TmlU. Secondly, does TmlU interact with MmpB, and can any interaction be narrowed down to a specific domain on MmpB. This hypothesis was explored through deletions and point mutation of the thioesterase domain and bacterial two hybrid tests.

4.2 Results

4.2.1 Expressing pAMHI in *P. fluorescens*

Plasmid pAMHI was constructed by Ahmed Omer-Bali (2013) by cutting out *tmlU* from a pET28a derivative using *Eco*RI and *Sal*I, and cloning it into the expression vector pJH10 between *Eco*RI and *Xho*I. The construct was verified by both colony PCR, restriction digests, and sequencing.

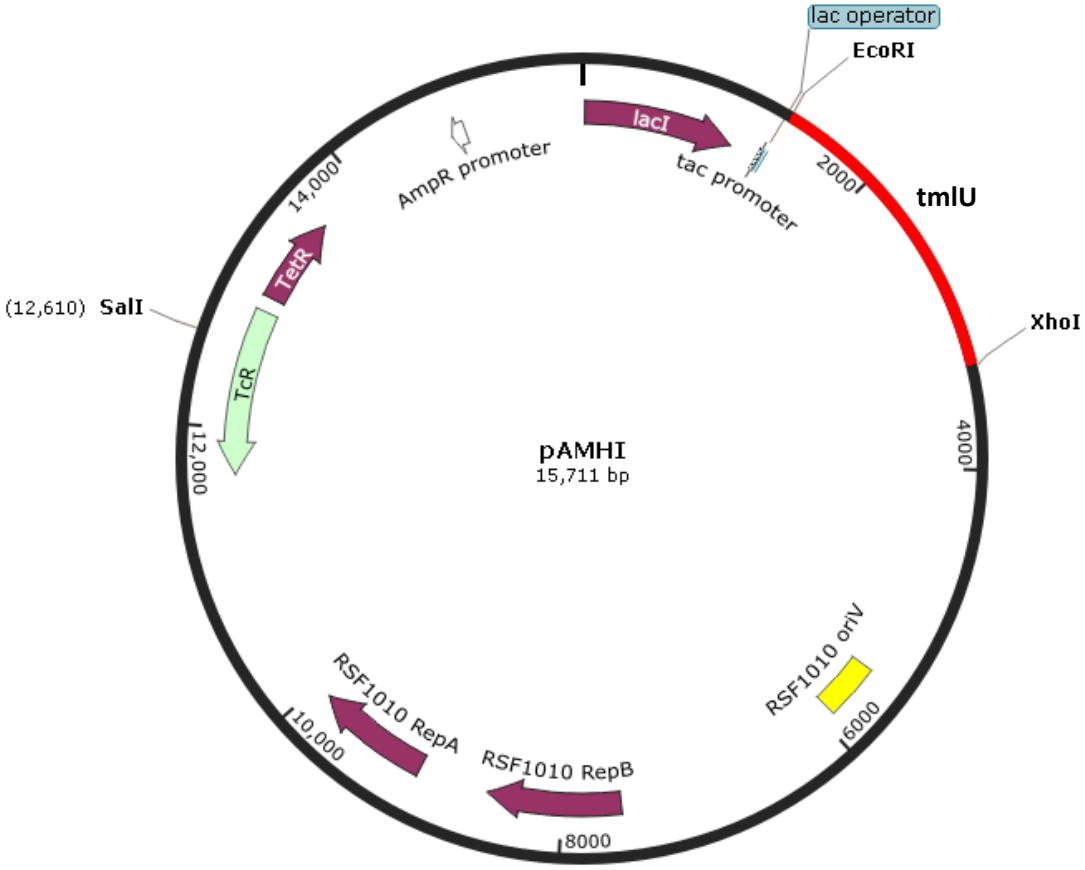

Figure 4.1 Map of the *tmlU* expression vector pAMH1. The *tmlU* open reading frame was cloned into the expression vector pJH10 between the *Eco*RI and *Xho*I sites.

4.2.2 HPLC analysis of *P. fluorescens*-pAMHI (*P. fluorescens* NCIMB 10586 strains expressing *tmlU*)

To provide a base line for the impact of *tmlU*, HPLC analysis was performed on the wild type strain *P. fluorescens* NCIMB 10586 and strains with pJH10 expressing *tmlU* in-*trans*, to determine the impact on pseudomonic acid production. HPLC data revealed that both *P. fluorescens* NCIMB 10586 WT *and P. fluorescens* NCIMB 10586(pJH10) produced pseudomonic acid A and B. The C_5 version of PA-B was observed when *tmlU* was expressed in-*trans* in *P. fluorescens* NCIMB 10586 WT. When expression was induced with 0.5 mM IPTG, all of the PA-B was found in the C_5 form (Figure 4.2).

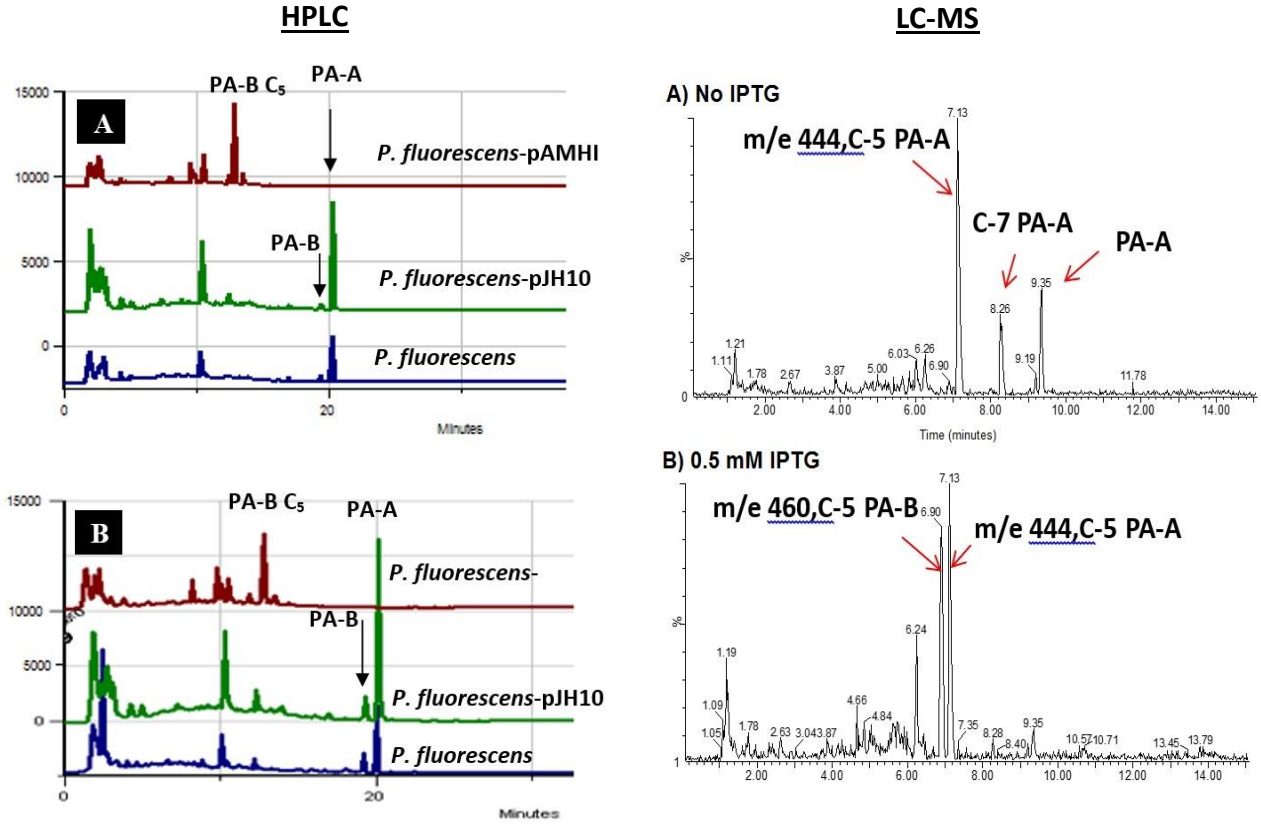

Figure 4.2 HPLC and LC-MS chromatograms of *P. fluorescens* WT with pAMH1 plasmid. A) Without IPTG induction, B) With 0.5mM IPTG induction. *P. fluorescens* and *P. fluorescens* (pJH10) are included as controls. All production cultures and HPLC analysis was performed in triplicate. Expression of TmlU causes a switch to truncated C5 PA-B production. Integration of the peak areas is included in Appendix A.

4.2.3 Effect of TmlU on *P. fluorescens* strains with single ACP (5, 6 or 7) deletions

In analysing the possible explanations for the effect of TmlU there seemed to be two obvious possibilities. First, the TmlU protein associates with MmpB in some way, and prevents it from undertaking more than one condensation. Second, that the activity of TmlU off-loads the growing acyl chain early. Previous work by Ahmed Omer-Bali had started to explore the first of these possibilities, based on the hypothesis that perhaps it was the ACPs that were the target of TmlU binding, and that removal of a subset of the three ACPs in MmpB would result in loss of the sensitivity to TmlU. Because there had been inconsistent results with the ACP deletion strains, HPLC analysis was performed on all the *P. fluorescens* strains with single deletions of ACP5, ACP6 and ACP7 (in triplicate) with and without IPTG induction. Wild type *P. fluorescens* NCIMB 10586 and wild type with pJH10 vector were used as controls. The HPLC chromatograms showed that TmlU still blocks mupirocin biosynthesis and causes the formation of the C_5 version of pseudomonic acid B which can be detected at 14 min retention time. The results were the same when *tmlU* was induced with 0.5mM IPTG (Figure 4.3).

Bioassays were performed using *Bacillus subtilis* 1064 as the sensitive bacterium, and plates of L-agar were supplemented with 0.5 mM IPTG to induce expression of the *tmlU* gene. Results in Figure 4.4 showed that clearing zone disappears completely when pAMHI was present in NCIMB10586ΔACP5 and NCIMB10586ΔACP7, while NCIMB10586ΔACP6 still formed a clearing zone although approximately 25% of the diameter of the wild type NCIMB10586(pAMHI). When *tmlU* expression from pAMH1 was induced with IPTG a more drastic effect was seen (Figure 4.5). No clearing zone was observed in any of the strains with pAMHI.

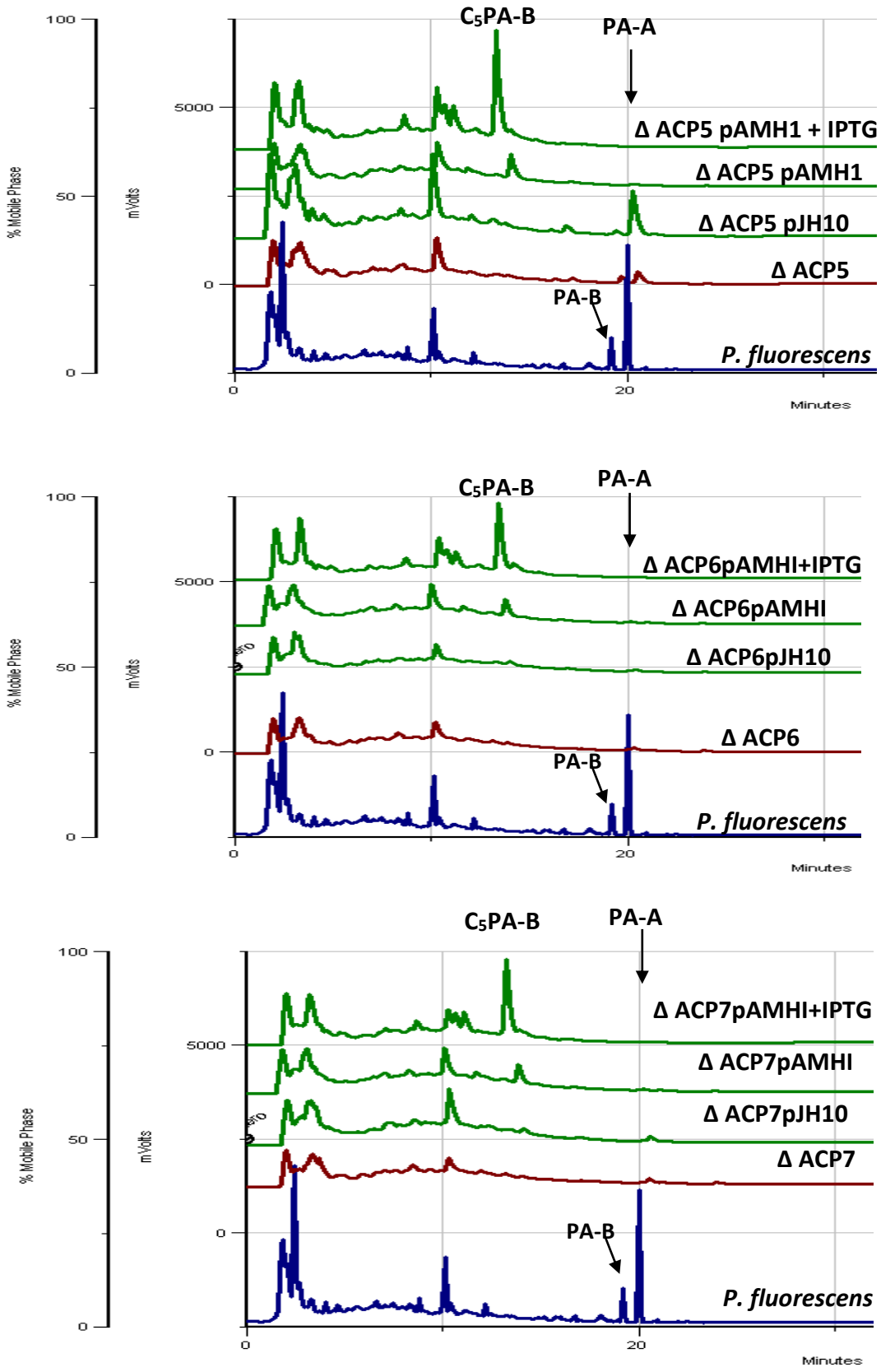

Figure 4.3 HPLC chromatograms of NCIMB 10586 strains with single deletion in one of the MmpB ACPs (5, 6, or 7) with pAMH1 plasmid in-*trans*. NCIMB 10586 WT was used as a control.

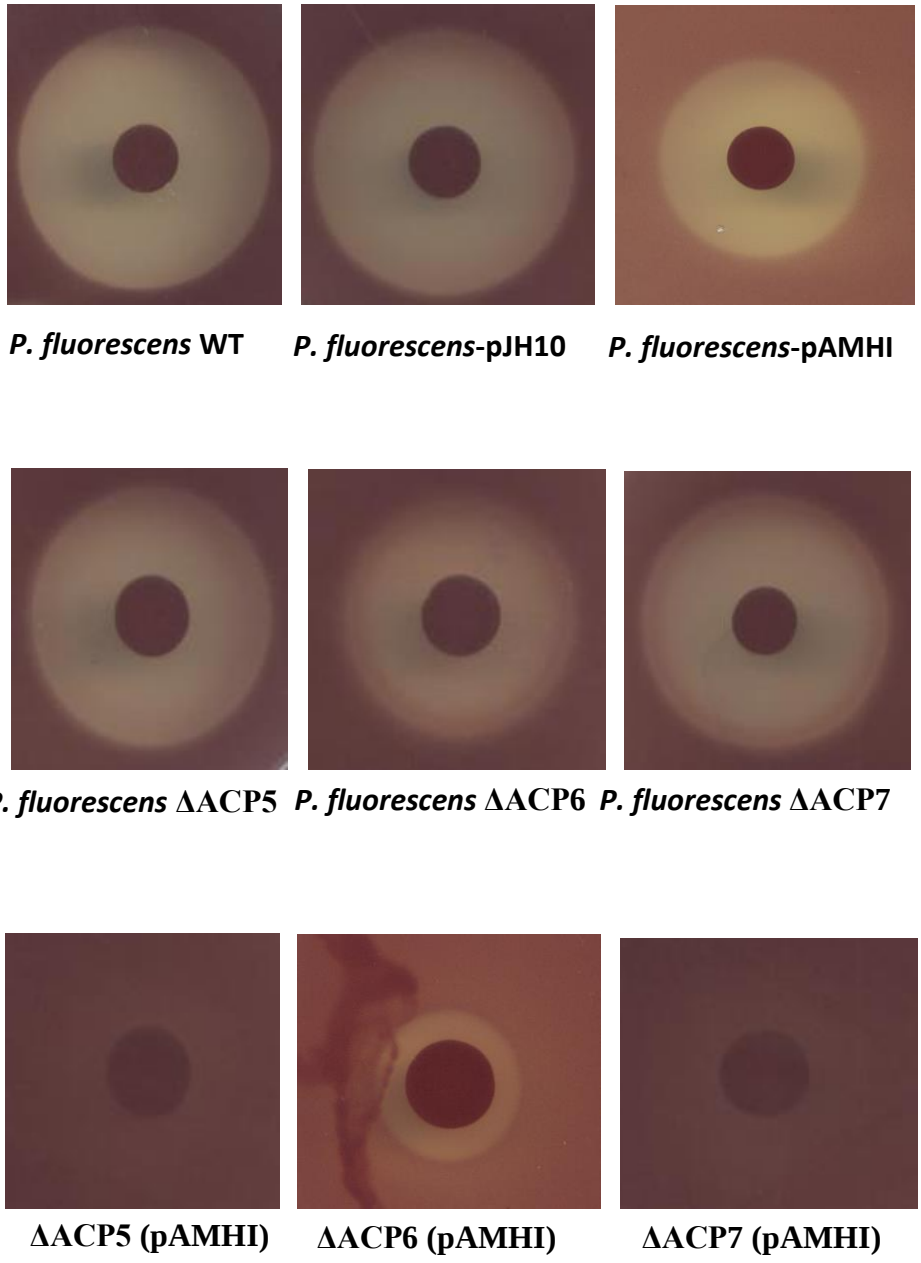

Figure 4.4 Bioassay to show the effect of *tmlU* expression on strains of *P. fluorescens* with deletion in one of the ACPs (ACP5, ACP6, or ACP7) of MmpB.

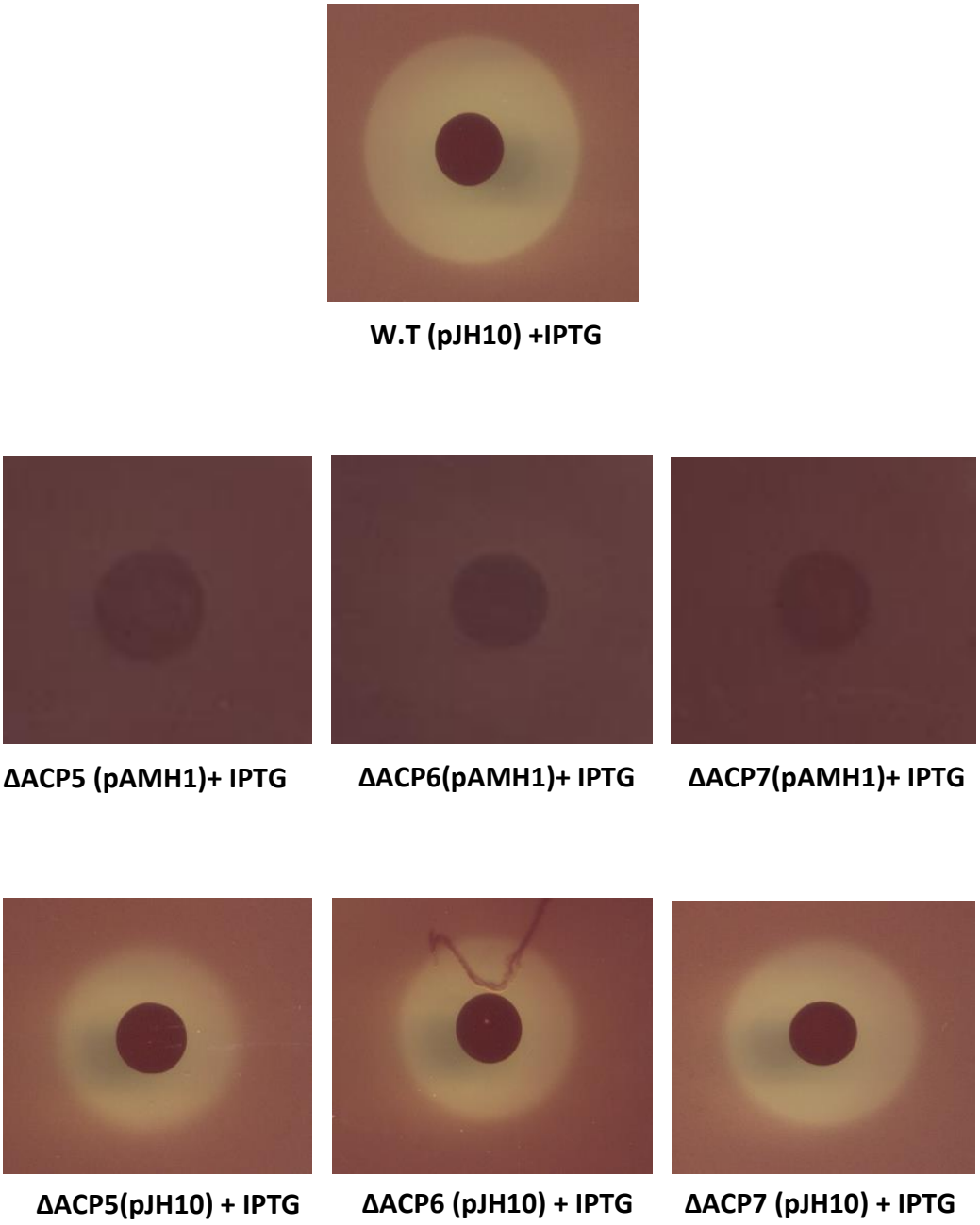

Figure 4.5 The effect of in-*trans* expression of *tmlU* when induced with IPTG on *P. fluorescens* NCIMB 10586 strains with deletion in one of the ACPs (ACP5, ACP6, or ACP7) of MmpB.

4.2.4 Effect of point mutations on TmlU enzymatic activity and their impact on Mupirocin production

The results obtained from the experiments designed to test the possible interaction between one of the ACPs in MmpB and TmlU were not conclusive enough to determine whether deletion of ACP6 is actually reducing the sensitivity towards TmlU. Therefore, it was decided to look at another aspect of this effect, namely the enzymatic activity of TmlU. It might be that this inhibitory effect is due to an enzymatic activity rather than a physical interaction between TmlU and part of MmpB.

4.2.4.1 TmlU site directed mutagenesis

To test this hypothesis, point mutations were made by site directed mutagenesis of different locations in the TmlU active site. Mutations of the amino acids were based on a sequence alignment of TmlU and firefly luciferase, which share a great deal of sequence and mechanistic similarities with peptide synthetases and acyl-CoA ligases (Figure 4.6). In the firefly luciferase, seven residues were found to be conserved and are likely to be significant in the process of binding ATP and adenylate formation: Gly200, Lys206, Glu344, Asp422, Arg437, Gly446 and Glu455 (Conti *et al*., 1996). The motif ^{198} [STG]--STG-G-[ST]--TSE--[GS] xs-[PALIVM]-K^{206} is the signature sequence for the luciferase super-family. When Lys206 was mutated to arginine in firefly luciferase the acyl-CoA ligase activity decreased drastically, whereas changing other amino acids in the motif had a lesser effect. Another motif which seems to be of great significance for firefly luciferase is [STA]-[GRK]-D, and mutating Asp422 resulted in a complete loss of enzymatic activity (Conti *et al*., 1996). The locations of the TmlU mutations within a homology model of the structure are indicated in (Figure 4.7).

Figure 4.6 Sequence alignments of TmlU with amide synthetases and acyl-CoA synthetases showing the conserved amino acids in these proteins. The boxed areas are the two motifs thought to be important for protein activity, and the red coloured residues represent the most conserved amino acids among the listed acyl-CoA synthetases. **1PG3**: Acetyl CoA Synthetase, **3CW9**: 4-Chlorobenzoyl-CoA Ligase and **3NYQ**: Malonyl-CoA Ligase

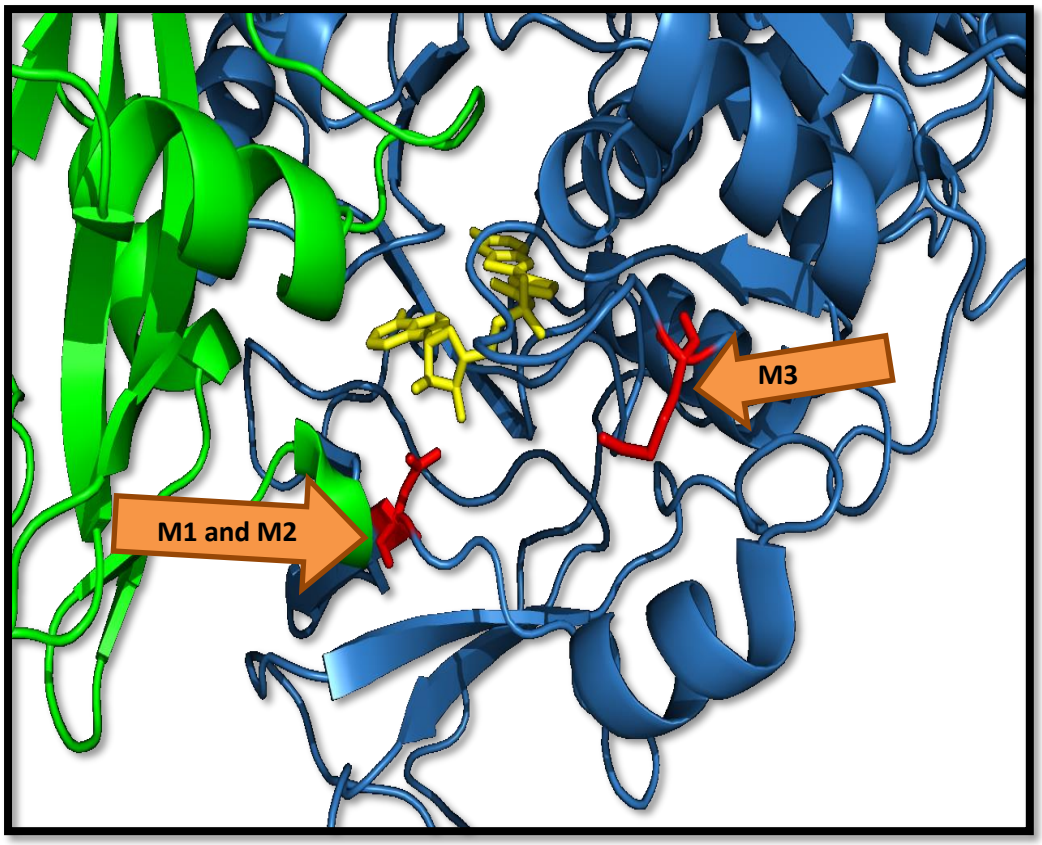

Figure 4.7 A computational model of TmlU from *Pseudoalteromonas* SANK73390 showing the positions of the introduced mutations. The mutations are made in the acyl-activating enzyme consensus motif and it appears to be necessary for binding of ATP and adenylate formation. M1 (D422A) and M2 (D422S) change the Aspartic acid (D) into Alanine and Serine respectively, while M3 (K206R) changes the Lysine in this motif to Arginine. This homology model was made by Jack Connolly, University of Birmingham.

The Quick-change Lightning Site-Directed Mutagenesis Kit was used to introduce the required mutations into TmlU. Amplification of *tmlU* with the different point mutations was achieved using the primers listed in Table 2.8. The active site codon **GAT** encoding Aspartic acid in wild type was replaced by **GCT** encoding Alanine in mutant TmlUM1 (D422A), and to **AGT** in mutant TmlUM2 (D422S). The codon AAG encoding Lysine 206 was changed to AGG encoding Arginine in mutant TmlUM3 (K206R). The fragments were amplified, ligated into pET28a vector and sequenced to check for the mutations and then cloned into pJH10.

Before transforming *E. coli* S17-1 with the constructed mutants, the plasmids were checked for insert by restriction digest and sequencing. The plasmids pJH10-TmlUM1, pJH10-TmlUM2 and pJH10-TmlUM3 were all digested with *Eco*RI and *Sac*I to yield 1 kb and 1.96 kb inserts respectively (Figure 4.8). The reason for the different restriction pattern observed for pJH10-TmlUM1 compared with pJH10-TmlUM2, is that changing the amino acid from Aspartic acid to Alanine introduced a *Sac*I restriction site almost in the middle of *tmlU*. This provided another method for checking that the mutation was there.

5'-GTTGGTTAAATACCGGAGATCTTGGCAAGTTCGATGC-3'

5'-GTTGGTTAAATACCGGAGCTCTTGGCAAGTTCGATGC-3'

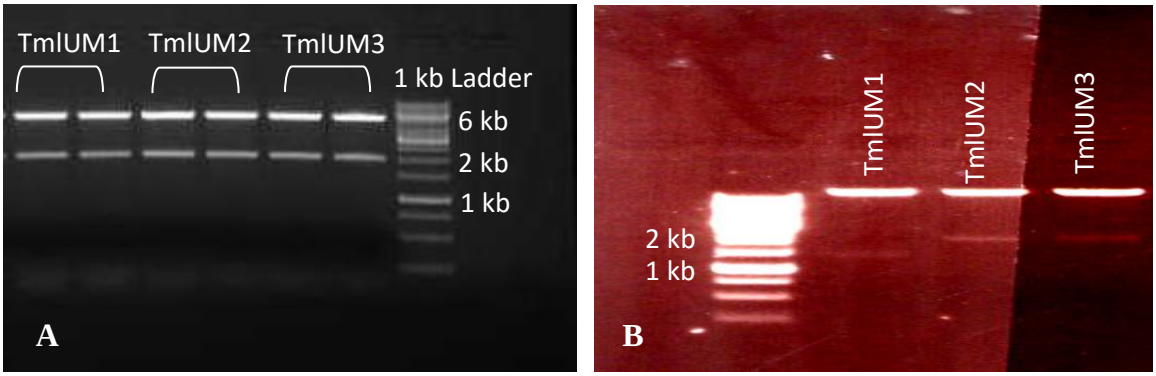

Figure 4.8 Analysis of the pJH-tmlU mutant expression plasmids. The sequences above show how changing aspartic acid to alanine introduces a *Sac*I site. Restriction digest analysis of: a) pET28a-TmlUM1, pET28a-TmlUM2 and pJH10-TmlUM3 digested with *Eco*RI and *Sal*I; b) pJH10-TmlUM1, pJH10-TmlUM2 and pJH10-TmlUM3 digested with *Eco*RI and *Sac*I. To confirm the size of the insert, the digestion products were run on a 1% agarose gel.

4.2.5 Effect of site directed mutagenesis of TmlU on its ability to interfere with Mupirocin production.

A bioassay was conducted on the strains *P. fluorescens* NCIMB10586-pAMH1, *P. fluorescens* NCIMB10586-pTmlUM1, *P. fluorescens*-pTmluM2 and *P. fluorescens*-pTmlUM3 in order to compare the effect of the mutant TmlU with wild type TmlU on the pseudomonic acid production. A large clearing zone can be seen when pTmlUM1 and pTmlUM2 were introduced into the wild type *P. fluorescens* NCIMB 10586. However, pTmlUM3 had the same effect as wild type TmlU in terms of blocking Pseudomonic acid A production. When the strains were induced with IPTG the clearing zone size decreased significantly (Figure 4.9 and Figure 4.10), which raised questions about whether the amide ligase activity of TmlU was deactivated.

To confirm the results obtained from the bioassay, HPLC analysis was performed to verify the production of pseudomonic acid A in the different strains with and without IPTG induction. In contrast to the bioassay results, the IPTG induced *P. fluorescens* (pTmlUM1) and *P. fluorescens* (pTmlUM2) did produce pseudomonic acid A, which confirms that the amide ligase of TmlU was actually deactivated. Whilst *P. fluorescens*-pTmlUM3 was consistent with the bioassay results, in producing the C_5 version of pseudomonic acid B and not pseudomonic acid A (Figure 4.11). The disappearance or at least decrease in strength of the negative effect of TmlU on Pseudomonic acid A production in mutants M1 and M2, suggests strongly that the biochemical activity of TmlU is needed for the truncation of the pseudomonic acid A, consistent with the hypothesis that was being tested. This might therefore suggest that truncation of the pseudomonic acid is due to premature capture of the incomplete hydroxy fatty acid by TmlU. If this is the case, then the normal thioesterase may not be needed for the release of the intermediate and this

would make a clear prediction – that loss of TE activity should have no effect on the TmlU effect.

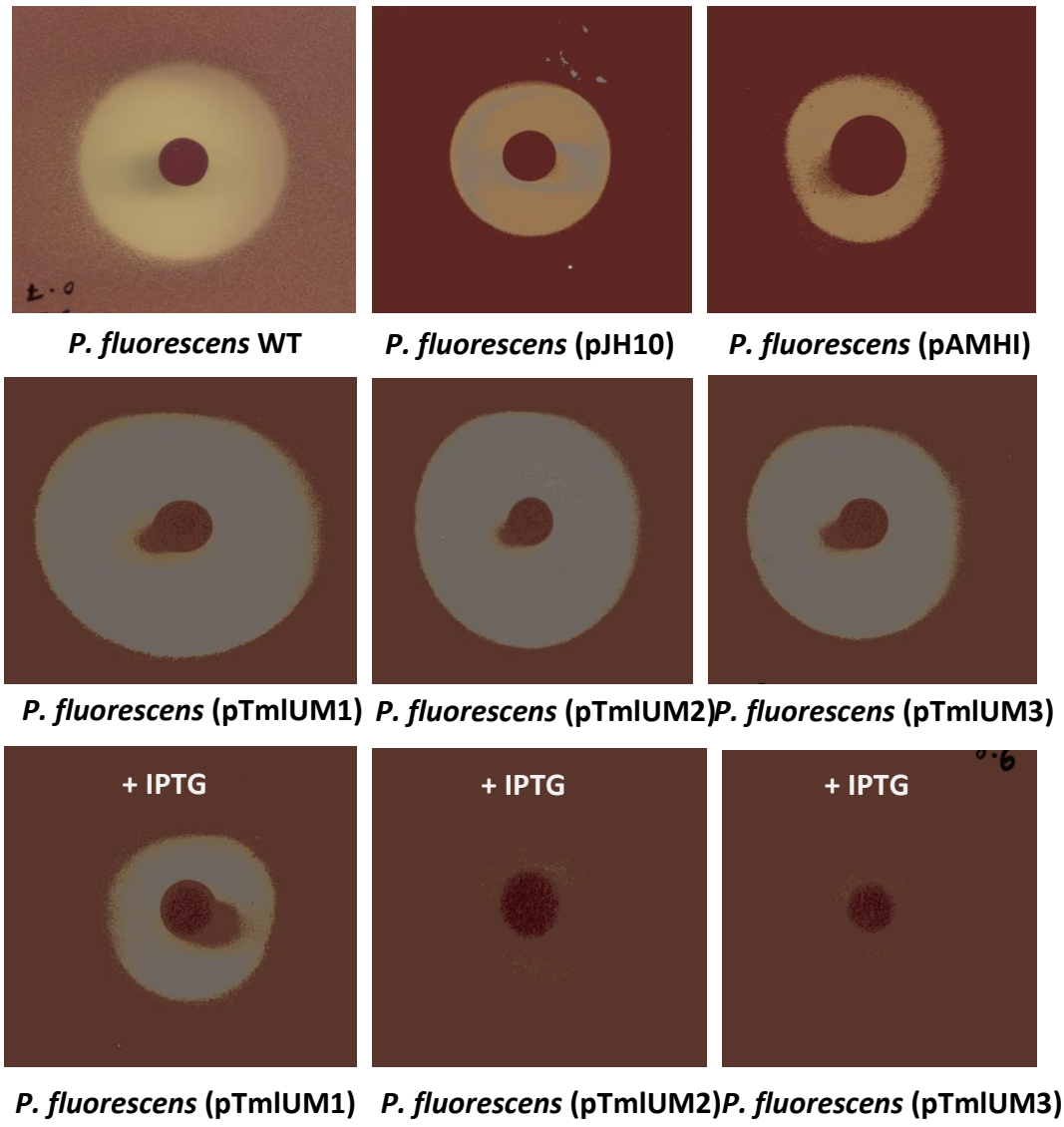

Figure 4.9 Bioassay to determine the effect of the mutations on mupirocin production as well as the enzymatic activity of TmlU. *Bacillus subtilis* was used as the test organism and *P. fluorescens* NCIMB 10586 was the producer organism.

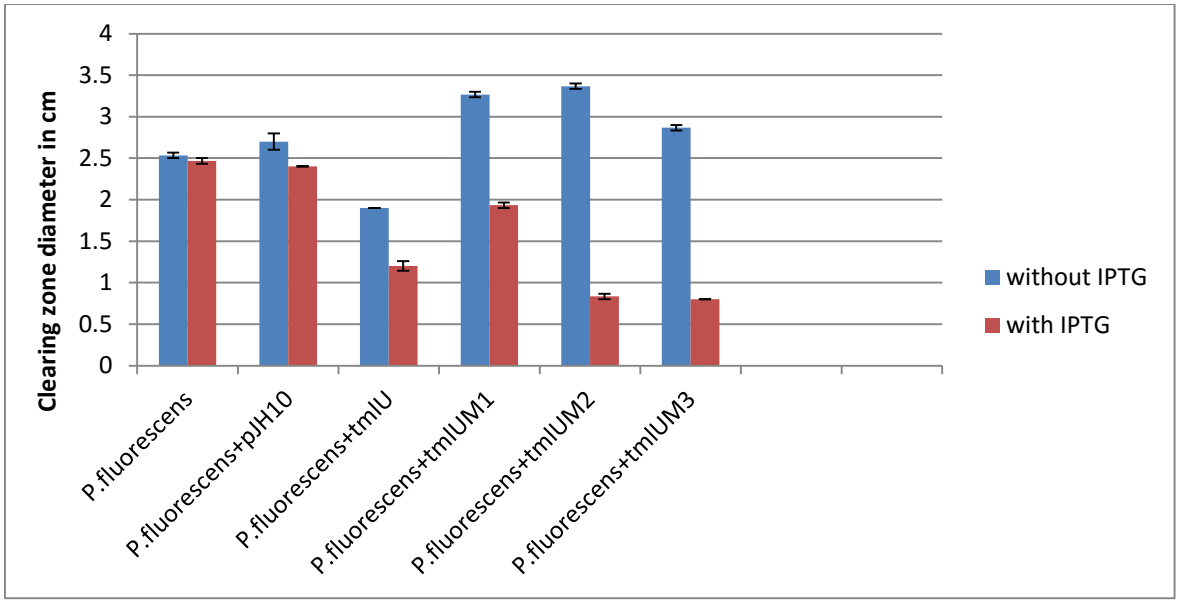

Figure 4.10 Quantitative bioassay of the NCIMB10586 WT expressing *tmlU* with different point mutations in the active site. All the samples were repeated in triplicate.

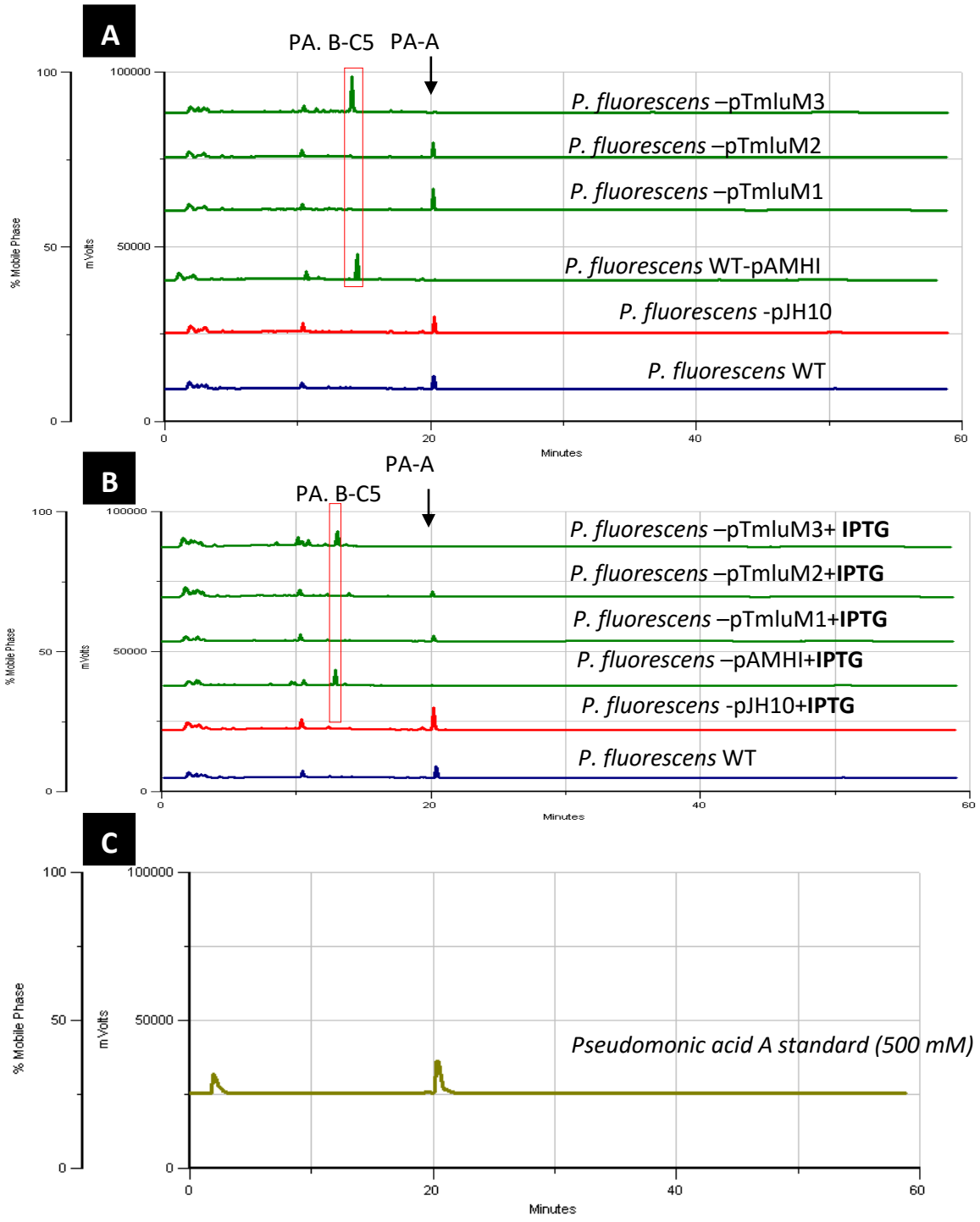

Figure 4.11 HPLC chromatograms showing the effect of TmlU mutations on *P. fluorescens* WT with and without IPTG induction (panel A and B respectively). Panel C shows a 500mM PA.A standard. No quantification through peak integration was performed on these chromatograms, as the purpose was to detect presence or absence of PA.A only.

4.2.6 Investigating whether MmpB thioesterase is necessary for the effect of TmlU

The current model for 9-hydroxynonanoic acid biosynthesis is that all the condensations occur on MmpB. Given the results obtained in the previous section it seemed reasonable that deleting the TE domain may have no effect on TmlU mediated truncation PA-A. This had already been tested based on a rather different hypothesis by (Omer-Bali, 2013) by deleting the thioesterase (TE) and introducing pAMHI to the *P. fluorescens-mmpBΔTE*. The results showed that deleting the TE in the wild type *P. fluorescens* abolished mupirocin production completely, and the same results were observed when *tmlU* was introduced to and expressed in *P. fluorescens* NCIMB10586-*mmpBΔTE*.

Deleting the thioesterase clearly prevented the premature release caused by TmlU. This means that either both the biochemical activity of TmlU and the TE domain of MmpB are required for premature release of the truncated PA-A/PA-B. Or that the effect of TmlU depends on its interaction with the TE domain, so that it is ready to capture the intermediate before release. The hypothesis is that the TE domain is needed to tether TmlU in the right place in order for it to release the truncated pseudomonic acid (C_5). A way to test this hypothesis would be to introduce mutations into the TE domain that knock out the biochemical activity but retain the domain structure, so that the TE-TmlU interaction can still occur if it is needed. According to the crystal structure of the thioesterase domain in fengycin biosynthesis cluster (Samel *et al*., 2006) the catalytic triad includes Serine84, Histidine201 and Aspartic acid111. Based on this model two single mutations were made in the TE domain of *P. fluorescens* - D111A and H201A (Figure 4.12)**.** The mutations were made by Splicing Overlap Extension technique (SOEing) explained in section 2.3.7 and illustrated in (Figure 2.1 and Figure 4.12b). The two TE mutations were cloned separately into pAKE604 generating two suicide plasmids

designated pTEMD (Figure 4.12c) and pTEMH. For the purpose of testing the interaction hypothesis *tmlU, tmlUM1* and *tmlUM2* were introduced to *P. fluorescens* strains with the mutated/inactive TE via conjugation, as explained in section 2.3.11.

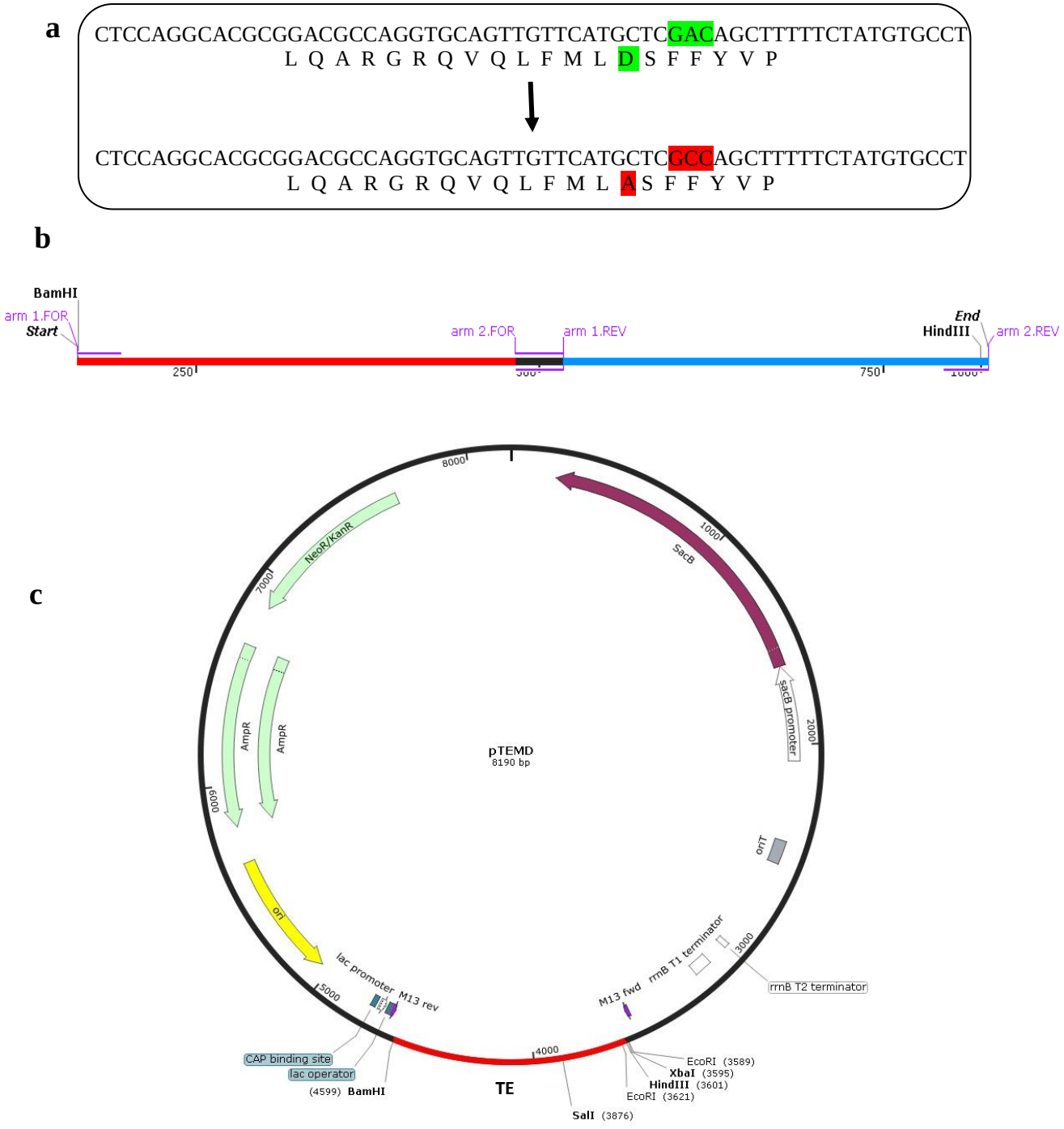

Figure 4.12 Construction of the D111A thioesterase point mutation to illustrate the method used. **a)** Locations of the D111A mutation in the TE domain, **b)** Schematic presentation of the SOEing PCR primers used to amplify TE with the required site directed mutations. **c)** Map of pTEMD showing the position of the inserted TE after amplification. The same method was used to generate plasmid pTEMH for the other mutation, H201A.

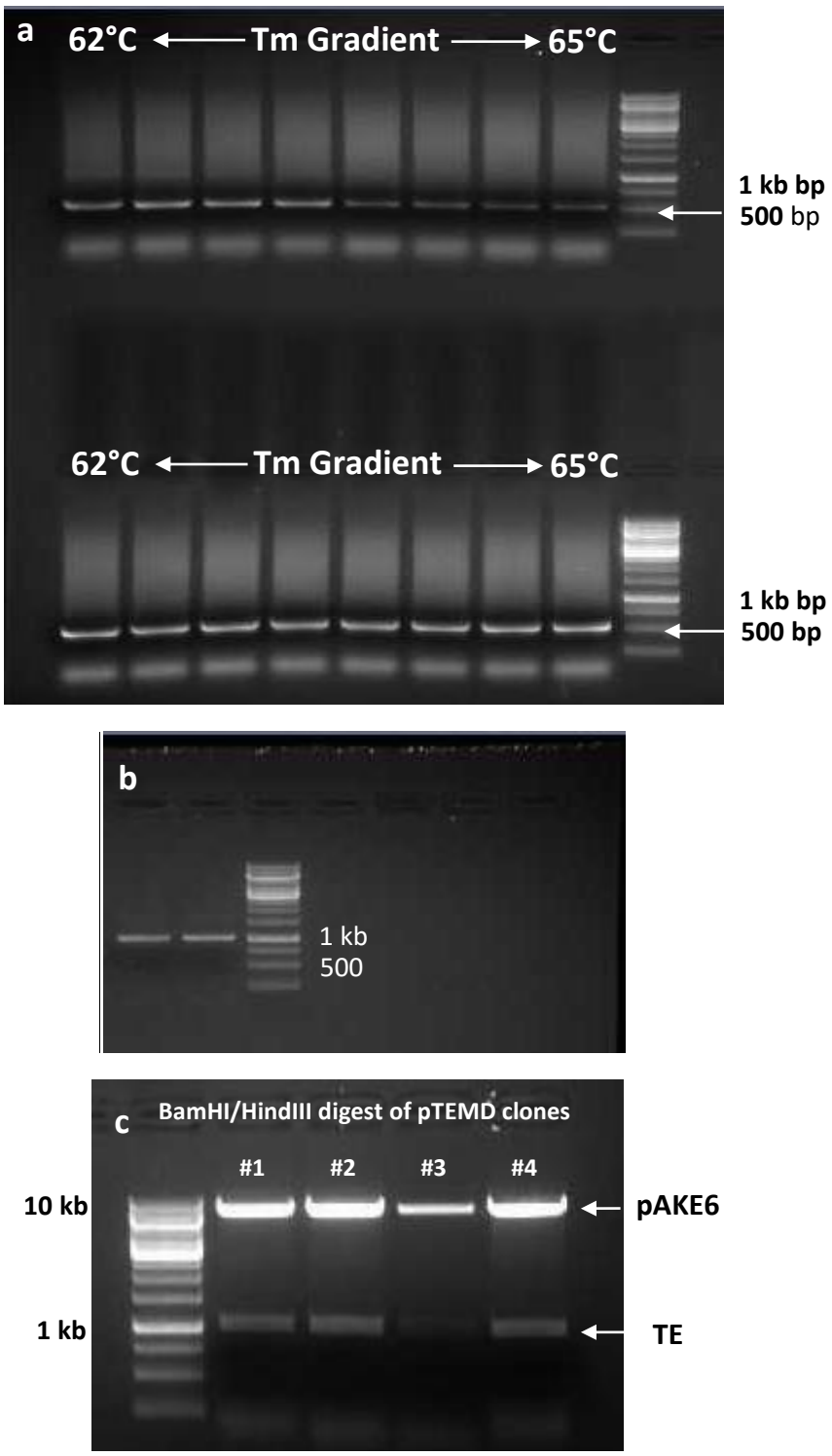

Figure 4.13 Construction of the suicide plasmid pTEMD designed to introduce the TE point mutation D111A. a) The two amplified arms of TE produced by gradient PCR; **b)** The complete TE fragments after SOEing PCR; and **c)** The *Bam*HI *Hind*III digestion of pAKE604 vector from different clones containing the TE mutated fragments.

4.2.7 Integrating the TE mutations into the *P. fluorescens* chromosome

To facilitate the integration of the D111A and H201A mutations into the chromosome by homologous recombination, suicide vectors pTEMD and pTEMH were introduced into *P. fluorescens* strains, via conjugation from *E. coli* S17-1. After purification, the transconjugant cointegrant strains were grown without selection and plated on 5% sucrose plates to select for excisants, as the presence of the *sacB* gene which encodes the enzyme levansucrase, will not allow the bacteria to grow in the presence of sucrose because it catalyses levan synthesis which is lethal to the Gram negative cells. Therefore, the only bacteria that would survive are the ones without the integrated plasmid. The colonies obtained on the sucrose plates were patched onto Ampicillin and Kanamycin plates to check for plasmid excision (Figure 4.14) and section 2.3.11.

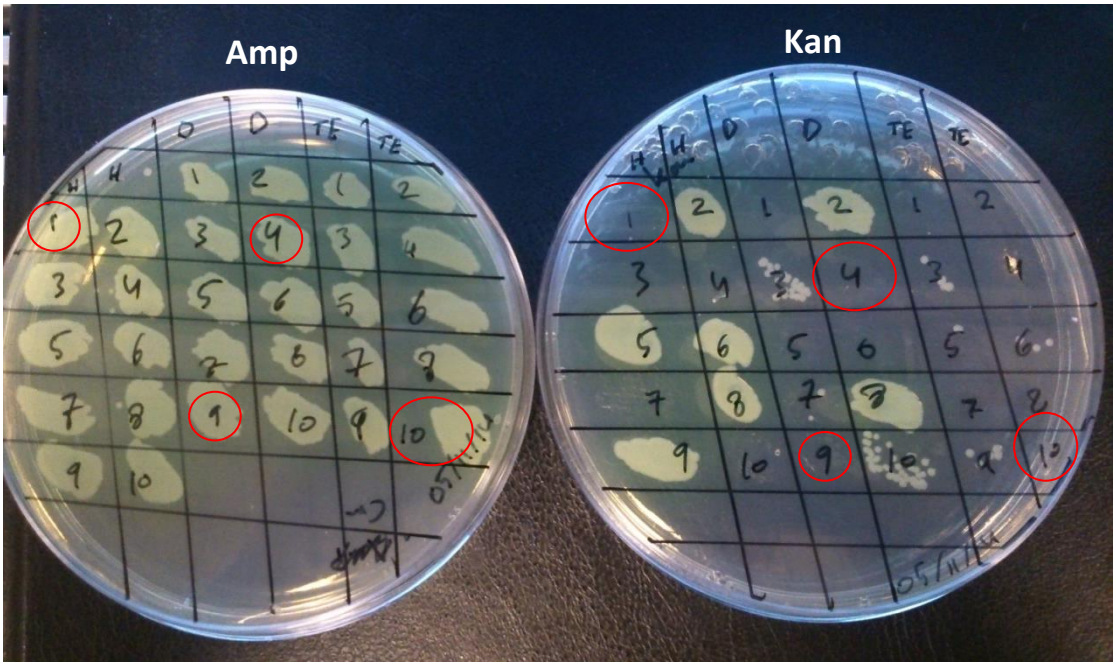

Figure 4.14 Screening for potential *mmpB* TE point mutants. Ten colonies were patched on replica plates to identify excisants of each possible mutant (D=D111A and H=H201A) along with a non-mutated parental control strain (TE). Circled colonies were selected for sequencing as they did not grow on the kanamycin plate, which suggests that the plasmid had excised, and they may contain the correct recombinant. Only the sequenced strains with the correct recombinant were used in the downstream applications.

The hypothesis developed so far is that the inhibitory effect of TmlU depends on the interaction with the TE domain, so that it is ready to capture the intermediate before the release. This hypothesis is tested in this section through the introduction of point mutations to the TE domain designed to knock out its enzymatic activity, whilst keeping the domain itself intact so the protein-protein interaction can still take place. HPLC was used to detect the production of PA-A by the mutant strains and WT (Figure 4.15). H201A did not completely abolish PA-A production, suggesting some thioesterase domain activity was retained. No PA-A was detected with D111A suggesting that TE activity had been abolished. Therefore, all following experiments were carried out on the D111A mutant.

P. fluorescens TE-D111A was transformed with pAMHI (expressing WT *tmlU*), pTmlUM1 and pTmlUM2, and analysed by HPLC to see if the presence of an enzymatically inactive thioesterase domain will allow TmlU to cause the release of the intermediate PA-B (C_5) (Figure 4.16). In *P. fluorescens* TE-D111A (pTmlUM1) and (pTmlUM2), where both TmlU and the TE domain are enzymatically inactivated by point mutation, no release of PA-A or PA-B (C_5) was observed. PA-B (C_5) was observed in the wild type *P. fluorescens* with TmlU as expected, and *P. fluorescens* TE-D111A (pAMHI). The HPLC profile for the control strains was as expected in terms of the compounds that were eluted.

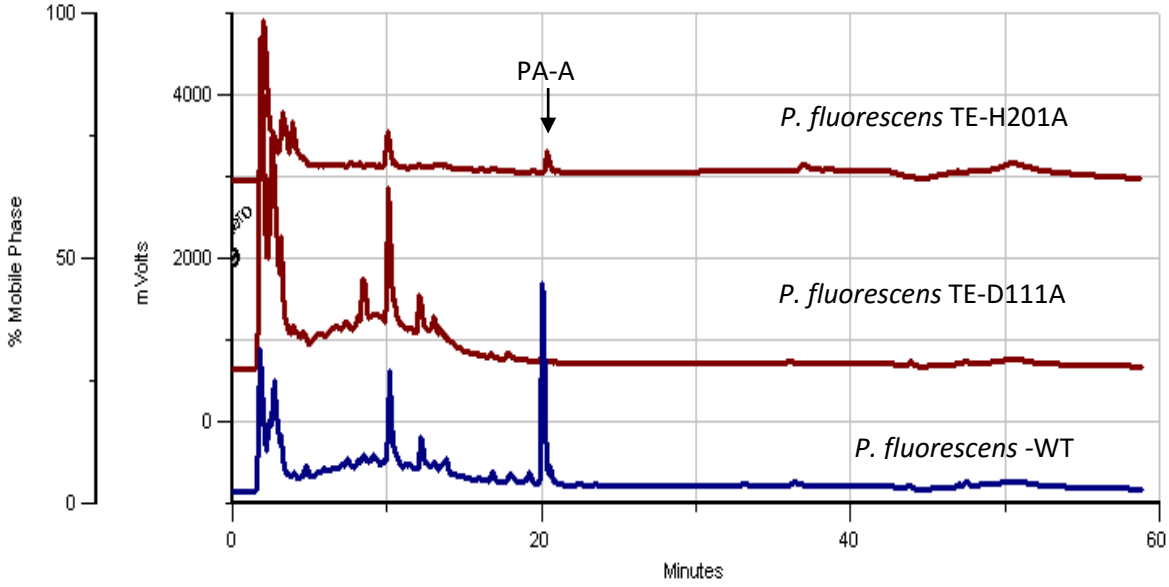

Figure 4.15 The effect of the TE point mutation. The HPLC chromatograph shows the effect of the two different point mutations on PA-A production.

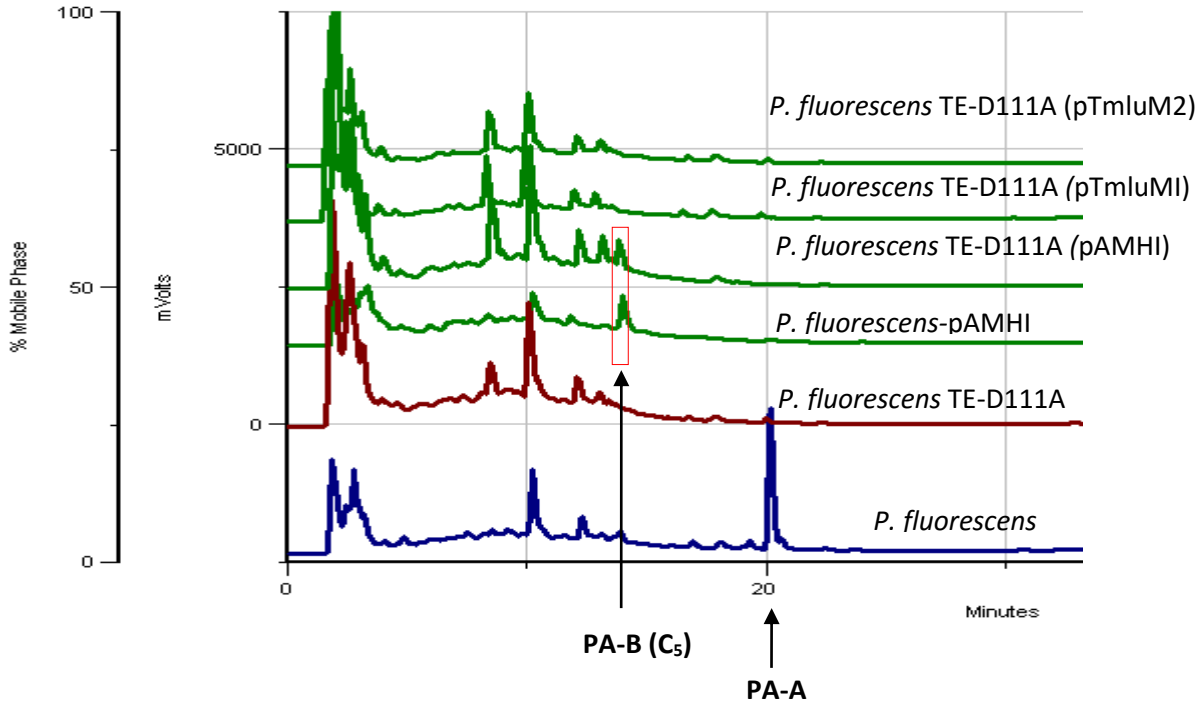

Figure 4.16 The effect of the TE-D111A point mutation on TmlU action. HPLC chromatograms showing production of PA-B (C5) when pAMHI is introduced to the *P. fluorescens* TE-D111A and *P. fluorescens* WT. *P. fluorescens* TE-D111A and *P. fluorescens*-pAMHI were used as controls.

4.2.8 Testing the interaction between Thioesterase and TmlU

The results in the previous section (4.2.7) indicated that for PA-B (C5) to be produced, both an intact TE domain and an active TmlU are needed. This suggests that TmlU might interact directly with the TE domain. The bacterial two hybrid system (BACTH) was used in order to test this hypothesis. The principle of this method is described in section 2.5. The first step was to clone both the open reading frames for both the thioesterase of *mmpB* (designated *te*) and *tmlU* into pKT25 and pUT18 respectively. This was achieved using *Xba*I and *Hind*III for restriction digest and the resulting plasmids were designated pUT18tmlU and pKT25TE. These two plasmids were then co-transformed into the host strain *E. coli*-BTH101. As a positive control, *E. coli*-BTH101 was also transformed with the two plasmids pUT18-zip and pKT25-zip, as they express the fusion proteins which come together as a result the dimerization of the leucine zipper motif. As a negative control, *E. coli*-BTH101 was transformed with the empty pUT18 and pKT25 vectors.

The bacterial strains were then plated on L-agar supplemented with 0.5mM IPTG and 40µg/ml X-gal, in addition to Ampicillin and Kanamycin for plasmid selection and incubated at 30°C for 24-72 hours. *E. coli*-BTH101 co-transformed with pUT18tmlU and pKT25TE produced blue colonies after 24 hours, while the negative strains produced lighter blue colonies. This suggested that there is an interaction as predicted. As an additional negative control *E. coli*-BTH101 was transformed with pUT18tmlU and pKT25, and pKT25TE with pUT18, both yielding light blue colonies. To check if TmlU behaves in the same way in its native system (the thiomarinol pathway), TmpB-TE (Figure 1.15) was also checked for interaction with TmlU. The results obtained were negative (Figure 4.17). To quantify and confirm the bacterial two hybrid results, β-galactosidase assays were conduct (Figure 4.18). The results provided evidence that TmlU and MmpB-TE from the

mup cluster do interact. However, no interaction was detected between TmlU and TmpB-TE from the pTMLI cluster, with a similar OD420 value to the negative control.

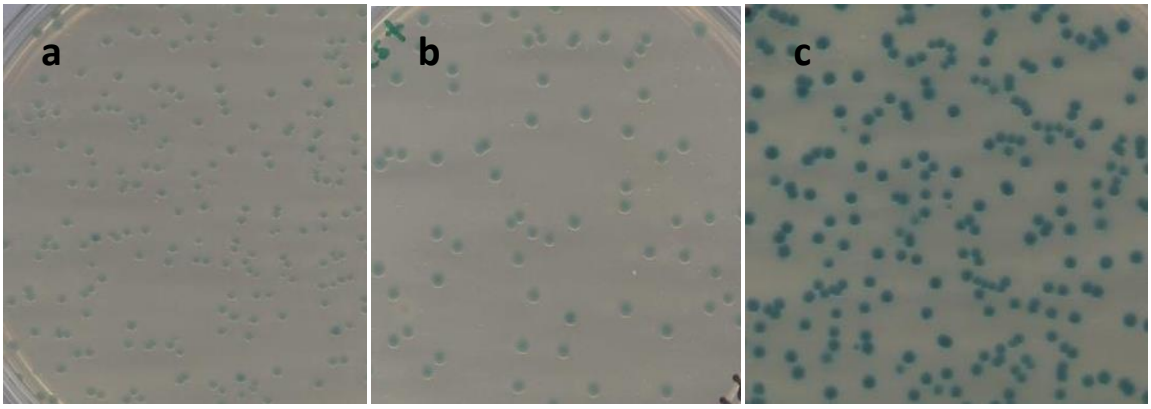

Figure 4.17 The results of using the Bacterial two hybrid system to test for interaction between TmlU and MmpBTE. **a)** BTH101 transformed with pUT18 and pKT25 vectors served as a negative control; **b)** BTH101 transformed with pUT18-tmlU and pKT25-TE which are the subject of the study; and **c)** the positive control where BTH101 strains were transformed with plasmids pUT18-zip and pKT25-zip

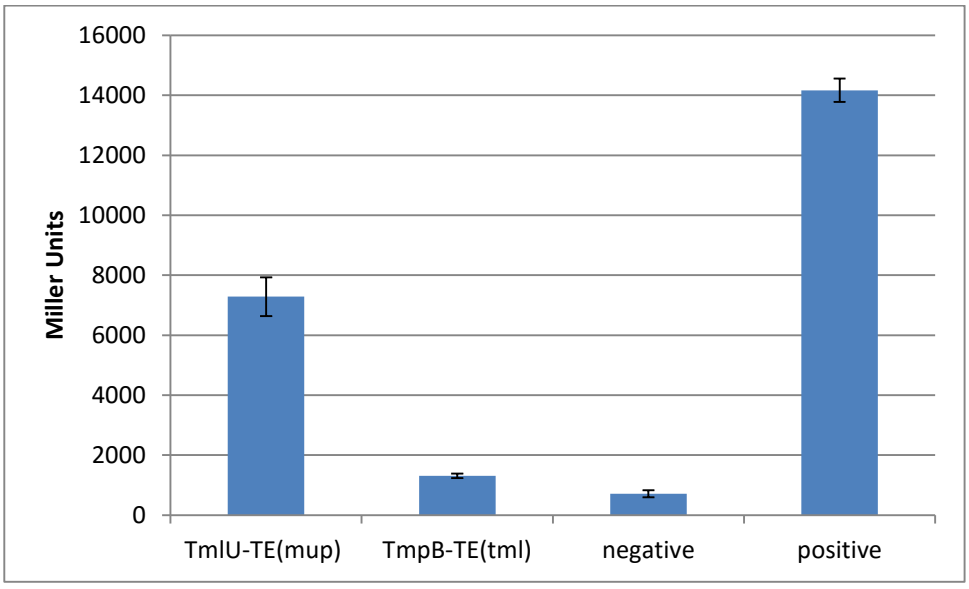

Figure 4.18 Beta-galactosidase assay to quantify the level of interaction between TmlU and MmpB-TE and TmpB-TE. As a positive control *E. coli*-BTH101 was transformed with the two plasmids pUT18-zip and pKT25-zip that express the fusion proteins which come together as a result the dimerization of the leucine zipper motif. As a negative control, *E. coli*-BTH101 was transformed with pUT18 and pKT25.

4.2.9 Discussion

Mutants of *Pseudoalteromonas* SANK73390, Δ*tmpD* (the largest PKS gene in the thiomarinol cluster) and Δ*tmlU* were previously examined for the potential of carrying out mutasynthesis. Feeding PA-A to ΔPKS mutants resulted in the formation of five different compounds: the pyrrothine derivatives of pseudomonic acid A and its 4-hydroxylated analogue, 4-hydroxypseudomonic acid A and two of 4-hydroxypseudomonic acid amides (Murphy *et al*., 2011). The ability of ΔPKS mutants to produce these compounds suggests that they are capable of adding pyrrothine to PA-A, in addition to catalysing its 4-hydroxylation. Similarly, marinolic acid was produced in both the ΔNRPS and Δ*tmlU* strains, demonstrating the ability of TmlU and the 4-hydroxylase to accept thiomarinol analogues. So to further exploit the activity of *tmlU*, it was cloned into *Pseudomonas fluorescens* NCIMB10586 using the IncQ vector pJH10 under the control of the *tac* promoter and the *lacI*^{q} gene (Murphy *et al*., 2011). When no IPTG was added to induce expression of *tmlU* a reduced amount of PA-A was produced. When *tmlU* expression was induced the C5 version of both PA-A and PA-B were produced.

The observations made by Ahmed Omer-Bali, suggested that the ACPs of MmpB may be the point at which TmlU interacts with MmpB. To follow up on this hypothesis, *tmlU* was introduced to *P. fluorescens* strains with ACP (5, 6 and 7) single deletions. The purpose of this experiment was to investigate the position where TmlU interacts with MmpB. Hence, this test was designed to determine which one of the ACPs is the interaction point with TmlU. However, despite the initially promising results from Ahmed (Omer-Bali, A. 2013), the results presented in this thesis demonstrate that the absence of any of the ACPs in MmpB does not change the inhibitory effect of TmlU on PA-A production. All the strains with the single deletions did not produce any PA-A. However,

these results are not consistent with what was observed in the bioassays or with what was reported by (Omer-Bali, 2013).

Because the results obtained from introducing *tmlU* to *P. fluorescens*-ΔACP6 were inconsistent, we had to think of another way to understand the causes of this inhibitory effect. Given the 9-HN truncation observed with TmlU expression, it seemed logical that MmpB could be involved in causing this sensitivity to TmlU. Therefore, investigation into any protein-protein interaction between TmlU and any of the other parts of MmpB was undertaken.

As deletions of different parts of in MmpB did not provide us with any clues regarding the inhibitory effect of TmlU, it seemed reasonable to test whether the enzymatic activity of TmlU is needed for inhibition, or if steric inhibition is sufficient (assuming that the mutation would not change the TmlU structure). The results obtained this experiment suggested that the activity of TmlU does play a role in causing the inhibitory effect as shown in Figure 4.11. Mutations 1 (D422A) and 2 (D422S) were observed to make *P. fluorescens* strains less sensitive to TmlU, however mutation 3 (K206R) did not seem to affect TmlU enzymatic activity, and behaved as wild type TmlU by blocking mupirocin production. This could be explained by the location of both mutations 1 and 2 in the AMP binding sites, whereas 3 is not.

Although very interesting, knowing that TmlU enzymatic activity is essential is only part of the puzzle, as it does not reveal which part of the biosynthetic pathway TmlU is interfering with. As previous results have demonstrated that the deletion of the *mmpB*-TE abolished mupirocin production, it could be that the TE is needed for the release, but not its enzymatic activity. TmlU could be associated with TE to be ready to capture its substrate from MmpB at or before release. Thus, in order to test this hypothesis a point

mutation was made in the TE active site to deactivate its enzymatic activity, preferably without altering the TE domain structure.

While introducing TmlU to *P. fluorescens-mmpB*ΔTE did not release any product, introducing *tmlU* to *P. fluorescens* with point mutations to the TE domain did indeed result in production of the truncated product PA-B (C_5). On the other hand, when the inactive TmlU was introduced to the point mutated TE strain, PA-B (C_5) was not produced. This indicated that TmlU activity is critical for this process to take place, and so is the presence of the TE domain, as it may be needed to tether TmlU in the right place (Figure 4.16).

To further investigate these predictions, the bacterial two hybrid system was used to test the interaction between TmlU and *mmpB*-TE. The results revealed that the TE and TmlU do seem to interact (Figure 4.17). When quantified by β-galactosidase assay (Figure 4.18), a level of interaction significantly higher than the negative controls was observed. Although the data presented provided an explanation for a significant part of the TmlU inhibitory effect, it does not explain how exactly this process takes place. Previous work on the mupirocin pathway demonstrated that about 30% of PA-B gets converted into PA-A when *P. fluorescens* NCIMB10586 strains that cannot produce PA-B are fed with PA-B (Gao *et al*., 2014). This is also observed in *P. fluorescens* strains where the TE domain is deleted, which implies that the TE is not needed for the release of the substrate from mAcpE. In which case PA-B should be easily converted to PA-A if it was to be released into the cytoplasm by after MmpB action. One explanation could be that TmlU and MupU compete to bind the TE, and if the binding of MupU was not efficient it might affect the processing of the PA-B substrates.

Previous experiments considered the possibility of MmpB being a dimer. In this scenario there would be two thioesterase domains in one complex. This hypothesis could

explain why we still see truncated versions of PA-A at a low TmlU level, as one of the TEs would be occupied with TmlU while the other is associated with MupU. This could mean that PA-B-CoA can be produced by TmlU, which is then used by MupU in order to load the mAcpE. When a high level of TmlU is expressed, this may lead to the occupation of both TEs by TmlU, preventing the efficient binding of MupU and processing to PA-A (Figure 4.19).

In light of these findings we can conclude that the reason for TmlU interference with mupirocin biosynthesis is its interaction with the TE domain. This proved to be important not only for the release of the truncated product but also for tethering TmlU, allowing capture of intermediates. These results also represent the first strong evidence that MmpB makes the 9-hydroxynonanoic acid.

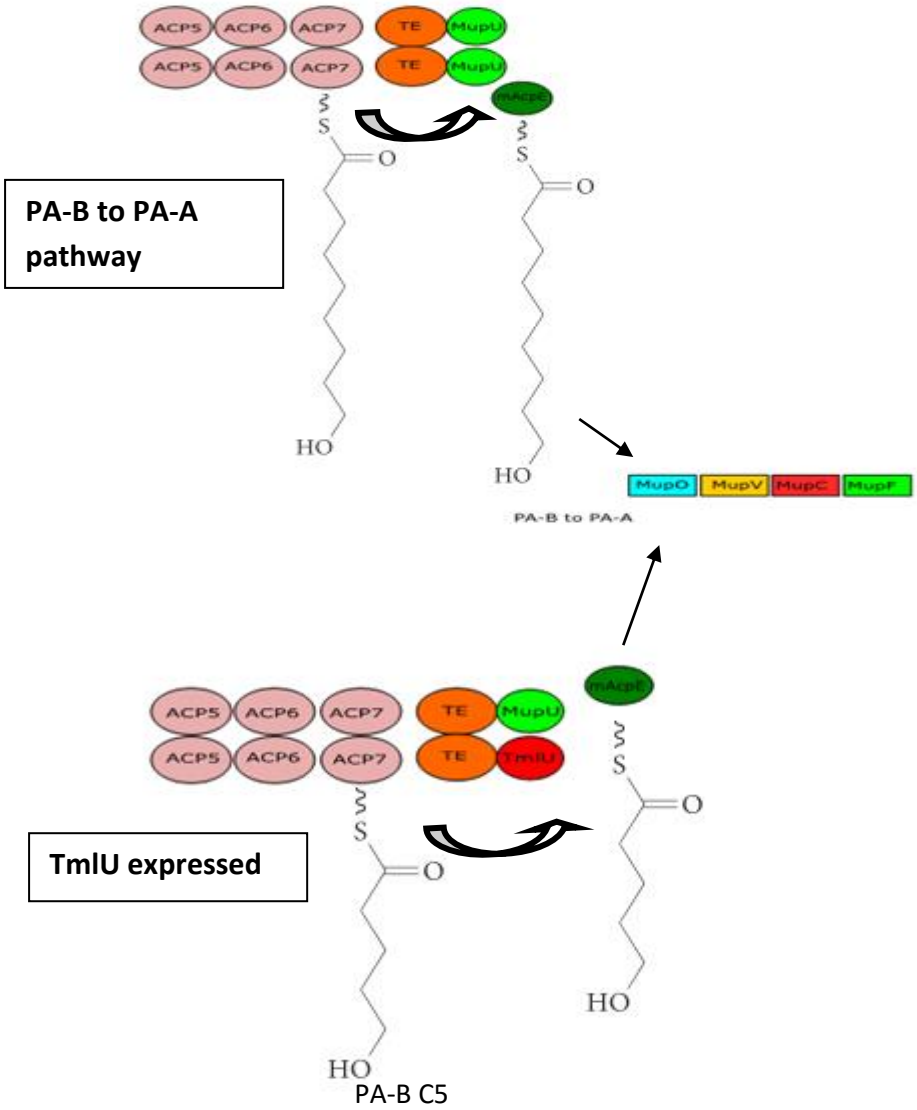

Figure 4.19 Schematic diagram showing putatively how TmlU affects the release of PA-A. The upper panel represents the wild type mupirocin tailoring pathway post MmpB. After release of the 9-HN intermediate catalysed by the MmpB TE domain, MupU loads the intermediate onto the discrete mAcpE, after which MupO, MupV, MupC and MupF complete tailoring to the final pseudomonic acid A product. The lower panel represents the hypothetical explanation for inhibition by TmlU. TmlU competes with MupU for binding the TE domains of the MmpB dimer. When TmlU binds it catalyses the premature release of truncated fatty acids. At low TmlU concentrations, sufficient MupU could bind the TE domain, explaining the various length PA-A forms observed. However, at high TmlU concentrations, MupU would not bind efficiently, explaining the observed switch to truncated PA-B forms.

Chapter 5

5 Expressing the Hol genes from the thiomarinol cluster in *P. fluorescens*

5.1 Introduction

Polyketides and NRPS peptides constitute major classes of natural products that exhibit a wide range of biological activities, which makes them of great importance to our current pharmacopeia. Combinatorial biosynthesis studies have without doubt opened the door to discovering the endless potential of the natural products as antimicrobial compounds. With more polyketides and NRPS being discovered with unusual domains or new module organization, the manipulation of such diverse machinery is becoming a very attractive strategy for drug discovery purposes.

In modular PKSs many of the techniques used to engineer the pathways are limited to individual domains or modules, while very few studies are involved in investigating the possibility of combining a whole protein subunit from different polyketides systems to create hybrid pathways with demonstrated therapeutic activities. Tang and coworkers applied this concept to *Streptomyces lividans* by co-transforming it with *pikAI* and *pikAII* which encode module 1 to 4 of picromycin, and the *eryAIII* and the *eryAIII* gene encoding subunit 3 which includes modules 5 to 6 of erythromycin (Tang *et al*., 2000). The result of this co-expression was a hybrid macrolactone 3-hydroxynarbonolide. Daptomycin is an antibiotic that is produced by an NRPS in *Streptomyces roseosporus*. When the NRPS genes from related pathways were expressed *in trans* in a ΔNRPS *Streptomyces roseosporus* strain, a full complementation was achieved (Miao *et al*., 2006). These studies prove that entire subunits or a complete set of genes can be used successfully to engineer polyketide biosynthetic pathways and produce derivatives with improved therapeutic properties.

In the thiomarinol biosynthesis pathway there are seven ORFs that make up the NRPS gene cluster responsible for producing holomycin: *holA* (NRPS), *holB* (oxidoreductase), *holC* (thioesterase), *holD* (dehydrogenase), *holE* (acyltransferase), *holF* (oxygenase), and *holG* (decarboxylase) (Figure 1.15). Several experiments were conducted to test the possibility of creating new hybrid families using SANK73390 strains that harbour mutations or deletions in the NRPS genes. It was reported that *ΔholA* mutants could incorporate different pseudomonic acid metabolites or even amines such as anhydroornithine into the thiomarinol pathway, by accepting alternative substrates. This suggests that these NRPSs are flexible enough to be used for mutasynthesis studies (Murphy *et al*., 2011). As a proof of concept this chapter reports an attempt to express the genes for the entire NRPS subunit from SANK 73390 *in trans* in *P. fluorescens* NCIMB 10586 to see if it is possible to create a thiomarinol–like hybrid using the mupirocin pathway rather than the marinolic acid pathway as the partner.

5.2 Results

5.2.1 Construction of pHolA-H

Given the length of the entire *hol* genes fragment (~11 kb) and to avoid introducing any errors during the amplification process, it made sense to divide the *hol* genes into three pieces. These were amplified separately and then assembled into one vector. In pTML1, there appear to be five transcriptional units (*tmlT* to *tmlN*, *tmlM* to *tacpB, tmlA* to *tmlF, tmlY* to *tmlP* and *tacpA* to *holH)***.** This suggests that the *hol* genes are likely to be transcribed from one promoter as one operon, and so it should be feasible to express all of them under control of the *tac* promoter (Fukuda *et al*., 2011). The natural ribosome binding sites (RBS) were used for cloning of all the *hol* genes. The 5.8 kb segment encoding the NRPS genes designated Hol1 was amplified using primers as shown

in Table 2.9, and cloned into the vector pGEM-T-Easy, (Figure 5.1a). The ligation was achieved by A-tailing the Hol1 fragment so it could be inserted between the 3´-T overhangs at the insertion site of pGEM-T-Easy generating the plasmid pGEMHol1. An important part of the strategy is that the fragment is flanked by the restriction sites *Xho*I and *Age*I to allow the sub-cloning in the next stage of this process.

In a similar manner pGEMHol2 was produced by amplifying 3.25 kb of the NRPS genes and ligating it into the vector pGEM-T-easy**.** The Hol2 DNA fragment is flanked with sites for the restriction enzymes *Age*I and *Avr*II.

The next step after constructing pGEMHol1 and pGEMHol2 was to insert both of Hol1 and Hol2 fragments into one plasmid. *Sbf*I cuts pGEM-T-Easy vector at the nucleotide 89, so pGEMHol1 was digested with *Age*I and *Sbf*I, while Hol2 was cut out of pGEMHol2 using the same restriction enzymes *Age*I and *Sbf*I as shown in Table 2.5**.** The resulting plasmid, which includes both Hol1 and Hol2 was named pGEMHol12. The third segment (Hol3 fragment) which constitutes 3.16 kb of the NRPS genes was designed to be flanked by *Avr*II and *Bst*bI restriction sites and was cloned into pGEM-T-easy vector in the same way as the Hol1 and Hol2 fragments to produce the plasmid pGEMHol3.

In order to assemble all the fragments into one vector, Hol3 was cut out of pGEMHol3 using restriction sites *Avr*II and *Sbf*I, and ligated into pGEMHol12 which had been digested with the same enzymes, producing pGEMHol123 (Figure 5.1b). To transfer all the genes that make up the *hol* NRPS from SANK 73390 into the expression vector pJH10 as a single piece, pJH10 was digested with *Xho*I and *Cla*I, while Hol123 was cut out using *Xho*I and *Bst*bI (which has ends compatible with *Cla*I) and the DNA ligated. The plasmid produced, designated pHOLA-H, was quality checked by digest and sequencing (Figure 5.1c).

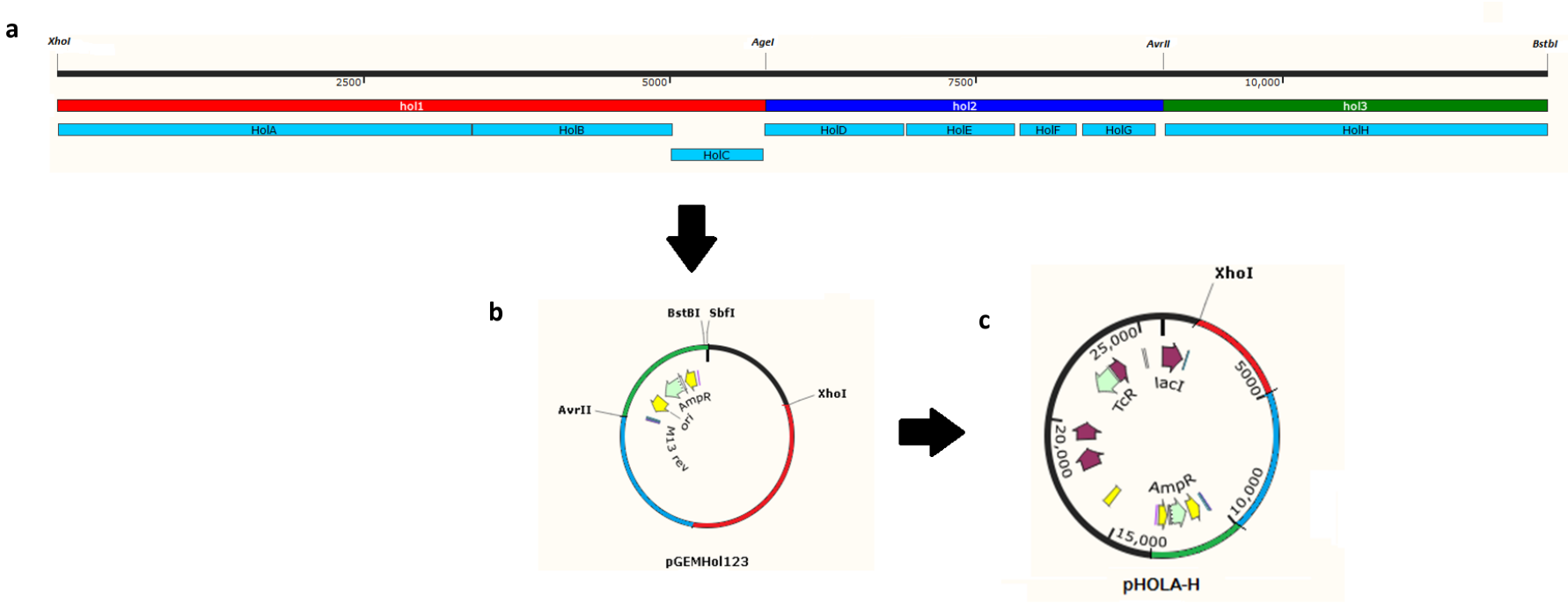

Figure 5.1 a) A linear map of the hol genes (blue segments). The amplified parts of the hol genes are represented by hol1, hol2 and hol3. **b)** hol1, hol2 and hol3 were cloned separately into pGEM- T-easy producing pGEMHol123. The entire fragment (Hol123) was flanked by *Xho*I and *Bstb*I sites. **c)** Construction of the IncQ expression vector encoding all the hol genes: *Bstb*I and *Cla*I have compatible cohesive ends, based on this it was decided to digest pJH10 vector with *Xho*I and *Cla*I and move the Hol123 fragment into the expression vector pJH10 by digesting pGEMHol123 with *Xho*I and *Bstb*I generating

5.2.2 Insertion of *tmlU* into the pHOLA-H expression plasmid

To create a hybrid pathway between holomycin and mupirocin, it is important to have the putative amide ligase TmlU present**.** Therefore, *tmlU* was amplified and cloned into pHOLA-H between the sites *Abs*I and *Pac*I to create pHolA-HtmlU.

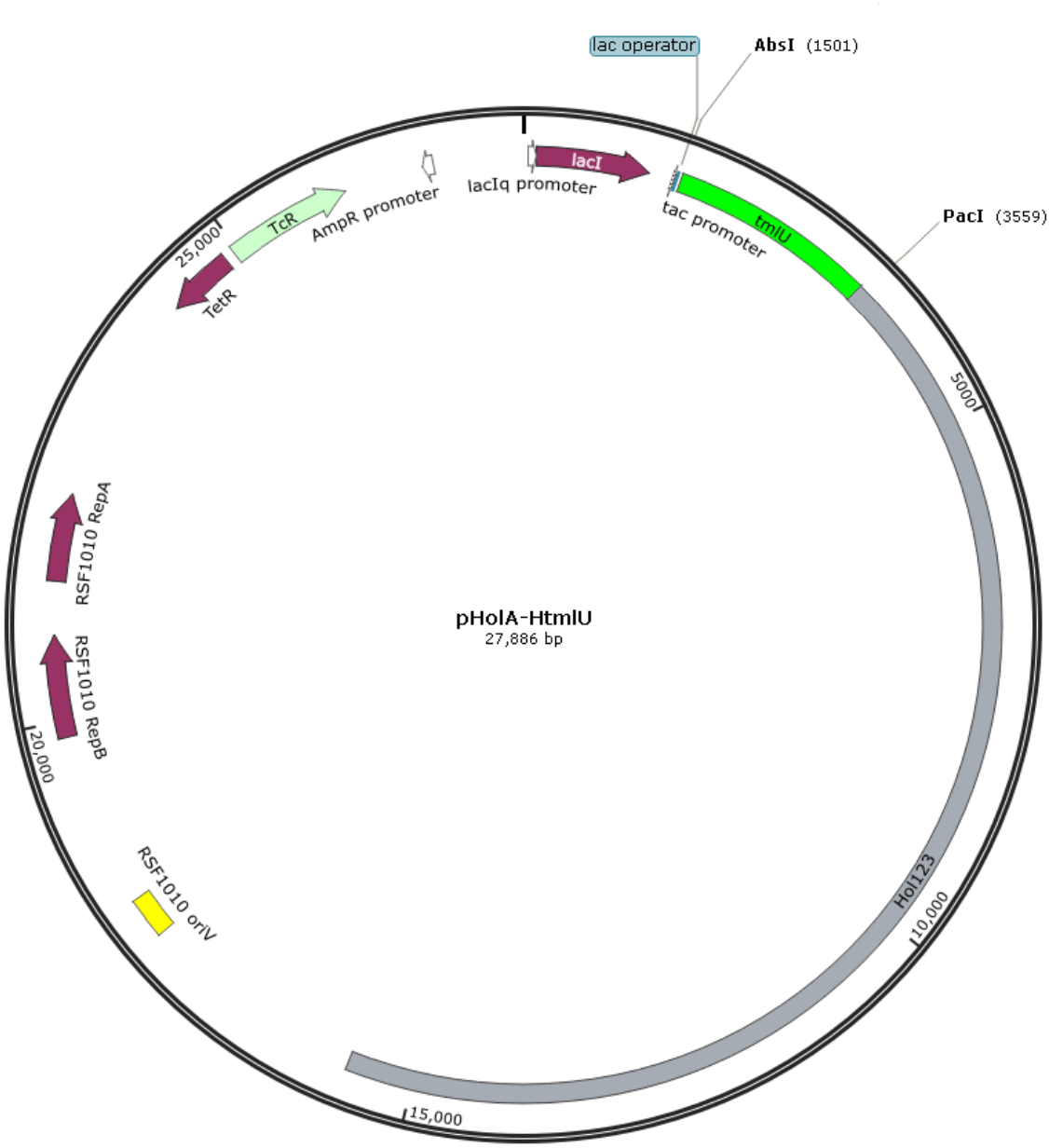

Figure 5.2 Map of the expression plasmid pHolA-HTmlU. A *tmlU* fragment was cloned into pHolA-H between the *Abs*I and *Pac*I sites.

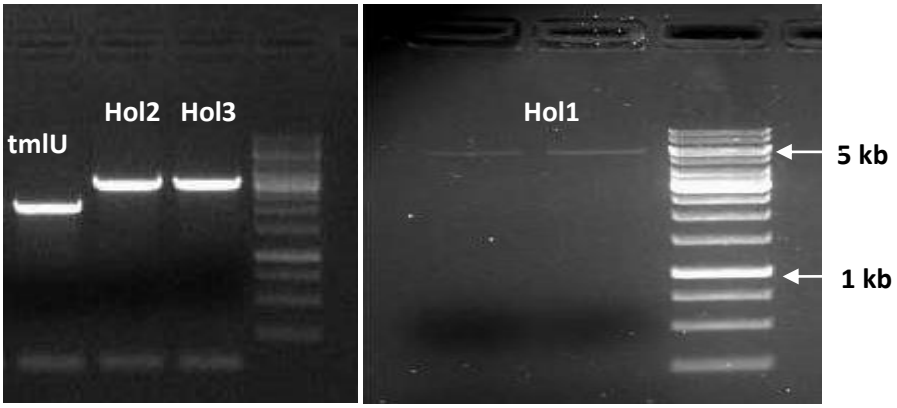

Figure 5.3 Verification of pHOLA-HtmlU by colony PCR.

5.2.3 Expression from pHOLA-HtmlU in *P. fluorescens* NCIB10586

Using the conjugation method explained in section 2.3.11, pHolA-HtmlU was transferred from *E. coli* S17-1 to *P. fluorescens* NCIB10586, both to determine any phenotypic effect of the *hol*-genes (pyrrothine) on *P. fluorescens*, and whether or not expressing pyrrothine genes would give rise to a new compound as a result of creation of a hybrid pathway. The thiomarinol NRPS part produces holomycin, which belongs to the pyrrothines. A key feature for the pyrrothines is the yellow pigment they produce, responsible for the bright yellow phenotype of SANK 73390 (Shiozawa *et al*., 1993). However, the obtained transformants looked white in colour despite containing pyrrothine genes as shown in (Figure 5.4).

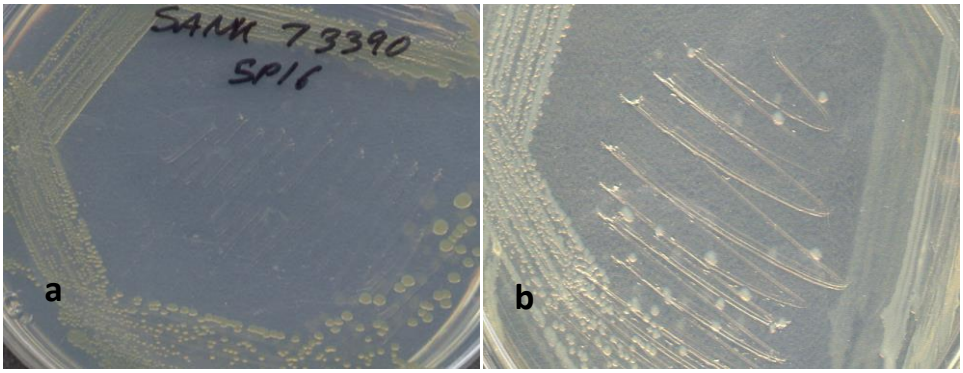

Figure 5.4 Phenotype comparison of **a)** SANK 73390 WT and **b)** *P. fluorescens* (pHOLA-H).

5.3 Discussion

The growing number of the biologically active compounds that are built up of hybrid pathways, provide diverse platforms to engineer novel metabolites. This applies in particular to engineering hybrid polyketide-peptide biosynthetic pathways starting from the many biosynthetic clusters that have been cloned and characterised. However, although the available biochemical and genetic data allow us to predict the function of domains and modules for both PKS and NRPS, there is still relatively little known about how domains and modules interact with each other. This makes the mission of creating new hybrids and effective pathways more challenging.

In *P. fluorescens*, one way to explore the potential of making a hybrid pathway is to test the possibility of expressing a set of genes in the mupirocin producer strain. If correctly expressed *P. fluorescens* might be able to produce both mupirocin and holomycin, and the presence of these two biosynthetic pathway may give a rise to a new compound which is a hybrid between the two as in the case of the thiomarinol system. This approach will also add to our knowledge of how these systems work and how flexible they are.

Many recent studies investigated the possibility of creating a hybrid scaffold by merging two pathways; an interesting observation is that both PKSs and NRPSs utilize a similar strategy to synthesise different classes of natural products (Du *et al*., 2001). In one of the studies, the Tylosin polyketide synthase (Tyl PKS) was produced in a *Streptomyces venezuelae* strain that lacks the pikromycin PKS gene cluster. The mutated *Streptomyces venezuelae* not only produced tylactone (a 16-membered ring macrolactone), but also produced a small amount of desosamine-glycosylated tylactone, which proved the possibility of creating a hybrid molecule (Jung *et al*., 2006). On a smaller scale, the ACP

of the actinorhodin polyketide synthase was swapped with ACPs from other pathways such as the granaticin, oxytetracycline and tetracenomycin pathways. These all produced aromatic polyketides similar to actinorhodin, and it was also observed that some ACP regions are interchangeable, yielding functional hybrid ACPs (Khosla *et al*., 1993). Although swapping and replacing domains in PKSs is a common practice to achieve a hybrid pathway, this nevertheless highlights the fact that building blocks from different biosynthetic pathways can be used to construct a functional hybrid compound. However, one of the best demonstrations of creating hybrid pathway was conducted in an *E. coli* strain, where different components from different biosynthetic systems have been expressed together. These components included, for example, a phosphopantetheinyl transferase gene from *Bacillus subtilis*, genes responsible for the methylmalonyl-CoA extender unit from *Streptomyces coelicolor* and many more required to make a complete and functional biosynthetic pathway. This eventually resulted in production of the expected compound from entirely hybridized machinery (Kinghorn *et al*., 2009).

The mupirocin and thiomarinol pathways share many features both structural and functional, and the idea of assembling parts of both into one hybrid pathway could be feasible, given the successful outcome of the previously conducted studies. The problem with cloning an entire functional pathway is that the antibiotic produced by that particular set of genes might be toxic to the bacterial cell, which makes it challenging to express. In this case the NRPS genes from the thiomarinol pathway encode the pyrrothine production pathway, which potentially could be harmful to *P. fluorescens*. However, transfer of the pHolA-H genes to *P. fluorescens* was successful, although the observed transfer frequency was low. While the colonies obtained contained the plasmid pHolA-H, the observation that they did not produce the yellow pigmentation characteristic of pyrrothines suggests the *hol* genes were either not expressed correctly, or not processed to the active form. In the

mupirocin biosynthetic pathway there are eleven type I ACPs in addition to five type II ACPs (mAcpA-E). ACPs rely on post-translational modification to convert the apoACP into the active holo-form. This process is catalysed by a phosphopantetheinyl tranferase (PPTase) and involves the attachment of a phosphopantetheine prosthetic group to a conserved serine residue. The role of the ACP in this process is to hold the acyl intermediates attached to the thiol of the phosphopantetheine moiety, which in turn supplies the KS active sites and some other catalytic domains with the necessary substrates. Three types of PPTases can be found based on sequence and ACP specificity: the first is the AcpS type of *Escherichia coli* which is normally responsible for the modification of ACPs of primary metabolism. The second type is related to the surfactin synthase PPTase of *Bacillus subtilis* and modifies carrier proteins in secondary metabolic pathways, including the ACPs in PKSs and NRPSs pathways. The third group of PPTases are found integrated as domains in multifunctional type I proteins and are usually found in fungal type I FASs (Lewis Mander, 2010, Shields *et al*., 2010).

Given that TmlN and MupN appear to be homologous (Figure 5.5), there was potential that MupN would convert the apoACP into the active holo-form through its phosphopantetheinyl transferase activity. However, given the lack of holomycin production in the *P. fluorescens* NCIMB10586, it may be that the *hol* ACPs specifically require TmlN (putative phosphopantetheinyl tranferase). If this were the case, then in order for the different parts of this assembly and especially the *hol* genes to be correctly processed after expression, a functional *tmlN* would be needed. Future work would therefore be to add this to the system to see if this achieves the desired functional hybrid pathway. Therefore, *tmlN* could be cloned into another, compatible vector such as pJS701, which is an IncP-9 expression plasmid. The effect of the presence such a vector co-maintained with pHolA-H in terms of pyrrothine production is yet to be determined.

Figure 5.5 Alignment of MupN from the mup cluster and TmlN from the pTML1. MupN is thought to be a Phosphopantetheinyl transferase. The sequence shows that TmlN might have the same function as MupM since they seem to have conserved areas.

Chapter 6

6 Attempts to bypass KS2 gatekeeper activity in the *mup* cluster

6.1.1 Introduction

Many steps of the mupirocin biosynthesis pathway have been elucidated, however some features of the *mup* cluster are still ambiguous as to the way mupirocin is synthesised. In this regard, tailoring regions in the mupirocin biosynthesis pathway are yet to be fully characterised, despite the insight gained from previous knock-out studies (Hothersall *et al*., 2007). While trying to identify the gene responsible for the 6-hydroxylation of monic acid, one possible candidate considered by Dr. Joanne Hothersall at the University of Birmingham (personal communication) was *mupA*. MupA is predicted to introduce the hydroxyl group at C6 based on its similarity to proteins such as OnnC and PedJ from the onnamide and pederin pathways respectively, in which they are proposed to add a hydroxyl group at C7. Considering the position of the 6-OH group in the backbone it could not be added until after the condensations performed by MmpD. The first module of MmpD joins carbons 14-13 to 12-11 plus carbon 17 due to the alpha methyl addition (bearing in mind the numbering system is in reverse order compared to the direction of synthesis). The second module adds carbons 10 and 9, the third adds carbons 8 and 7 plus the carbon 16 due to alpha methyl addition, whilst the fourth adds carbons 6 and 5. Thus the earliest that 6-hydroxyation could occur is after the condensation performed by module 4. Moving to MmpA, the KS of module 1 is predicted to be non-elongating (KS^0) because of its sequence family, and because only two further elongations are needed to complete the monic acid backbone which are performed by MmpA modules 2 (adding carbons 4 and 3) and 3 (adding carbons 2 and 1 as well as carbon 15 of the beta-branch methyl group), (Figure 6.1) (Haines *et al*., 2013).

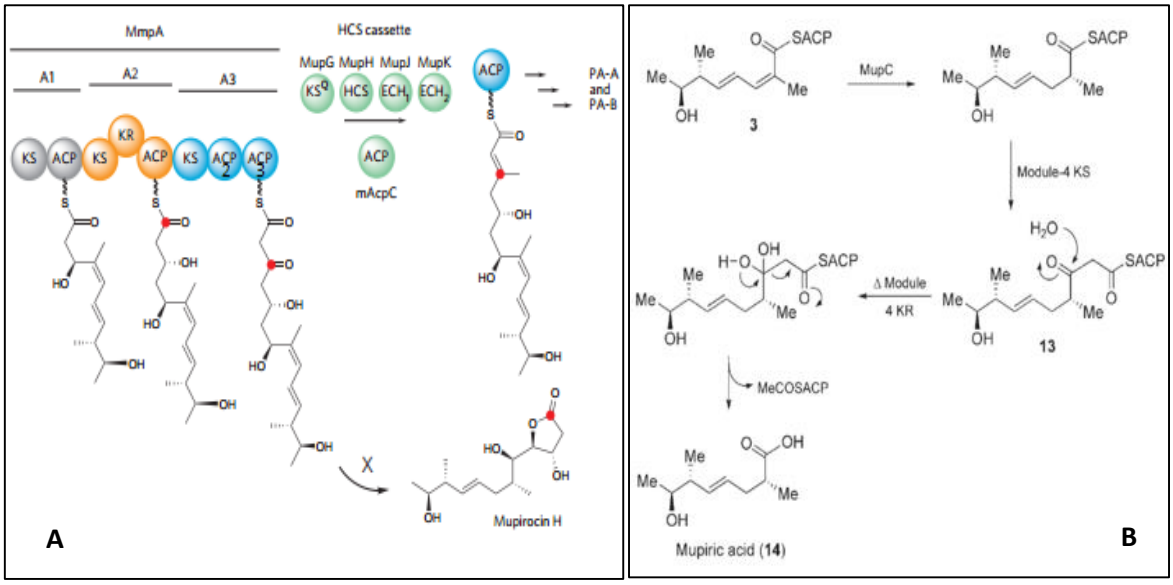

Figure 6.1 Biosynthetic pathway for PA-A showing mupirocin H production when HCS is inactivated. a) Proposed biosynthetic pathway of monic acid and the formation of mupirocin H. ACP domains ACP2 and ACP3 are involved in the third module of MmpA. The red dots represent the position of C3 in pseudomonic acid as it progresses through the biosynthetic pathway. b) Proposed biosynthesis of mupiric acid. Adapted from (Haines *et al.*, 2013).

Mupirocin H, the intermediate released in elevated quantities when the *mupH* encoding part of the beta-branching cassette is mutated, depends on the presence of the 6-OH as part of the off-loading and ring formation. So we can also deduce that the 6-OH must have been added at an earlier stage, shortly after the addition of carbons 6 and 5. One possibility is that it happens on the non-elongating module of MmpA and since *mupA* is located immediately adjacent to it, there would be a sort of genetic logic that would make this a neat hypothesis. To test this hypothesis *mupA* was deleted and also point mutations were made in the active site of *mupA* (G127A, D134A) by Dr. Joanne Hothersall. LC-MS was performed by our collaborators in the University of Bristol to identify the secondary metabolites produced by the mutant strains. This revealed that the strains with deleted *mupA* produced mupiric acid but interestingly no mupirocin H, while the ones with point mutations in *mupA* had a similar profile to the *P. fluorescens* wild type.

The interesting observation here is that when *mupA* is deleted no other intermediates longer than mupiric acid were produced, which suggests that MupA is acting after MmpD. In the same way accumulation of mupirocin H indicates that the mutated protein acts at some point after the MupH cassette. This deletion has also shown that the intermediates lacking the α-hydroxyl produced by *P. fluorescens ΔmupA* cannot go beyond or past MmpD. In this chapter, we investigate whether *mupA* is in fact responsible for adding this α-hydroxyl, and if yes, what makes the 6-hydroxylated intermediates capable of proceeding further in the biosynthetic pathway, compared to the non-hydroxylated intermediates?

In many *trans*-AT PKSs, the KS is proposed to play the role of gatekeeper by transferring specific intermediates through the assembly line (Gay *et al*., 2013) (Nguyen *et al*., 2008). Assuming that this is the case with the KS-mupA2 (in the second module of the MmpA subunit), it is possible that this KS is specific for α-hydroxylated intermediates, hence it does not allow any non-hydroxylated intermediates to pass through. To test this hypothesis Dr. Rohit Farmer at the University of Birmingham performed a docking study. A homology model of KS-mupA2 dimer was generated to imitate the decarboxylation stage of the Claisen condensation, where the substrate is attached to the catalytic cysteine in the KS active site, and the malonate is attached to the phosphopantetheine arm of the ACP (Figure 6.2 and Figure 6.3).

An interesting observation is that a DNYK motif seems to be conserved between the KSs in MmpA and TmpA, but not in the other KSs (Figure 6.4). This observation led to the idea of swapping the KS-mupA2 loop with the loops from KS-mupA1 and KS-mupA3 as these two do not require an α-hydroxylated substrate and might allow the pathway to continue.

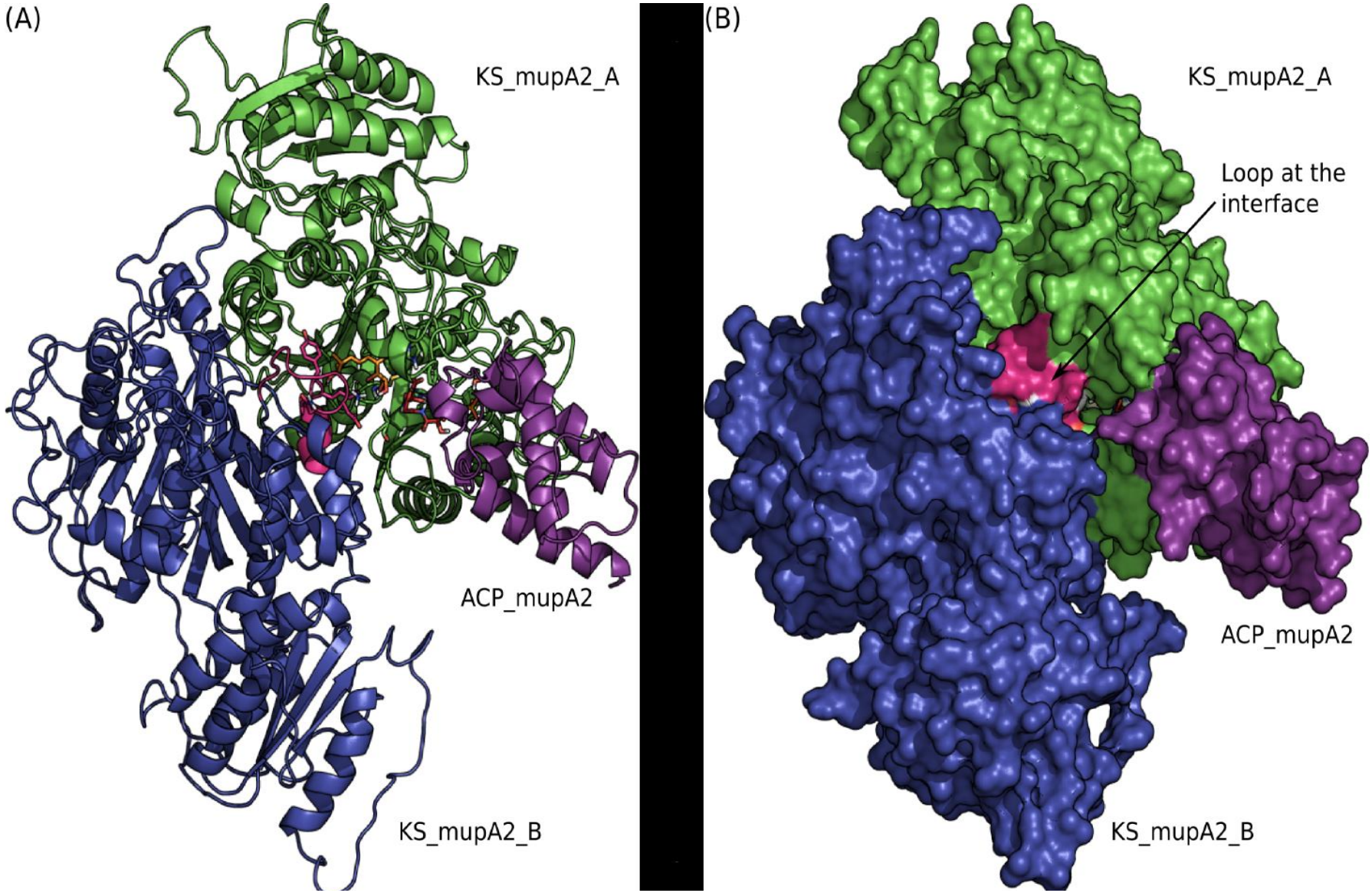

Figure.6.2 Cartoon and surface illustrations of the KS-mupA dimer with the dockedACP-mupA2. The chains A and B of KS-mupA2 dimer are coloured in green and blue respectively, while the interface loop is coloured in pink. (A) The cartoon illustration shows the phosphopantetheine-polyketide intermediate as sticks.

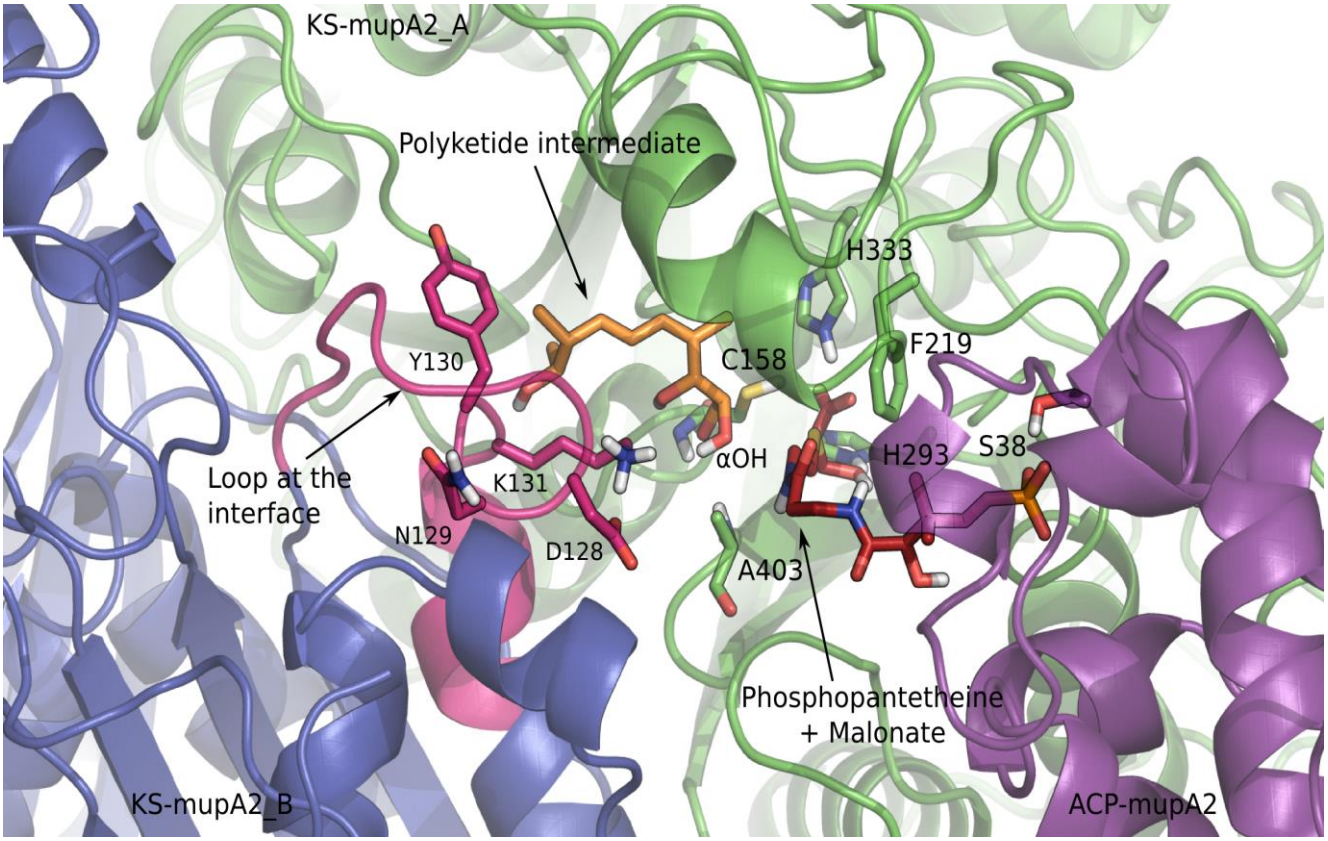

Figure.6.3 A close up view of the DNYK motif which is shown in pink coloured sticks (Dr. Rohit Farmer – University of Birmingham)

```
KS-mupA1     DWKGSAT--------GVFIAAERNEY--HLNLLQAQIDPGEGLDQAASMLANRVSHFYDL
KS-mupA2     SLEQEKV--------GVFVGVSKAGH-DNY-------------KDSFFSIANRVSYRFGF
KS-mupA2SS   ----EEE--------EEEE--------------------------HHHHHHHHHHH----
KS-mupA3     GLAASARHEDAEGMVGVFVGVTYEEY-QLYGAQQTAEGRPLVLSMSPSSIANRVSFVNGF
KS-mupD1     ALAGSRT--------GVFVAAFNYDYKQLLESAGLPIDAHHSTGNAAAVIANRISHFYDL
KS-mupD2     QRRAEV---------SVYVGCEQGDYDQLFDDMPPPQSFW---GNAPSIVPARIAYYLDL
KS-mupD3     ALRRT----------GVYVGVMYQEY-QLFGAEQTLLGRPMALSGSSASIANRVSWSLGL
KS-mupD4     ATEGQPV--------GVYVGASASDYRSLFAEAAPAQAFW---GNASSIIPARIAYHLDL
KS-tmpA1     SLRGSNT--------GVFVGFERNEY--LLNLIESGHDTGESLHQSDSMIANNISYFFDF
KS-tmpA2     ELESDTV--------GVFVGISKAGF-DNY-------------KDSYFSAANRISYRFNF
KS-tmpA3     ALAQSTMIDKTPGVVGVYVGVTYQEY-QLYGAQETMLGNPMVLSMSPSSIANRVSYFCDF
KS-tmpD1     TLSGQNV--------GVYIGAFNFDYKELLEKHERPIEAYQSTGTANAIIANRISHFYDF
KS-tmpD2     SIDGNAV--------SIYVGCEQGDYERLFADSPLPQSFW---GNAPSIIPARLSYHLNL
KS-tmpD3     SKLGDHV--------GVFVGVMYSEY-QLYGAQQGVLGTPISLGGSAASIANRVSFSLNF
KS-tmpD4     PEFGENA--------GVYVGCNSGDYKNILSDEAPAQAFW---GNAGSITPARLSYYLNL
```

Figure 6.4 Alignment of the KS domains from the *mup* cluster and the *tml* cluster showing the conserved motif in MmpA and TmpA which was swapped in KS-mupA2 (in the second module of the MmpA) with KS-mupA1 and KS-mupA3.

6.2 Results

6.2.1 Experimental design

As explained in section 6.1.1 the idea was to replace the KS2-MmpA loop with the KS1-MmpA and KS3-MmpA loops in both the *P. fluorescens* wild type and *P. fluorescens ΔmupA*, (Figure 6.5). The primers were designed to be suitable for the SOEing PCR method, such that the loops from KS1-mmpA and KS2 mmpA were included in the primers as shown in Table 2.10.

```
ks2_mmpa   IAIIGMAGVYPKSADLSAFWDCLANAGDCIETVPEQRWSLDEHFNADRQRAIQEGKSYGK
ks1_mmpa   VAIIGLSANVAQSASVRQFWQALDDDRSLIEEIPATRFDFTSWYAGSN---IEEGKMRTR
ks3_mmpa   VAIIGLAGRYPQARTLEEFWQVLSQGRDCISEIPTERWDHSRYYSADE---DAPGKTYAR

ks2_mmpa   WGGFIEGLDDFDPMFFNFSLAEATYMHPKERQFIQCAWHALEDAGYTPASLEQEK-----
ks1_mmpa   WGGFIPAIDQFDPVFFGMLPAEARKMDPQQRLLLMSVRQTFEDAGYRHTDWKGSA-----
ks3_mmpa   WGGFIDGVAEFDPAFFGISPREAMAMEPQERLFLQTAHEAIEDAGYTRQGLAASARHEDA

ks2_mmpa   ---VGVFVGVSKAGHDNY-------------KDSFFSIANRVSYRFGFTGPSLPVDTACS
ks1_mmpa   ---TGVFIAAERNEYHLNLLQAQIDPGE-GLDQAASMLANRVSHFYDLRGPSERIDAMCA
ks3_mmpa   EGMVGVFVGVTYEEYQLYGAQQTAEGRPLVLSMSPSSIANRVSFVNGFHGPSMAIDAMCA

ks2_mmpa   SSLTAVHEACLHLQAGECTVAVVGGVNAYTHPSTFAEFARLGVLSADGKSRAFGAGANGF
ks1_mmpa   GGAVALHHAVTALRSGQINAAIVGACNLLLRPDVFVTLSQSGQMSPEPTVRSFGAGADGY
ks3_mmpa   SSLTTIHLACQSLHSGECQVALAGGVNVSIHPAKFLMLGAGKFASRRGRCESFGASGSGY

ks2_mmpa   VPGEGVGALLLKPLERALADGDMVHGVIAASAVNH-GGKANGYTVPNPEAQRAMIRLALD
ks1_mmpa   LRGEGVCSLLLKPLSKAEADGDHIYGLIRNTAVNYNGGDAASIAAPSVSAHSSLVQDCYR
ks3_mmpa   VPSEGVGAVLLKPLHQAQADGDRIYGVIRGSAINH-GGRTNGYAVPNPAAQAAVISRALR
```

Figure 6.5 The KS2 -mupA amino acids highlighted in yellow were replaced by the loops of KS1-mmpA and KS3-mmpA highlighted in green.

Following a successful amplification, the required fragment was cloned into pAKE604 suicide vector in order to integrate the replaced loops into the chromosomal DNA of *P. fluorescens ΔmupA* (Figure 6.6). The chromosomal integration method and suicide vector excision are described in detail in section 2.3.11.

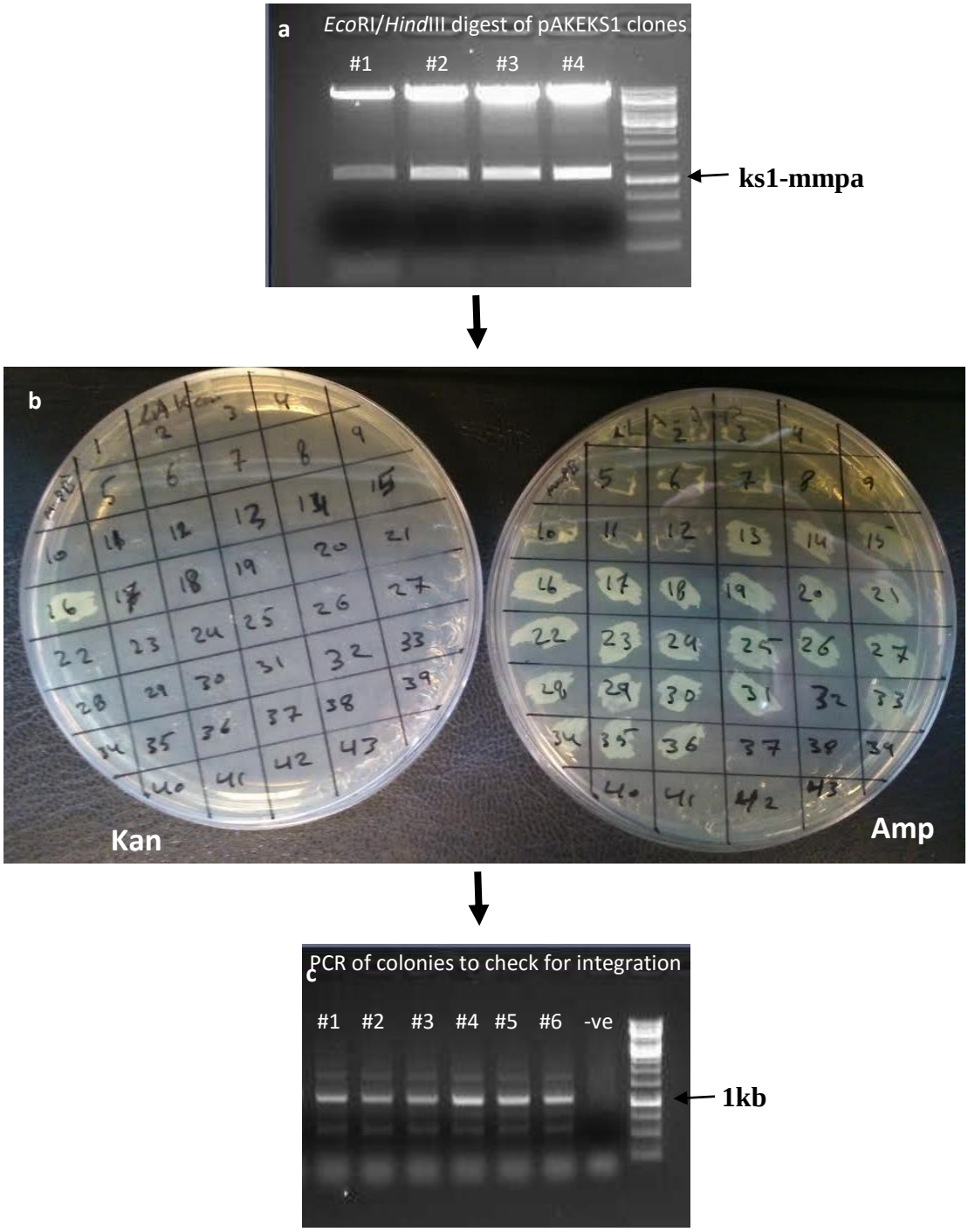

Figure 6.6 (a) Multiple pAKEKS1 clones digested with *Eco*RI and *Hind*III to check if it contains the ks1-mmpA fragment; **(b)** Replica plating to screen for excision of the suicide plasmid; and **(c)** Colony PCR of *P. fluorescens* to check if that integration has taken place.

6.2.2 Analysis of products

The hypothesis was that MupA hydroxylates pseudomonic acid at the 6-OH position. Deletion of *mupA* results in production of mupiric acid only, which is produced by MmpD, implying that the chain cannot pass through KS2-MmpA and the pathway is somehow blocked. It was hypothesized that the KS2 loop specificity for hydroxylated products is the reason for this blockage, and if the loop was replaced with loops from other KSs like KS1-MmpA or KS3-MmpA this would solve the issue, as these KSs do not require α-hydroxylated substrates to pass the growing chain. Therefore, it was logical to expect the new product to be more hydrophobic than pseudomonic acid A and hence it would elute later than 20 minutes (PA-A retention time). *P. fluorescens ΔmupA*-(KS1) and *P. fluorescens ΔmupA*-(KS3) were analysed by HPLC to check for pseudomonic acid A derivatives along with relevant controls (Figure 6.7). As expected the strain with the deleted *mupA* did not produce pseudomonic acid A, while the strain with the replaced loop (KS2 loop swapped with KS1 loop) *P. fluorescens* ΔmupA-KS1 did produce a new peak with a retention time of 22-23 minutes (Figure 6.7 a). However, this was later identified by LC-MS as a non-pseudomonic acid product by our collaborators in Bristol. The KS2 loop swap was also done in the *P. fluorescens* WT and the resultant product had a similar profile and retention time to *P. fluorescens* ΔmupA-KS1 (Figure 6.7 b).

The strain *P. fluorescens* ΔmupA-KS3 where the KS2 loop was replaced with the KS3 loop was also analysed by HPLC but the results were different to those from the *P. fluorescens* ΔmupA-KS1 as there was no product at all, and the HPLC traces looked quite similar to the *P. fluorescens ΔmupA*. KS3 loop was also introduced to the wild type *P. fluorescens* and the same results were obtained (Figure 6.8).

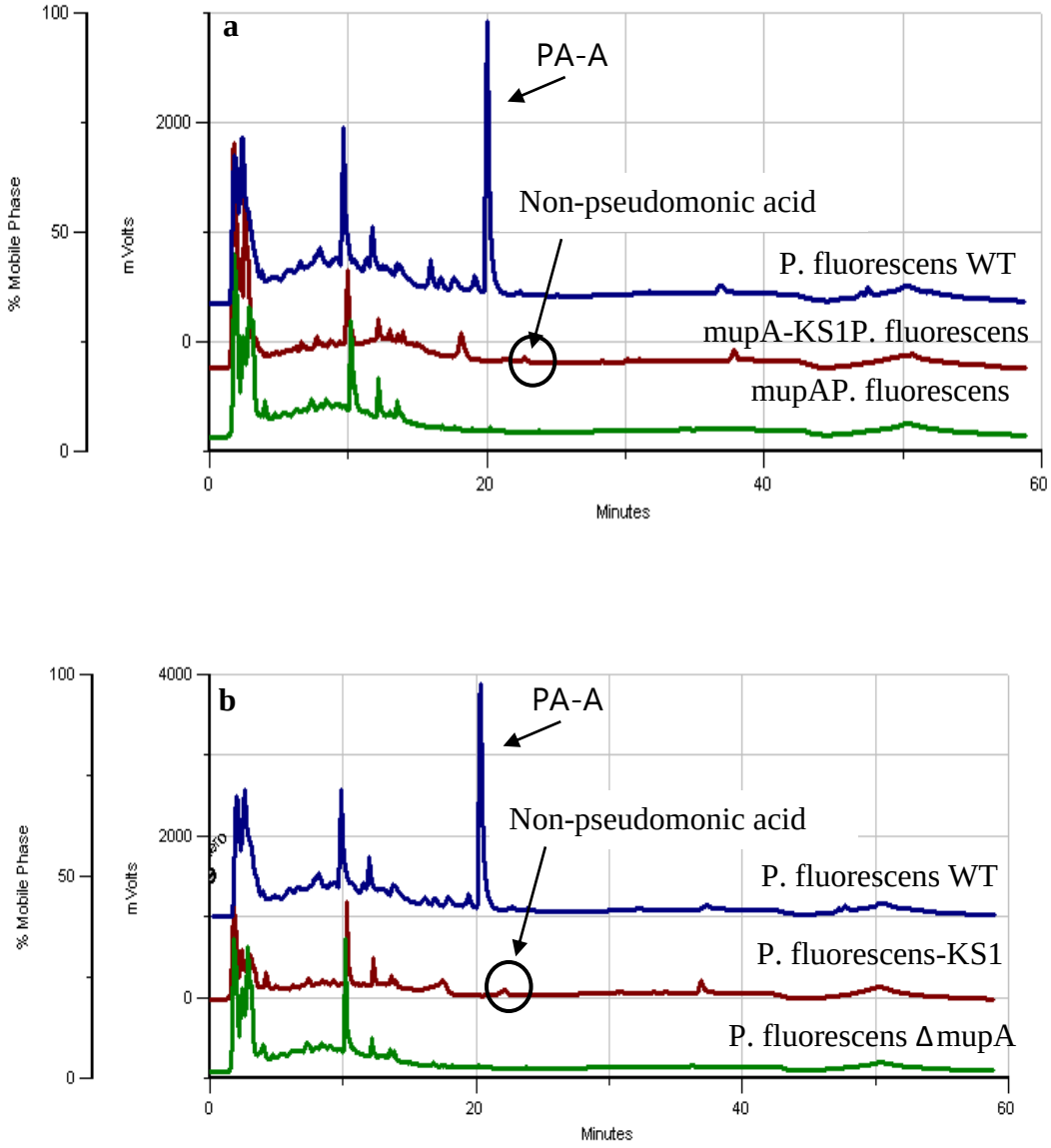

Figure 6.7 HPLC analysis of **a)** *P. fluorescens ΔmupA-KS1* and **b)** *P. fluorescens-KS1* , *P. fluorescens* WT and *P. fluorescens ΔmupA* were used as controls.

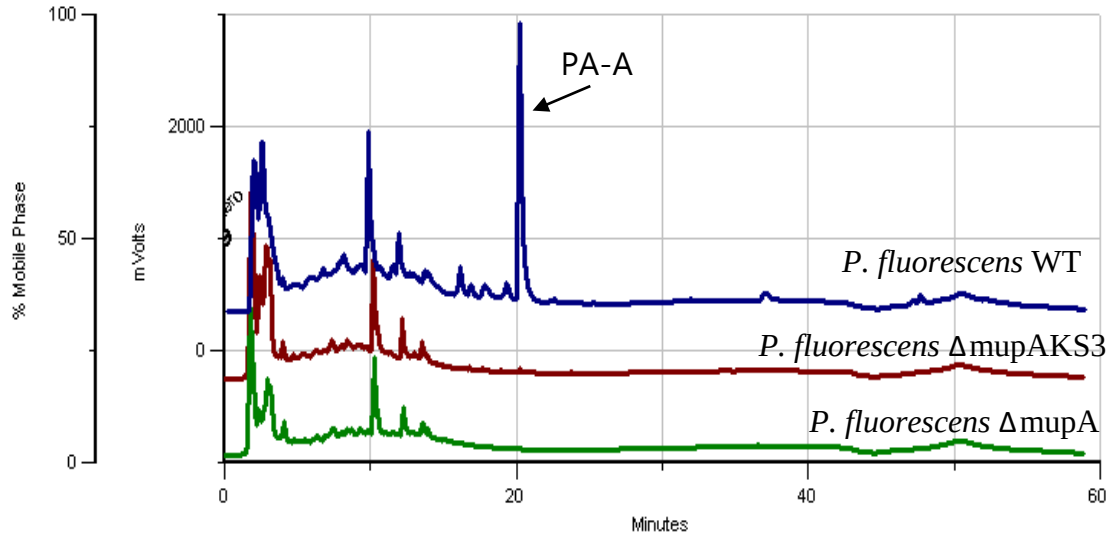

Figure 6.8 HPLC traces of *P. fluorescens ΔmupAKS3* *P. fluorescens WT* and *P. fluorescens ΔmupA* were used as controls.

6.3 Discussion

Mupirocin biosynthesis is thought to begin with creation of the C_{12} pentaketide moiety by MmpD. The basis for this deduction goes back to the accumulation of mupiric acid by a mutant *P. fluorescens* strain with a deletion in the KR of MmpD domain 4. This observation meant that the intermediate produced was not able to carry on through the biosynthetic pathway to the stage of a fully formed monic acid.

In order to study the biosynthetic pathway of Mupirocin and identify genes and proteins involved in the pathway several deletions and mutations have been made. For this Chapter the mutation(s) of interest were created by Dr. Joanne Hothersall, with the aim of identifying which part of the cluster is responsible for adding the 6-hydroxyl group. Given the position of this α-hydroxyl it was proposed that *mupA*, which is a tailoring gene in the mupirocin biosynthetic pathway, might be responsible for this hydroxylation as discussed

in the introduction. Therefore, a mutant strain of *P. fluorescens* was created with *mupA* deleted.

The results obtained from analysing *P. fluorescens* NCIMB10586 *ΔmupA* with HPLC confirmed that, consistent with the proposal, the only product released by the mutant was mupiric acid, which is a shunt product released by module 4 of MmpD. With that in mind the next step mainly revolved around testing whether MupA is in fact a hydroxylase, and if so what is preventing a non-hydroxylated product from continuing on down the assembly line, which is the case when *mupA* is deleted. One explanation would be that if MupA is acting as a hydroxylase, the non-hydroxylated substrate resulting from *mupA* deletion would not be recognized by the KS in MmpA. Hence the chain would not be extended to proceed to the next module.

An example of *trans*-AT ketosynthase intolerance is the KS5 of the bacillaene pathway, which does not accept an acyl chain with methyl branching at the β-position. This was demonstrated to be due to a key residue in BaeL-KS5 which controls KS5 tolerance to branching. The sequence of Bael-KS5 was compared to another 150 KSs domains from various *trans*-AT PKSs. Sequence analysis revealed that the presence of Gly and Ala is crucial for accepting the carbon branch in the acyl chain (Kohlhaas *et al*., 2013).

KS specificity in PKS systems has been an interesting research area recently, and with the advancing computational studies a lot has been revealed regarding the basis of the KS specificity and how it works. However, when it comes to bioengineering, functional testing is still a necessity to understand the rules of rational engineering of the different PKS systems (Hertweck, 2015).

The computational modelling of the KS-mupA2 revealed the unique motif DNYK which is conserved in both MmpA and TmpA but not in the rest of the KSs of either

pathway. However, when *P. fluorescens-ΔmupA* KS3 and *P. fluorescens-ΔmupA* KS1 were analysed by HPLC the obtained peaks were non-pseudomonic acid derivatives, which suggested that the pathway is still blocked. The only piece of information we have regarding the 6-hydroxylation is that the gene responsible for it is most likely to be acting after MmpD. In addition to MupA there is another candidate that could add the hydroxyl group, MupL (a putative hydrolase), and so to see the effect of swapping the loops we need to introduce the non-hydroxylated substrate into *P.fluorescen ΔmupL*. Future work will need to address this issue further.

Chapter 7

7 General Discussion

7.1 General outlook

With the inevitable rise of resistance against the current and the future antibiotics, it is critical to find ways to keep up with the rapidly evolving bacteria and slow down the selective pressure which is not only dangerous but also costly. One of the successful strategies to produce new antibiotics was to use old antibiotics as a scaffold through synthetic tailoring. Microbial natural products played a major role in the resurgence of antimicrobial agent production, and since their discovery in the 1950s polyketides remain an important driving factor in the process of discovering new sources of antimicrobial compounds. Therefore, the subject of this thesis is highly relevant to the current issue of antibiotic resistance and trying to revive the field of drug discovery with not only new antimicrobial compounds, but also new classes of antibiotics by exploiting the potential of polyketides to provide us with a vast range of new molecules through molecular engineering and mutasynthesis.

7.2 Discussion of key conclusions

7.2.1 Genes *simL, clouL, couL* and *novL* could be used in engineering *P. fluorescens* to accept different precursors

It has been proven by (Anderle *et al*., 2007a) that polyketide synthases can be tolerant of accepting different precursors such as in the case of the aminocoumarins but it has also been shown that similar proteins are not guaranteed to have similar effects on a particular pathway regardless of their structural and functional resemblance. This was evident when CloL and CouL, which share 91% sequence identity, were found to be very different when it came to substrate specificity. While CouL accepted a wide range of

substrates and was rather promiscuous, CloL showed a very strict selectivity for substrates and very few were accepted. This promiscuity of at least some of these different amide ligases encouraged us to hope that they would work to join aminocoumarin to mupirocin or marinolic acid. Although it looks like *simL*, *couL*, *cloL* and *novL* have no negative effect on Mupirocin production, they do cause some sort of change in the pathway particularly *simL* and *cloL*. Looking at the HPLC traces in (Figure 3.8) we notice that in the case of *cloL* and *simL* the PA-A peak starts to decrease when the concentration of the aminocoumarin is increased, but the same cannot be said about *couL* where the PA-A peak seems to be unaffected by the aminocoumarin concentration. It might be that both *cloL* and *simL* are actually incorporating aminocoumarin into the mupirocin pathway, hence the disappearance of the PA-A peak. However, as there are no obvious new peaks in any of the fed strains there is still the possibility of needing another enzyme in order for the amide synthetases to be processed or accept other substrates, as is the case with TmlU and HolE (Section 4.1). More research is needed to identify the observed peaks and whether they are a result of successful substrate incorporation or if we need to include an additional enzyme into the feeding method to facilitate this process.

7.2.2 Can an entire set of genes from the thiomarinol biosynthetic pathway be cloned and expressed *in trans*?

Chapter 5 of this thesis describes the cloning of the full set of *hol* genes from thiomarinol biosynthetic pathway and their expression in-*trans* in *P. fluorescens* NCIMB10586 that produces mupirocin. The ability to successfully do this should provide us with new insight into mutasynthesis, especially if it had been possible to show that the *hol* genes are responsible for producing holomycin, thus representing the possibility of creating a product similar to thiomarinol in case this approach had been successful.

The genes involved were cloned sequentially, keeping their natural RBSs intact. When the *hol* genes were introduced to *P. fluorescens* the colonies looked like typical *P. fluorescens* colonies without the yellow pigmentation expected if they were producing pyrrothine. It is a possibility that pyrrothine is not being produced due to the absence of *tmlN* which is the putative phosphopantetheinyl tranferase. This problem could be solved by cloning *tmlN* on a different expression vector. Another hurdle to be passed might be the survival of *P. fluorescens* itself, since producing pyrrothine might be toxic for the cells in which case *tmlM* should be included in the experimental design as it is the equivalent of *mupM*, the gene responsible for producing mupirocin-resistant IleS2.

7.2.3 Protein-protein interaction might be the reason behind the inhibitory effect of TmlU on mupirocin production

Regardless of whether TmlU works alone to join holomycin and marinolic acid together or the whole process is performed using TmlU and HolE, the fact that introducing *tmlU* to the wild type *P. fluorescens* stops full length mupirocin from being produced demonstrates again that PKSs, although flexible to a certain extent, are more complex than our current ideas suggest, and proves that we still have not unlocked some of the rules that control the biosynthetic pathways. Chapter 4 of this study sheds the light on some of the dynamics involved in accepting and offloading intermediates in the mupirocin biosynthetic pathway.

From the results obtained in Chapter 4 it is evident that TmlU is somehow obstructing the normal flow of events in the Mupirocin biosynthetic pathway. More particularly it seems like *tmlU* is blocking the second and the third round of condensation which prevents the conversion of the 3-hydroxypropionic acid to 9-hydroxynonanoic acid. Inactivation of the CoA ligase in TmlU by point mutations revealed that the enzymatic activity is required for release of the truncated products. Further investigation has also

shown that releasing the intermediate requires the thioesterase TE to be present as no product was released when TE was deleted, despite *tmlU* being expressed in-*trans*. When the thioesterase was inactivated by point mutations and *tmlU* was introduced to the *P. fluorescens* strain, the C5-PA-B reappeared, which suggested the possibility of a protein – protein interaction. This observation drew attention to the fact that both TmlU and TE need to be intact even if not enzymatically active in order for the truncated product to be released, and TmlU may well be associated with TE to be ready to capture its substrate from MmpB at or before release. Further investigation confirmed the possibility of interaction by using the bacterial two hybrid system followed by the β-galactosidase assay. The hypothesis formulated based on the results of this chapter proposes that the TE is necessary for the TmlU effect to take place, perhaps because it tethers TmlU in the right place to release the C5-PA-B. There is also the possibility of MupU being involved in this inhibitory effect especially in situations where TmlU levels are low. In the latter scenario one TE of the dimer may be occupied by MupU while the other is occupied by TmlU, which could explain in a way why we still get the truncated PA-A even with TmlU present. In this case TmlU will compete with MupU to be tethered to TE which results in TmlU processing a truncated intermediate (Figure 4.19). The results presented in this chapter are the most important part of this thesis and represent a very significant step towards a better understanding of the biosynthetic pathway of mupirocin and how to improve our strategies to create a hybrid molecule using mupirocin as a scaffold.

7.3 Future work

Creating effective hybrids requires a good understanding of the rules governing interactions between polyketide modules. Although most of the mupirocin biosynthetic pathway has been elucidated, there are still parts of this system that need more research in order to successfully incorporate new molecules into the pathway. Feeding different compounds to *P. fluorescens* strains can be very useful, but more input is required as to at which stage this will result in a successful incorporation. There is also the issue of which gene will catalyze the joining of two different molecules. These questions could be addressed by trying feeding at different intervals or possibly trying other amide ligases from different pathways.

In order to express a gene correctly all the elements involved should be incorporated, and in case of cloning the *hol* genes there are still missing pieces in this construct that are needed to produce pyrrothine. TmlN is the equivalent of MupN in the *mup* cluster. MupN has been proved to be essential to activate the ACPs of primary metabolism in the mupirocin biosynthetic pathway, it is therefore possible that providing the Hol genes with their own PPTase is critical to their function, and so cloning *tmlN* is the next step to do in order to try to activate the construct pHolA-H (Shields *et al*., 2010). However, fitness cost is one of the main concerns in studies like this as the main fragments are cloned into a 13 kb vector, while the fragment itself is about 11 kb which brings the entire plasmid size to almost 25 kb. Adding TmlN and TmlM will obviously add to this, so the aim should be to clone the two genes into the same vector (pJS701) which is compatible with pJH10-based plasmids.

In regards to the KS2 loop specificity, the hypothesis was built on the basis that *mupA* is involved in hydroxylating pseudomonic acid A at the carbon 6 position. As replacing the KS2 loop with loops from both KS1 and KS3 did not result in the pathway going any further, it is possible that *mupA* does not do what we predicted it to do and in fact if these loops were introduced into a strain like *P. fluorescens ΔmupL*, the pathway might actually pass this bottleneck as *mupL* is a putative hydrolase.

Since it has been recently found that TmlU is in fact a CoA-ligase that needs the acyl transferase HolE to join the two parts of thiomarinol together, it might be feasible to check if HolE also interacts with thioesterase or if it is only TmlU that does this. Previously complementation studies were carried out to test if *tmlU* could complement *P. fluorescens ΔmupU* based on weak similarities (Fukuda *et al*., 2011); although *tmlU* did not complement *mupU*, it would be interesting to see if MupU and the MmpB TE interact. This could give us a better picture about where and how TmlU is interacting within the mupirocin biosynthetic pathway, through its similarity with MupU as it is proposed that MupU transfers the growing polyketide chain to the mAcpE. This could be achieved by using either the bacterial two hybrid system or possibly co-purifying the TE with TmlU and MupU separately, as it would serve as a more solid proof that these two proteins do interact.

REFERENCES

References

A.J.BIRCH (1963) The biosynthesis of antibiotics. *Pure and Applied Chemistry,* 7.

ABE, I. Engineered biosynthesis of plant polyketides: structure-based and precursor-directed approach. *Top Curr Chem,* 297**,** 45-66.

AGNES, M. R. & SCOTT, R. B. (2007) *Polyketides,* American Chemical Society.

ALLEN, H. K., TRACHSEL, J., LOOFT, T. & CASEY, T. A. (2014) Finding alternatives to antibiotics. *Annals of the New York Academy of Sciences,* 1323**,** 91-100.

AMARAL, L., BOEREE, M. J., GILLESPIE, S. H., UDWADIA, Z. F. & VAN SOOLINGEN, D. (2009) Thioridazine cures extensively drug-resistant tuberculosis (XDR-TB) and the need for global trials is now! *International Journal of Antimicrobial Agents,* 35**,** 524-526.

AMINOV, R. I. (2010) A brief history of the antibiotic era: lessons learned and challenges for the future. *Front Microbiol,* 1**,** 2010.

ANDERLE, C., HENNIG, S., KAMMERER, B., LI, S.-M., WESSJOHANN, L., GUST, B. & HEIDE, L. (2007a) Improved Mutasynthetic Approaches for the Production of Modified Aminocoumarin Antibiotics. *Chemistry & Biology,* 14**,** 955-967.

ANDERLE, C., HENNIG, S., KAMMERER, B., LI, S. M., WESSJOHANN, L., GUST, B. & HEIDE, L. (2007b) Improved mutasynthetic approaches for the production of modified aminocoumarin antibiotics. *Chem Biol,* 14**,** 955-67.

ANTONIO, M., MCFERRAN, N. & PALLEN, M. J. (2002) Mutations Affecting the Rossman Fold of Isoleucyl-tRNA Synthetase Are Correlated with Low-Level Mupirocin Resistance in Staphylococcus aureus. *Antimicrobial Agents and Chemotherapy,* 46**,** 438-442.

ARIAS, C. A. & MURRAY, B. E. (2012) The rise of the Enterococcus: beyond vancomycin resistance. *Nat Rev Microbiol,* 10**,** 266-78.

ARTSIMOVITCH, I. & VASSYLYEV, D. G. (2006) Is it easy to stop RNA polymerase? *Cell Cycle,* 5**,** 399-404.

AUGUST, P. R., TANG, L., YOON, Y. J., NING, S., MULLER, R., YU, T. W., TAYLOR, M., HOFFMANN, D., KIM, C. G., ZHANG, X., HUTCHINSON, C. R. & FLOSS, H. G. (1998) Biosynthesis of the ansamycin antibiotic rifamycin: deductions from the molecular analysis of the rif biosynthetic gene cluster of Amycolatopsis mediterranei S699. *Chem Biol,* 5**,** 69-79.

BERMINGHAM, A. & DERRICK, J. P. (2002) The folic acid biosynthesis pathway in bacteria: evaluation of potential for antibacterial drug discovery. *BioEssays,* 24**,** 637-648.

BERTANI, G. (1951) Studies on lysogenesis. I. The mode of phage liberation by lysogenic Escherichia coli. *J Bacteriol,* 62**,** 293-300.

BHULLAR, K., WAGLECHNER, N., PAWLOWSKI, A., KOTEVA, K., BANKS, E. D., JOHNSTON, M. D., BARTON, H. A. & WRIGHT, G. D. (2012) Antibiotic Resistance Is Prevalent in an Isolated Cave Microbiome. *PLoS ONE,* 7**,** e34953.

BRODERSEN, D. E., CLEMONS JR, W. M., CARTER, A. P., MORGAN-WARREN, R. J., WIMBERLY, B. T. & RAMAKRISHNAN, V. (2000) The Structural Basis for the Action of the Antibiotics Tetracycline, Pactamycin, and Hygromycin B on the 30S Ribosomal Subunit. *Cell,* 103**,** 1143-1154.

BROWN, M. G. & BALKWILL, D. L. (2009) Antibiotic resistance in bacteria isolated from the deep terrestrial subsurface. *Microb Ecol,* 57**,** 484-93.

BUSCH, B. & HERTWECK, C. (2009) Evolution of metabolic diversity in polyketide-derived pyrones: Using the non-colinear aureothin assembly line as a model system. *Phytochemistry,* 70**,** 1833-1840.

BUSH, K. (2012) Antimicrobial agents targeting bacterial cell walls and cell membranes. *Rev Sci Tech,* 31**,** 43-56.

CAMPBELL, J. W. & CRONAN, J. E. (2001) BACTERIAL FATTY ACID BIOSYNTHESIS: Targets for Antibacterial Drug Discovery. *Annual Review of Microbiology,* 55**,** 305-332.

CANE, D. E. (2010) Programming of Erythromycin Biosynthesis by a Modular Polyketide Synthase. *The Journal of Biological Chemistry,* 285**,** 27517-27523.

CARLET, J., JARLIER, V., HARBARTH, S., VOSS, A., GOOSSENS, H. & PITTET, D. (2012) Ready for a world without antibiotics? The Pensieres Antibiotic Resistance Call to Action. *Antimicrob Resist Infect Control,* 1**,** 11.

CASSELS, R., OLIVA, B. & KNOWLES, D. (1995) Occurrence of the regulatory nucleotides ppGpp and pppGpp following induction of the stringent response in staphylococci. *Journal of Bacteriology,* 177**,** 5161-5.

CDC (2015) Methicillin-resistant Staphylococcus aureus (MRSA) Infections (08/01/2015), Centre for disease control and prevention.

CHAIN, E. B. & MELLOWS, G. (1977) Pseudomonic acid. Part 1. The structure of pseudomonic acid A, a novel antibiotic produced by Pseudomonas fluorescens. *J Chem Soc Perkin 1***,** 294-309.

CHAN, D. I. & VOGEL, H. J. (2010) Current understanding of fatty acid biosynthesis and the acyl carrier protein. *Biochem J,* 430**,** 1-19.

CHATTERJEE, S. S. & OTTO, M. (2013) Improved understanding of factors driving methicillin-resistant Staphylococcus aureus epidemic waves. *Clin Epidemiol,* 5**,** 205-17.

CHEMLER, J. A., BUCHHOLZ, T. J., GEDERS, T. W., AKEY, D. L., RATH, C. M., CHLIPALA, G. E., SMITH, J. L. & SHERMAN, D. H. (2012) Biochemical and Structural Characterization of Germicidin Synthase: Analysis of a Type III Polyketide Synthase That Employs Acyl-ACP as a Starter Unit Donor. *Journal of the American Chemical Society,* 134**,** 7359-7366.

CHENG, Y. Q., COUGHLIN, J. M., LIM, S. K. & SHEN, B. (2009) Type I polyketide synthases that require discrete acyltransferases. *Methods Enzymol,* 459**,** 165-86.

CLARDY, J., FISCHBACH, M. A. & CURRIE, C. R. (2009) The natural history of antibiotics. *Current Biology,* 19**,** R437-R441.

CLARDY, J., FISCHBACH, M. A. & WALSH, C. T. (2006) New antibiotics from bacterial natural products. *Nat Biotech,* 24**,** 1541-1550.

CLATWORTHY, A. E., PIERSON, E. & HUNG, D. T. (2007) Targeting virulence: a new paradigm for antimicrobial therapy. *Nat Chem Biol,* 3**,** 541-548.

CONTI, E., FRANKS, N. P. & BRICK, P. (1996) Crystal structure of firefly luciferase throws light on a superfamily of adenylate-forming enzymes. *Structure (London, England : 1993),* 4**,** 287-298.

COOPER, S. M., COX, R. J., CROSBY, J., CRUMP, M. P., HOTHERSALL, J., LAOSRIPAIBOON, W., SIMPSON, T. J. & THOMAS, C. M. (2005a) Mupirocin W, a novel pseudomonic acid produced by targeted mutation of the mupirocin biosynthetic gene cluster. *Chemical Communications***,** 1179-1181.

COOPER, S. M., LAOSRIPAIBOON, W., RAHMAN, A. S., HOTHERSALL, J., EL-SAYED, A. K., WINFIELD, C., CROSBY, J., COX, R. J., SIMPSON, T. J. & THOMAS, C. M. (2005b) Shift to Pseudomonic Acid B Production in P. fluorescens NCIMB10586 by Mutation of Mupirocin Tailoring Genes mupO, mupU, mupV, and macpE. *Chemistry & Biology,* 12**,** 825-833.

COX, G. & WRIGHT, G. D. (2013) Intrinsic antibiotic resistance: Mechanisms, origins, challenges and solutions. *International Journal of Medical Microbiology,* 303**,** 287-292.

COSTA, V. M., KING, C. E., KALAN, L., MORAR, M., SUNG, W. W. L., SCHWARZ, C., FROESE, D., ZAZULA, G., CALMELS, F., DEBRUYNE, R., GOLDING, G. B., POINAR, H. N. & WRIGHT, G. D. (2011) Antibiotic resistance is ancient. *Nature,* 477**,** 457-461.

DAS, A. & KHOSLA, C. (2009) Biosynthesis of aromatic polyketides in bacteria. *Acc Chem Res,* 42**,** 631-9.

DAUM, S. J. & LEMKE, J. R. (1979) Mutational Biosynthesis of New Antibiotics. *Annual Review of Microbiology,* 33**,** 241-265.

DAVIES, J. & DAVIES, D. (2010) Origins and Evolution of Antibiotic Resistance. *Microbiology and Molecular Biology Reviews,* 74**,** 417-433.

DITTMANN, E., NEILAN, B. A. & BORNER, T. (2001) Molecular biology of peptide and polyketide biosynthesis in cyanobacteria. *Appl Microbiol Biotechnol,* 57**,** 467-73.

DU, L., SÃNCHEZ, C. S. & SHEN, B. (2001) Hybrid Peptide-Polyketide Natural Products: Biosynthesis and Prospects toward Engineering Novel Molecules. *Metabolic Engineering,* 3**,** 78-95.

DUNN, Z. D., WEVER, W. J., ECONOMOU, N. J., BOWERS, A. A. & LI, B. (2015) Enzymatic Basis of "Hybridity" in Thiomarinol Biosynthesis. *Angew Chem Int Ed Engl,* 2015**,** 201411667.

EL-SAYED, A. K., HOTHERSALL, J., COOPER, S. M., STEPHENS, E., SIMPSON, T. J. & THOMAS, C. M. (2003) Characterization of the mupirocin biosynthesis gene cluster from Pseudomonas fluorescens NCIMB 10586. *Chem Biol,* 10**,** 419-30.

EL-SAYED, A. K., HOTHERSALL, J. & THOMAS, C. M. (2001) Quorum-sensing-dependent regulation of biosynthesis of the polyketide antibiotic mupirocin in Pseudomonas fluorescens NCIMB 10586. *Microbiology-Sgm,* 147**,** 2127-2139.

ENRIQUE RAVINA, H. K. (2011) The Evolution of Drug Discovery. *Weinheim, Germany: Wiley-VCH*

EVANS, B. S., ROBINSON, S. J. & KELLEHER, N. L. (2011) Surveys of Non-Ribosomal Peptide and Polyketide Assembly Lines in Fungi and Prospects for Their Analysis in vitro and in vivo. *Fungal genetics and biology : FG & B,* 48**,** 49-61.

FAIR, R. J. & TOR, Y. (2014) Antibiotics and Bacterial Resistance in the 21st Century. *Perspectives in Medicinal Chemistry,* 6**,** 25-64.

FLOSS, H. G. & YU, T.-W. (2005) RifamycinMode of Action, Resistance, and Biosynthesis. *Chemical Reviews,* 105**,** 621-632.

FUKUDA, D., HAINES, A. S., SONG, Z., MURPHY, A. C., HOTHERSALL, J., STEPHENS, E. R., GURNEY, R., COX, R. J., CROSBY, J., WILLIS, C. L., SIMPSON, T. J. & THOMAS, C. M. (2011) A natural plasmid uniquely encodes two biosynthetic pathways creating a potent anti-MRSA antibiotic. *PLoS One,* 6**,** e18031.

FULLER, A. T., MELLOWS, G., WOOLFORD, M., BANKS, G. T., BARROW, K. D. & CHAIN, E. B. (1971) Pseudomonic acid: an antibiotic produced by Pseudomonas fluorescens. *Nature,* 234**,** 416-7.

GAO, S.-S., HOTHERSALL, J., WU, J. E., MURPHY, A. C., SONG, Z., STEPHENS, E. R., THOMAS, C. M., CRUMP, M. P., COX, R. J., SIMPSON, T. J. & WILLIS, C. L. (2014) Biosynthesis of Mupirocin by Pseudomonas fluorescens NCIMB 10586 Involves Parallel Pathways. *Journal of the American Chemical Society,* 136**,** 5501-5507.

GAO, X., WANG, P. & TANG, Y. (2010) Engineered polyketide biosynthesis and biocatalysis in Escherichia coli. *Applied Microbiology and Biotechnology,* 88**,** 1233-1242.

GAY, DARRENÂ C., GAY, G., AXELROD, ABRAMÂ J., JENNER, M., KOHLHAAS, C., KAMPA, A., OLDHAM, NEILÂ J., PIEL, J. R. & KEATINGE-CLAY, ADRIANÂ T. (2013) A Close Look at a Ketosynthase from a Trans-Acyltransferase Modular Polyketide Synthase. *Structure,* 22**,** 444-451.

GOTTLIEB, T. & NIMMO, G. R. (2011) Antibiotic resistance is an emerging threat to public health: an urgent call to action at the Antimicrobial Resistance Summit 2011. *Med J Aust,* 194**,** 281-283.

GROSS, H. & LOPER, J. E. (2009) Genomics of secondary metabolite production by Pseudomonas spp. *Natural Product Reports,* 26**,** 1408-1446.

GUAN, X., XUE, X., LIU, Y., WANG, J., WANG, Y., WANG, J., WANG, K., JIANG, H., ZHANG, L., YANG, B., WANG, N. & PAN, L. (2013) Plasmid-mediated quinolone resistance, current knowledge and future perspectives. *Journal of International Medical Research,* 41**,** 20-30.

GURNEY, R. & THOMAS, C. M. (2011) Mupirocin: biosynthesis, special features and applications of an antibiotic from a gram-negative bacterium. *Appl Microbiol Biotechnol,* 90**,** 11-21.

HAINES, A. S., DONG, X., SONG, Z., FARMER, R., WILLIAMS, C., HOTHERSALL, J., PŁOSKOŃ, E., WATTANA-AMORN, P., STEPHENS, E. R., YAMADA, E., GURNEY, R., TAKEBAYASHI, Y., MASSCHELEIN, J., COX, R. J., LAVIGNE, R., WILLIS, C. L., SIMPSON, T. J., CROSBY, J., WINN, P. J., THOMAS, C. M. & CRUMP, M. P.

(2013) A conserved motif flags acyl carrier proteins for β-branching in polyketide synthesis. *Nat Chem Biol,* 9**,** 685-692.
HARDY, K. J., HAWKEY, P. M., GAO, F. & OPPENHEIM, B. A. (2004) Methicillin resistant Staphylococcus aureus in the critically ill. *British Journal of Anaesthesia,* 92**,** 121-130.
HASHIMOTO, M., NONAKA, T. & FUJII, I. (2014) Fungal type III polyketide synthases. *Natural Product Reports,* 31**,** 1306-1317.
HAWKEY, P. M. (2003) Mechanisms of quinolone action and microbial response. *J Antimicrob Chemother,* 51 Suppl 1**,** 29-35.
HAY, M., THOMAS, D. W., CRAIGHEAD, J. L., ECONOMIDES, C. & ROSENTHAL, J. (2014) Clinical development success rates for investigational drugs. *Nat Biotech,* 32**,** 40-51.
HE, J. & HERTWECK, C. (2005) Functional Analysis of the Aureothin Iterative Type I Polyketide Synthase. *Chembiochem,* 6**,** 908-912.
HEIDE, L. (2009a) The aminocoumarins: biosynthesis and biology. *Natural Product Reports,* 26**,** 1241-1250.
HEIDE, L. (2009b) Genetic engineering of antibiotic biosynthesis for the generation of new aminocoumarins. *Biotechnology Advances,* 27**,** 1006-1014.
HERMANN, T. (2005) Drugs targeting the ribosome. *Current Opinion in Structural Biology,* 15**,** 355-366.
HERTWECK, C. (2009) The biosynthetic logic of polyketide diversity. *Angew Chem Int Ed Engl,* 48**,** 4688-716.
HERTWECK, C. (2015) Decoding and reprogramming complex polyketide assembly lines: prospects for synthetic biology. *Trends in Biochemical Sciences,* 40**,** 189-199.
HERTWECK, C., LUZHETSKYY, A., REBETS, Y. & BECHTHOLD, A. (2007) Type II polyketide synthases: gaining a deeper insight into enzymatic teamwork. *Nat Prod Rep,* 24**,** 162-90.
HOPWOOD, D. A. (1997) Genetic Contributions to Understanding Polyketide Synthases. *Chem Rev,* 97**,** 2465-2498.
HOPWOOD, D. A. & SHERMAN, D. H. (1990) Molecular genetics of polyketides and its comparison to fatty acid biosynthesis. *Annu Rev Genet,* 24**,** 37-66.
HOTHERSALL, J., MURPHY, A., IQBAL, Z., CAMPBELL, G., STEPHENS, E., WU, J. E., COOPER, H., ATKINSON, S., WILLIAMS, P., CROSBY, J., WILLIS, C., COX, R., SIMPSON, T. & THOMAS, C. (2011) Manipulation of quorum sensing regulation in Pseudomonas fluorescens NCIMB 10586 to increase mupirocin production. *Applied Microbiology and Biotechnology,* 90**,** 1017-1026.
HOTHERSALL, J., WU, J., RAHMAN, A. S., SHIELDS, J. A., HADDOCK, J., JOHNSON, N., COOPER, S. M., STEPHENS, E. R., COX, R. J., CROSBY, J., WILLIS, C. L., SIMPSON, T. J. & THOMAS, C. M. (2007) Mutational analysis reveals that all tailoring region genes are required for production of polyketide antibiotic mupirocin by pseudomonas fluorescens - Pseudomonic acid B biosynthesis precedes pseudomonic acid A. *Journal of Biological Chemistry,* 282**,** 15451-15461.
HOWDEN, B. P., DAVIES, J. K., JOHNSON, P. D. R., STINEAR, T. P. & GRAYSON, M. L. (2010) Reduced Vancomycin Susceptibility in Staphylococcus aureus, Including Vancomycin-Intermediate and Heterogeneous Vancomycin-Intermediate Strains: Resistance Mechanisms, Laboratory Detection, and Clinical Implications. *Clinical Microbiology Reviews,* 23**,** 99-139.
HURDLE, J. G., O'NEILL, A. J., INGHAM, E., FISHWICK, C. & CHOPRA, I. (2004) Analysis of mupirocin resistance and fitness in Staphylococcus aureus by molecular genetic and structural modelling techniques. *Antimicrob. Agents Chemother.,* 48**,** 4366-4376.
HUTCHINSON, C. R., KENNEDY, J., PARK, C., KENDREW, S., AUCLAIR, K. & VEDERAS, J. (2000) Aspects of the biosynthesis of non-aromatic fungal polyketides by iterative polyketide synthases. *Antonie Van Leeuwenhoek,* 78**,** 287-95.
JOSEPH, A. L., JOE, J. H. & RAYMOND, J. T. (2013) Antimicrobial activity of metals: mechanisms, molecular targets and applications. *Nature Reviews Microbiology,* 11**,** 371-384.

JUNG, W. S., LEE, S. K., HONG, J. S., PARK, S. R., JEONG, S. J., HAN, A. R., SOHNG, J. K., KIM, B. G., CHOI, C. Y., SHERMAN, D. H. & YOON, Y. J. (2006) Heterologous expression of tylosin polyketide synthase and production of a hybrid bioactive macrolide in Streptomyces venezuelae. *Appl Microbiol Biotechnol,* 72**,** 763-9.

KAHRSTROM, C. T. (2014) Antimicrobials: Tailor-made poisons for pathogens. *Nat Rev Micro,* 12**,** 791-791.

KHOSLA, C., MCDANIEL, R., EBERT-KHOSLA, S., TORRES, R., SHERMAN, D. H., BIBB, M. J. & HOPWOOD, D. A. (1993) Genetic construction and functional analysis of hybrid polyketide synthases containing heterologous acyl carrier proteins. *Journal of Bacteriology,* 175**,** 2197-2204.

KINGHORN, A. D., CHIN, Y.-W. & SWANSON, S. M. (2009) Discovery of Natural Product Anticancer Agents from Biodiverse Organisms. *Current opinion in drug discovery & development,* 12**,** 189-196.

KOHANSKI, M. A., DWYER, D. J. & COLLINS, J. J. (2010) How antibiotics kill bacteria: from targets to networks. *Nat Rev Microbiol,* 8**,** 423-35.

KOHLHAAS, C., JENNER, M., KAMPA, A., BRIGGS, G. S., AFONSO, J. P., PIEL, J. & OLDHAM, N. J. (2013) Amino acid-accepting ketosynthase domain from a trans-AT polyketide synthase exhibits high selectivity for predicted intermediate. *Chemical Science,* 4**,** 3212-3217.

KUO, A., BLOUGH, N. V. & DUNLAP, P. V. (1994) Multiple N-acyl-L-homoserine lactone autoinducers of luminescence in the marine symbiotic bacterium Vibrio fischeri. *Journal of Bacteriology,* 176**,** 7558-7565.

LEUNG, E., WEIL, D. E., RAVIGLIONE, M. & NAKATANI, H. (2011) The WHO policy package to combat antimicrobial resistance. *Bulletin of the World Health Organization,* 89**,** 390-392.

LEWIS, I. M. (1929) BACTERIAL ANTAGONISM WITH SPECIAL REFERENCE TO THE EFFECT OF PSEUDOMONAS FLUORESCENS ON SPORE FORMING BACTERIA OF SOILS. *Journal of Bacteriology,* 17**,** 89-103.

LEWIS MANDER, H.-W. L. (2010) Comprehensive Natural Products II: Chemistry and Biology: 10 Volume Set.

LI, Y., CHEN, H., DING, Y., XIE, Y., WANG, H., CERNY, R. L., SHEN, Y. & DU, L. (2014) Iterative Assembly of Two Separate Polyketide Chains by the Same Single-Module Bacterial Polyketide Synthase in the Biosynthesis of HSAF. *Angewandte Chemie International Edition,* 53**,** 7524-7530.

LIVERMORE, D. M. (2003) Bacterial Resistance: Origins, Epidemiology, and Impact. *Clinical Infectious Diseases,* 36**,** S11-S23.

LUFT, T., LI, S. M., SCHEIBLE, H., KAMMERER, B. & HEIDE, L. (2005) Overexpression, purification and characterization of SimL, an amide synthetase involved in simocyclinone biosynthesis. *Arch Microbiol,* 183**,** 277-85.

MAGNUSON, K., JACKOWSKI, S., ROCK, C. O. & CRONAN, J. E. (1993) Regulation of fatty acid biosynthesis in Escherichia coli. *Microbiological Reviews,* 57**,** 522-542.

MCDANIEL, R., EBERT-KHOSLA, S., HOPWOOD, D. A. & KHOSLA, C. (1995) Rational design of aromatic polyketide natural products by recombinant assembly of enzymatic subunits. *Nature,* 375**,** 549-54.

MCNEIL, J. C., HULTEN, K. G., KAPLAN, S. L. & MASON, E. O. (2011) Mupirocin Resistance in Staphylococcus aureus Causing Recurrent Skin and Soft Tissue Infections in Children. *Antimicrobial Agents and Chemotherapy,* 55**,** 2431-2433.

MIAO, V., COÃ«FFET-LE GAL, M.-F., NGUYEN, K., BRIAN, P., PENN, J., WHITING, A., STEELE, J., KAU, D., MARTIN, S., FORD, R., GIBSON, T., BOUCHARD, M., WRIGLEY, S. K. & BALTZ, R. H. (2006) Genetic Engineering in Streptomyces roseosporus to Produce Hybrid Lipopeptide Antibiotics. *Chemistry & Biology,* 13**,** 269-276.

MISHRA, R., SHUKLA, P., HUANG, W. & HU, N. (2014) Gene mutations in Mycobacterium tuberculosis: Multidrug-resistant TB as an emerging global public health crisis. *Tuberculosis*.

MOELLERING, R. C. (2010) NDM-1: A Cause for Worldwide Concern. *New England Journal of Medicine,* 363**,** 2377-2379.

MUNN, P. & JONES, R. (2001) *Honey and Healing,* International Bee Research Association.

MURPHY, A. C., FUKUDA, D., SONG, Z., HOTHERSALL, J., COX, R. J., WILLIS, C. L., THOMAS, C. M. & SIMPSON, T. J. (2011) Engineered Thiomarinol Antibiotics Active against MRSA Are Generated by Mutagenesis and Mutasynthesis of Pseudoalteromonas SANK73390. *Angewandte Chemie International Edition,* 50**,** 3271-3274.

MURPHY, A. C., GAO, S.-S., HAN, L.-C., CAROBENE, S., FUKUDA, D., SONG, Z., HOTHERSALL, J., COX, R. J., CROSBY, J., CRUMP, M. P., THOMAS, C. M., WILLIS, C. L. & SIMPSON, T. J. (2014) Biosynthesis of thiomarinol A and related metabolites of Pseudoalteromonas sp. SANK 73390. *Chemical Science,* 5**,** 397-402.

NAIR, R., PERENCEVICH, E., BLEVINS, A., GOTO, M., NELSON, R. & SCHWEIZER, M. (2015) Clinical effectiveness of mupirocin for preventing S. aureus infections in non-surgical settings: a meta-analysis. *Antimicrobial Resistance and Infection Control,* 4**,** O5.

NAKANO, C., OZAWA, H., AKANUMA, G., FUNA, N. & HORINOUCHI, S. (2009) Biosynthesis of aliphatic polyketides by type III polyketide synthase and methyltransferase in Bacillus subtilis. *J Bacteriol,* 191**,** 4916-23.

NEU, H. C. (1992) The crisis in antibiotic resistance. *Science,* 257**,** 1064-73.

OBRITSCH, M. D., FISH, D. N., MACLAREN, R. & JUNG, R. (2005) Nosocomial Infections Due to Multidrug-Resistant Pseudomonas aeruginosa: Epidemiology and Treatment Options. *Pharmacotherapy: The Journal of Human Pharmacology and Drug Therapy,* 25**,** 1353-1364.

OLIVEIRA, N. E. M. D., CAVALCANTI, E. D. A. C., LAPORT, M. S., BASTOS, M. D. C. D. F. & GIAMBIAGI-DEMARVAL, M. (2009) Constitutive expression of the ileS-2 gene responsible for high-level mupirocin resistance in Staphylococcus aureus. *Journal of Medical Microbiology,* 58**,** 1582-1584.

OMER-BALI, A. (2013) *PhD thesis (Biosciences).* University of Birmingham.

PAPPA, K. A. (1990) The clinical development of mupirocin. *J Am Acad Dermatol,* 22**,** 873-9.

PATEL, J. B., GORWITZ, R. J. & JERNIGAN, J. A. (2009) Mupirocin resistance. *Clin Infect Dis,* 49**,** 935-41.

PIDOT, S. J., COYNE, S. B., KLOSS, F. & HERTWECK, C. (2014) Antibiotics from neglected bacterial sources. *Special issue: Antiinfectives.*

PIEL, J. (2010) Biosynthesis of polyketides by trans-AT polyketide synthases. *Natural Product Reports,* 27**,** 996.

POJER, F., WEMAKOR, E., KAMMERER, B., CHEN, H., WALSH, C. T., LI, S.-M. & HEIDE, L. (2003) CloQ, a prenyltransferase involved in clorobiocin biosynthesis. *Proceedings of the National Academy of Sciences,* 100**,** 2316-2321.

PROJAN, S. J. (2003) Why is big Pharma getting out of antibacterial drug discovery? *Current Opinion in Microbiology,* 6**,** 427-430.

RAHMAN, A. S., HOTHERSALL, J., CROSBY, J., SIMPSON, T. J. & THOMAS, C. M. (2005) Tandemly Duplicated Acyl Carrier Proteins, Which Increase Polyketide Antibiotic Production, Can Apparently Function Either in Parallel or in Series. *Journal of Biological Chemistry,* 280**,** 6399-6408.

RAMSEY, M. A., BRADLEY, S. F., KAUFFMAN, C. A., MORTON, T. M., PATTERSON, J. E. & REAGAN, D. R. (1998) Characterization of Mupirocin-Resistant Staphylococcus aureus from Different Geographic Areas. *Antimicrobial Agents and Chemotherapy,* 42**,** 1305-1305.

RAWLINGS, B. J. (2001) Type I polyketide biosynthesis in bacteria (Part A-erythromycin biosynthesis). *Natural Product Reports,* 18**,** 190-227.

RINEHART, K. L. (1977) Mutasynthesis of new antibiotics. *Pure and Applied Chemistry.*

SAMEL, S. A., WAGNER, B. R., MARAHIEL, M. A. & ESSEN, L.-O. (2006) The Thioesterase Domain of the Fengycin Biosynthesis Cluster: A Structural Base for the Macrocyclization of a Non-ribosomal Lipopeptide. *Journal of Molecular Biology,* 359**,** 876-889.

SCHRODER, W., GOERKE, C. & WOLZ, C. (2012) Opposing effects of aminocoumarins and fluoroquinolones on SOS response in *Staphylococcus aureus*. *International Journal of Medical Microbiology,* 302**,** 90-90.

SEAH, C., ALEXANDER, D. C., LOUIE, L., SIMOR, A., LOW, D. E., LONGTIN, J. & MELANO, R. G. (2012) MupB, a New High-Level Mupirocin Resistance Mechanism in Staphylococcus aureus. *Antimicrobial Agents and Chemotherapy,* 56**,** 1916-1920.

SEOW, K. T., MEURER, G., GERLITZ, M., WENDT-PIENKOWSKI, E., HUTCHINSON, C. R. & DAVIES, J. (1997) A study of iterative type II polyketide synthases, using bacterial genes cloned from soil DNA: a means to access and use genes from uncultured microorganisms. *Journal of Bacteriology,* 179**,** 7360-8.

SHARMA, D., S. K., YOUSUF, DEBARAJ & MUKHERJEE, P. K. (2010) Opportunity, Challenge and Scope of Natural Products in Medicinal Chemistry. *Kerala, India: Research Signpost*

SHIELDS, J. A., RAHMAN, A. S., ARTHUR, C. J., CROSBY, J., HOTHERSALL, J., SIMPSON, T. J. & THOMAS, C. M. (2010) Phosphopantetheinylation and specificity of acyl carrier proteins in the mupirocin biosynthetic cluster. *Chembiochem,* 11**,** 248-55.

SHIER, W. T., RINEHART, K. L. & GOTTLIEB, D. (1969) Preparation of Four New Antibiotics from a Mutant of Streptomyces Fradiae. *Proceedings of the National Academy of Sciences of the United States of America,* 63**,** 198-204.

SHIOZAWA, H., KAGASAKI, T., KINOSHITA, T., HARUYAMA, H., DOMON, H., UTSUI, Y., KODAMA, K. & TAKAHASHI, S. (1993) Thiomarinol, a new hybrid antimicrobial antibiotic produced by a marine bacterium. Fermentation, isolation, structure, and antimicrobial activity. *J Antibiot (Tokyo),* 46**,** 1834-42.

SILVIAN, L. F., WANG, J. & STEITZ, T. A. (1999) Insights into Editing from an Ile-tRNA Synthetase Structure with tRNAIle and Mupirocin. *Science,* 285**,** 1074-1077.

SIMPSON, T. J. (1987) The biosynthesis of polyketides. *Nat Prod Rep,* 4**,** 339-76.

SNEADER, W. (2006) Antibiotics. *Drug Discovery.* John Wiley & Sons, Ltd.

SPELLBERG, B., POWERS, J. H., BRASS, E. P., MILLER, L. G. & EDWARDS, J. E. (2004) Trends in Antimicrobial Drug Development: Implications for the Future. *Clinical Infectious Diseases,* 38**,** 1279-1286.

STAUNTON, J. & WEISSMAN, K. J. (2001) Polyketide biosynthesis: a millennium review. *Nat Prod Rep,* 18**,** 380-416.

STAUNTON, J. & WILKINSON, B. (1997) Biosynthesis of Erythromycin and Rapamycin. *Chemical Reviews,* 97**,** 2611-2630.

SUTHERLAND, R., BOON, R. J., GRIFFIN, K. E., MASTERS, P. J., SLOCOMBE, B. & WHITE, A. R. (1985) Antibacterial activity of mupirocin (pseudomonic acid), a new antibiotic for topical use. *Antimicrobial Agents and Chemotherapy,* 27**,** 495-498.

TANG, L., FU, H. & MCDANIEL, R. (2000) Formation of functional heterologous complexes using subunits from the picromycin, erythromycin and oleandomycin polyketide synthases. *Chemistry & Biology,* 7**,** 77-84.

TAYLOR, P. W. (2013) Alternative natural sources for a new generation of antibacterial agents.

TENOVER, F. C. (2006) Mechanisms of antimicrobial resistance in bacteria. *Am J Infect Control,* 34**,** S64-73.

TENSON, T. & MANKIN, A. (2006) Antibiotics and the ribosome. *Mol Microbiol,* 59**,** 1664-77.

THOMAS, C. M., HOTHERSALL, J., WILLIS, C. L. & SIMPSON, T. J. (2010) Resistance to and synthesis of the antibiotic mupirocin. *Nat Rev Microbiol,* 8**,** 281-9.

TIMMINS, G. S. (2009) Drugs: From Discovery to Approval:Drugs: From Discovery to Approval. *Drug Dev Ind Pharm*.

TUAN, J. S., WEBER, J. M., STAVER, M. J., LEUNG, J. O., DONADIO, S. & KATZ, L. (1990) Cloning of genes involved in erythromycin biosynthesis from Saccharopolyspora erythraea using a novel actinomycete-Escherichia coli cosmid. *Gene,* 90**,** 21-9.

UDWADIA, Z. F. (2012) MDR, XDR, TDR tuberculosis: ominous progression. *Thorax,* 67**,** 286-288.

VAN RIJEN, M. M. L., BONTEN, M., WENZEL, R. P. & KLUYTMANS, J. A. J. W. (2008) Intranasal mupirocin for reduction of Staphylococcus aureus infections in surgical patients

with nasal carriage: a systematic review. *Journal of Antimicrobial Chemotherapy,* 61**,** 254-261.

WALSH, C. (2003) Antibiotics: Actions, Origins, Resistance. *Washington DC: ASM Press*

WANG, J., SOISSON, S. M., YOUNG, K., SHOOP, W., KODALI, S., GALGOCI, A., PAINTER, R., PARTHASARATHY, G., TANG, Y. S., CUMMINGS, R., HA, S., DORSO, K., MOTYL, M., JAYASURIYA, H., ONDEYKA, J., HERATH, K., ZHANG, C., HERNANDEZ, L., ALLOCCO, J., BASILIO, Á., TORMO, J. R., GENILLOUD, O., VICENTE, F., PELAEZ, F., COLWELL, L., LEE, S. H., MICHAEL, B., FELCETTO, T., GILL, C., SILVER, L. L., HERMES, J. D., BARTIZAL, K., BARRETT, J., SCHMATZ, D., BECKER, J. W., CULLY, D. & SINGH, S. B. (2006) Platensimycin is a selective FabF inhibitor with potent antibiotic properties. *Nature,* 441**,** 358-361.

WATANABE, T., IZAKI, K. & TAKAHASHI, H. (1982) New polyenic antibiotics active against gram-positive and -negative bacteria. II. Screening of antibiotic producers and taxonomical properties of Gluconobacter sp. W-315. *J Antibiot,* 35**,** 1148-55.

WEISSMAN, K. J. & LEADLAY, P. F. (2005) Combinatorial biosynthesis of reduced polyketides. *Nat Rev Microbiol,* 3**,** 925-36.

WHO (2001) WHO Global Strategy for Containment of Antimicrobial Resistance.

WORTHINGTON, R. J. & MELANDER, C. (2013) Combination approaches to combat multidrug-resistant bacteria. *Trends in Biotechnology,* 31**,** 177-184.

WRIGHT, G. D. & POINAR, H. (2012) Antibiotic resistance is ancient: implications for drug discovery. *Trends Microbiol,* 20**,** 157-9.

YU, D. Y., XU, F. C., ZENG, J. & ZHAN, J. X. (2012) Type III polyketide synthases in natural product biosynthesis. *Iubmb Life,* 64**,** 285-295.

ZHENG, J. & KEATINGE-CLAY, A. T. (2012) The status of type I polyketide synthase ketoreductases. *Medchemcomm,* 4**,** 34-40.

Appendix A

Integrated HPLC peak areas.

All production cultures and HPLC analysis was performed in triplicate. The peak areas listed below are the average of these triplicates, ±SEM (standard error of the mean).

Fig 3.3 (PA.A) peak area integration

Strain	**Mean ± SEM (V^2)**
P. fluorescens wt	34.72±1.15
P. fluorescens pJH10	78.18±9.17
P. fluorescens pJH10 SimL	40.53±1.75
P. fluorescens pJH10 NovL	130.55±9.94
P. fluorescens pJH10 CloL	98.20±1.70
P. fluorescens pJH10 CouL	125.55±7.52

Fig 3.5 Thiomarinol peak area integration

Strain	**Mean ± SEM (V^2)**
SANK73390 wt	30.82±0.42
SANK73390 pNOVL	27.62±0.44
SANK73390 pSIML	27.96±0.53
SANK73390 pCLOL	26.96±0.29
SANK73390 pCOUL	26.92±1.44

Fig 4.2 (PA.A C5) peak area integration

Strain	**Mean ± SEM (V^2)**
P. fluorescens pAMHI	102.67±4.32
P. fluorescens pAMHI+IPTG	36.43±1.53

Fig 4.3 (PA.A C5) peak area integration

Strain	**Mean ± SEM (V^2)**
*P. fluorescens*ΔACP5 pAMHI	113.08±3.34
*P. fluorescens*ΔACP6 pAMHI	84.87±1.38
*P. fluorescens*ΔACP7 pAMHI	81.43±0.33